UNCLASSIF

ORNL-2159
Progress cy. 6

CENTRAL RESEARCH LIBRARY
DOCUMENT COLLECTION

MARTIN MARIETTA ENERGY SYSTEMS LIBRARIES
3 4456 0350295 7

CHEMISTRY DIVISION

SEMIANNUAL PROGRESS REPORT

FOR PERIOD ENDING JUNE 20, 1956

CENTRAL RESEARCH LIBRARY
DOCUMENT COLLECTION

LIBRARY LOAN COPY

DO NOT TRANSFER TO ANOTHER PERSON

If you wish someone else to see this document, send in name with document and the library will arrange a loan.

OAK RIDGE NATIONAL LABORATORY
OPERATED BY
UNION CARBIDE NUCLEAR COMPANY
A Division of Union Carbide and Carbon Corporation
UCC
POST OFFICE BOX P · OAK RIDGE, TENNESSEE

UNCLASSIFIED

Printed in USA. Price 55 cents. Available from the

Office of Technical Services
U. S. Department of Commerce
Washington 25, D. C.

LEGAL NOTICE

This report was prepared as an account of Government sponsored work. Neither the United States, nor the Commission, nor any person acting on behalf of the Commission:

A. Makes any warranty or representation, express or implied, with respect to the accuracy, completeness, or usefulness of the information contained in this report, or that the use of any information, apparatus, method, or process disclosed in this report may not infringe privately owned rights; or

B. Assumes any liabilities with respect to the use of, or for damages resulting from the use of any information, apparatus, method, or process disclosed in this report.

As used in the above, "person acting on behalf of the Commission" includes any employee or contractor of the Commission to the extent that such employee or contractor prepares, handles or distributes, or provides access to, any information pursuant to his employment or contract with the Commission.

UNCLASSIFIED

ORNL-2159

Contract No. W-7405-eng-26

CHEMISTRY DIVISION

SEMIANNUAL PROGRESS REPORT

for Period Ending June 20, 1956

E. H. Taylor, Director
M. A. Bredig, Associate Director

DATE ISSUED

SEP 28 1956

OAK RIDGE NATIONAL LABORATORY
Operated by
UNION CARBIDE NUCLEAR COMPANY
A Division of Union Carbide and Carbon Corporation
Post Office Box P
Oak Ridge, Tennessee

MARTIN MARIETTA ENERGY SYSTEMS LIBRARIES

3 4456 0350295 7

UNCLASSIFIED

Chemistry Division progress reports previously issued in this series are as follows:

ORNL-65	March, April, May, 1948
ORNL-176	June, July, August, 1948
ORNL-229	September, October, November, 1948
ORNL-336	December, 1948, January and February, 1949
ORNL-286	Period Ending June 30, 1949
ORNL-499	Period Ending September 30, 1949
ORNL-607	Period Ending December 31, 1949
ORNL-685	Period Ending March 31, 1950
ORNL-795	Period Ending June 30, 1950
ORNL-870	Period Ending September 30, 1950
ORNL-1036	Period Ending December 31, 1950
ORNL-1053	Period Ending March 31, 1951
ORNL-1116	Period Ending June 30, 1951
ORNL-1153	Period Ending September 30, 1951
ORNL-1260	Period Ending December 31, 1951
ORNL-1285	Period Ending March 31, 1952
ORNL-1344	Period Ending June 30, 1952
ORNL-1432	Period Ending September 30, 1952
ORNL-1482	Period Ending December 31, 1952
ORNL-1587	Period Ending June 20, 1953
ORNL-1674	Period Ending December 20, 1953
ORNL-1755	Period Ending June 20, 1954
ORNL-1832	Period Ending December 20, 1954
ORNL-1940	Period Ending June 20, 1955
ORNL-2046	Period Ending December 20, 1955

ORNL-2159
Progress

INTERNAL DISTRIBUTION

1. C. E. Center
2. Biology Library
3. Health Physics Library
4-6. Central Research Library
7-12. Laboratory Records Department
13. Laboratory Records, ORNL R.C.
14. Reactor Experimental Engineering Library
15. A. M. Weinberg
16. L. B. Emlet (K-25)
17. J. P. Murray (Y-12)
18. J. A. Swartout
19. E. H. Taylor
20. E. J. Murphy
21. E. D. Shipley
22. S. C. Lind
23. M. L. Nelson
24. W. H. Jordan
25. R. R. Dickison
26. F. L. Culler
27. A. H. Snell
28. A. Hollaender
29. M. T. Kelley
30. R. A. Charpie
31. K. Z. Morgan
32. T. A. Lincoln
33. A. S. Householder
34. C. S. Harrill
35. C. E. Winters
36. D. W. Cardwell
37. E. M. King
38. J. A. Lane
39. G. E. Boyd
40. M. A. Bredig
41. R. W. Stoughton
42. R. B. Briggs
43. G. W. Parker
44. C. J. Borkowski
45. G. H. Jenks
46. K. A. Kraus
47. H. A. Levy
48. R. S. Livingston
49. T. E. Willmarth
50. C. H. Secoy
51. C. J. Hochanadel
52. W. H. Baldwin
53. A. R. Brosi
54. R. N. Lyon
55. S. A. Reynolds
56. P. F. Thomason
57. E. G. Bohlmann
58. C. P. Keim
59. C. D. Susano
60. D. D. Cowen
61. P. M. Reyling
62. R. Livingston
63. G. H. Cartledge
64. E. R. Van Artsdalen
65. G. C. Williams
66. R. W. Johnson
67. J. R. McNally, Jr.
68. E. P. Wigner (consultant)
69. S. J. Cromer
70. M. J. Skinner
71. D. S. Billington
72. H. G. MacPherson (consultant)
73. J. L. Gabbard
74. R. W. Dodson (consultant)
75. H. Eyring (consultant)
76. V. Schomaker (consultant)
77. J. W. Kennedy (consultant)
78. G. T. Seaborg (consultant)
79. C. E. Larson (consultant)

EXTERNAL DISTRIBUTION

80. R. F. Bacher, California Institute of Technology
81. Division of Research and Development, AEC, ORO
82. Boeing Airplane Company

83-667. Given distribution as shown in TID-4500 (12th ed.) under Chemistry category (200 copies – OTS)

DISTRIBUTION PAGE TO BE REMOVED IF REPORT IS GIVEN PUBLIC DISTRIBUTION

CONTENTS

CHEMISTRY DIVISION PUBLICATIONS FROM DECEMBER 20, 1955 TO JUNE 20, 1956 ix

SUMMARY 1

NUCLEAR CHEMISTRY 6
- Capture Cross Section of U^{236} 6
- Measurement of L/K Electron Capture Ratios 6
- Studies on Short-lived Fission Products 7
  - Energy Levels in Ru^{101} from the Disintegration of 13.5-min Tc^{101g} 7
  - Decay of 2.7-min Rb^{90} 8
  - Decay of 32-min Cs^{138} 9
  - Decay of 14.6-hr Nb^{90} 9

ISOLATION AND CHEMICAL PROPERTIES OF SYNTHETIC ELEMENTS 11
- Extraction and Recovery of Neptunium from Chalk River Uranium Solution 11
- Chemistry of Technetium 11
  - Heat Capacity of Potassium Hexachlororhenate from 15 to 320°K 11
- Solvent Extraction of Heptavalent Technetium 16

RADIATION CHEMISTRY 21
- Effect of Ionizing Radiation on Heterogeneous Catalysts 21
- Amorphous Ice 21
  - Thermal Behavior 21
  - Effect of Gamma Rays 22
- Electrons in Solution 23
- Radiation Studies on Nitrate Solutions 24
- An All-Platinum System for High-Temperature, High-Pressure Studies 25
- Radiation-induced Decomposition of Concentrated Solutions of the Alkali-Metal Nitrates 25
- Radiation-induced Chemical Reactions 26
  - Ceric Ion–Formic Acid 26
  - $K_2Cr_2O_7$–Thallous Ion 27
  - $K_2Cr_2O_7$–Halide Ion 28
- Effect of Radiation upon the Exchange of Hydrogen and Ethanol 28

ORGANIC CHEMISTRY 30
- Hydrogen-Deuterium Isotope Effect in the Acid-catalyzed Rearrangement of Triphenylethylene Glycol 30
- *p*-Tolyl/Phenyl Migration Ratio in the Rearrangement of 1,2-Di-*p*-tolyl-1-phenylethylene Glycol 30
- *o*-Tolyl/Phenyl Migration Ratio in the Rearrangement of 1,2-Diphenyl-1-*o*-tolylethylene Glycol and Related Compounds 32
- Relative Stabilizing Effects of an Anisyl Group and Two Phenyls on the Formation of Carbonium Ions 33
- Distribution of P^{32}-labeled Organo-Phosphorus Compounds Between Immiscible Solvents 34
  - Preparation of Di-2-ethylhexyl Hydrogen Phosphate-P^{32} 35

CHEMISTRY OF AQUEOUS SYSTEMS 36
- Rapid Separation by Ion Exchange 36
  - Diffusion Coefficient of Pb(II) in a Strong-Base Anion Exchange Resin 36

Rapid Separation of 2.6-min Ba^{137} from 37-year Cs^{137} with Zirconium Phosphate Used as a Cation Exchanger 37
Anion Exchange Studies 37
Adsorption of Th(IV) from Sulfuric Acid and Ammonium Sulfate Solutions 37
Hydrolysis of Th(IV) 38
Ultracentrifugation of Inorganic Solutions 39
Pb(II) and Sn(IV) 39
Mo(VI) in Acidic Solutions 39
Hg(I) and Hg(II) Nitrate 40
Adsorption on Inorganic Materials 40
Introduction 40
Adsorption of Chromate by Zirconium Oxide 40
Cation Exchange Properties of the Oxides 40
Anion Exchange Properties of Oxides Containing Bi(III) 41
Cation Exchange Properties of "Zirconium Molybdate" – Separation of the Alkaline Earths 41
Cation Exchange Properties of Zirconium Arsenate 41
Concentrated Polymer Solutions of Th(IV) 42
Measurement of Solubilities with Packed Columns 42
Fundamental Studies on Ion Exchange Resins 43
Thermodynamic Calculation of Anion Exchange Selectivities 43
Selectivity of a Sulfonium Type of Strong-Base Anion Exchanger 45
Selectivity of Cation Exchange Resins of Variable Capacity 46
Ionic Interactions in Organic Ion Exchangers 46
Solubility of Ag_2SO_4 in Various Electrolyte Media 48
Introduction 48
Experimental 48
Results and Discussion 48
Preparation of a Lead Dioxide Electrode for Use at High Temperatures 53
Introduction 53
Experimental 53
Results and Discussion 54
Isopiestic Equipment for Thermodynamic Studies at Elevated Temperatures 56
Stabilization of ThO_2 Sols 59
Concentrated Salt Solutions for Reactor Fuel Media or Heat Exchanger Fluids 59
A Study of Dilute Solutions in the System UO_2SO_4-$CuSO_4$-$NiSO_4$-H_2SO_4-H_2O 61

CHEMISTRY OF CORROSION 66
Passivation and Inhibition 66
Potentiostatic Studies on Stainless Steel Electrodes in Sulfuric Acid Solution 68
Electrode Potentials Under Radiation 71

NONAQUEOUS SYSTEMS AT HIGH TEMPERATURES 77
High-Temperature Calorimetry 77
Fused Salts 77
Electrical Conductance and Density of Fused Halides 77
Electrical Conductance and Density of Molten Nitrates 80
Self-Diffusion in Molten Salts 81
Cryoscopy 82
Fluorine Exchange Between Salts and Gases 82
Liquid Metal–Salt Solutions 83

Phase Equilibria of the Potassium–Potassium Halide Systems 83
Electrical Conductivity in Molten Salt-Metal Solutions 85
Color of Liquid Alkali Metals Containing Salt 85
Partial Vapor Pressures Over Mixtures of Salts 86
Diffraction Studies of Liquids 86
An X-Ray Study of Molten Cesium Iodide 86

CHEMICAL PHYSICS 89
Radio-Frequency Spectroscopy 89
Gas Yields from Irradiated Acids 89
Pure Quadrupole Spectroscopy 89
Paramagnetic Resonance 89
Neutron Diffraction Studies 91
A Single-Crystal Neutron Diffraction Study of AlO(OH) 91
Vibrational Spectra of Deuterated Ethanols 92
Experiments with Molecular Beams 92

CHEMISTRY DIVISION PUBLICATIONS FROM DECEMBER 20, 1955 TO JUNE 20, 1956

UNCLASSIFIED PUBLICATIONS

Nuclear Chemistry

N. H. Lazar, E. Eichler, and G. D. O'Kelley, "Nuclear Levels in Sr^{88} from the Disintegration of Rb^{88} and Y^{88}," *Phys. Rev.* **101**, 727 (1956).

G. D. O'Kelley, N. H. Lazar, and E. Eichler, "Decay Chain Ca^{49}-Sc^{49}-Ti^{49}," *Phys. Rev.* **101**, 1059 (1956).

G. D. O'Kelley, N. H. Lazar, and E. Eichler, "Decay of Rb^{89}," *Phys. Rev.* **102**, 223 (1956).

N. H. Lazar and G. D. O'Kelley, "Decay of Nb^{90}," *Bull. Am. Phys. Soc.* **1**(4), 163 (1956).

J. Halperin, R. W. Stoughton, D. E. Ferguson, C. V. Ellison, D. C. Overholt, and C. M. Stevens, "Effective Cross Sections of Pa^{233} and Np^{239} for Thermal Reactor Neutrons," *Proceedings of the International Conference on the Peaceful Uses of Atomic Energy*, **7**, 258, United Nations, New York (1956).

J. Halperin, R. W. Stoughton, C. V. Ellison, and D. E. Ferguson, "Effective Capture Cross Section of Pa^{233} for Thermal Reactor Neutrons," *Nuclear Sci. Engr.* **1**, 1 (1956).

J. Halperin, R. W. Stoughton, C. M. Stevens, D. E. Ferguson, and D. C. Overholt, "An Effective Capture Cross Section of Np^{239} for Thermal Reactor Neutrons," *Nuclear Sci. Engr.* **1**, 108 (1956).

Isolation and Chemical Properties of Synthetic Elements

R. H. Busey, "The Heat Capacity of Rhenium Heptoxide from 15 to 300°K. Entropy and Free Energy," *J. Am. Chem. Soc.* **78**, 3263 (1956).

G. E. Boyd and Q. V. Larson, "Report on the Occurrence of Technetium on the Earth's Crust," *J. Phys. Chem.* **60**, 707 (1956).

Radiation Chemistry

C. Hochanadel, "The Radiation Induced Reaction of Hydrogen and Oxygen in Water at 25°C to 250°C," *Proceedings of the International Conference on the Peaceful Uses of Atomic Energy*, **7**, 521, United Nations, New York (1956).

J. W. Boyle, C. J. Hochanadel, T. J. Sworski, J. A. Ghormley, and W. F. Kieffer, "The Decomposition of Water by Fission Recoil Particles," *Proceedings of the International Conference on the Peaceful Uses of Atomic Energy*, **7**, 576, United Nations, New York (1956).

J. A. Ghormley, "Luminescence of Ice Subjected to Ionizing Radiations," *J. Chem. Phys.* **24**, 111 (1956).

T. J. Sworski, "Relative Rate Constants for Reaction of OH Radical with Sulfuric Acid, Formic Acid and Cerous Ion," *J. Am. Chem. Soc.* **78**, 1768 (1956).

J. W. Boyle and H. A. Mahlman, "Radiation Chemistry of Thorium Nitrate Breeder-Blanket Solutions," *Abstracts of Papers, Second Annual Meeting of the American Nuclear Society*, Chicago (1956).

T. J. Sworski, "Mechanism for the Reduction of Ceric Ion by Thallous Ion Induced by Cobalt-60 Gamma Radiation," *Radiation Research* **4**, 483 (1956).

Organic Chemistry

H. J. Schaeffer and C. J. Collins, "Molecular Rearrangements. VI. The Dehydration of *cis*- and of *trans*-2-Phenylcyclohexanol," *J. Am. Chem. Soc.* **78**, 124 (1956).

E. J. Dewitt, C. T. Lester, and G. A. Ropp, "The Application of Isotope Dilution Techniques in Studies of Reaction Rates and Equilibria: The Effect of Diene Structure on the Rate of the Diels-Alder Reaction," *J. Am. Chem. Soc.* **78**, 2101 (1956).

E. Grovenstein, Jr., and G. A. Ropp, "Carbon-13 Isotope Fractionation as a Criterion of the Mechanism of Bromodecarboxylation of 3,5-Dibromo-4-hydroxybenzoic Acid," *J. Am. Chem. Soc.* **78**, 2560 (1956).

Chemistry of Aqueous Systems

J. S. Johnson, K. A. Kraus, and R. W. Holmberg, "Hydrolytic Behavior of Metal Ions. V. Ultracentrifugation of Hafnium(IV)," *J. Am. Chem. Soc.* **78**, 26 (1956).

K. A. Kraus and H. O. Phillips, "Anion Exchange Studies. XIX. Anion Exchange Properties of Hydrous Zirconium Oxide," *J. Am. Chem. Soc.* **78**, 249 (1956).

K. A. Kraus and H. O. Phillips, "Adsorption of Inorganic Materials. I. Cation Exchange Properties of Zirconium Phosphate," *J. Am. Chem. Soc.* **78**, 694 (1956).

K. A. Kraus, T. A. Carlson, and J. S. Johnson, "Cation Exchange Properties of Zirconium(IV) – Tungsten(VI) Precipitates," *Nature* **177**, 1128 (1956).

K. A. Kraus, G. E. Moore, and F. Nelson, "Anion Exchange Studies. XXI. Th(IV) and U(IV) in Hydrochloric Acid. Separation of Thorium, Protactinium and Uranium," *J. Am. Chem. Soc.* **78**, 2692 (1956).

M. H. Lietzke and R. W. Stoughton, "The Solubility of Silver Sulfate in Sulfuric Acid Media at High Temperatures. Effects on the Silver, Silver Sulfate Electrode," *J. Am. Chem. Soc.* **78**, 3023 (1956).

G. E. Myers and G. E. Boyd, "A Thermodynamic Calculation of Cation Exchange Selectivities," *J. Phys. Chem.* **60**, 521 (1956).

Chemistry of Corrosion

G. H. Cartledge, "The Mechanism of the Inhibition of Corrosion by the Pertechnetate Ion. II. The Reversibility of the Inhibiting Mechanism," *J. Phys. Chem.* **60**, 28 (1956).

G. H. Cartledge, "The Mechanism of the Inhibition of Corrosion by the Pertechnetate Ion. III. Studies on the Perrhenate Ion," *J. Phys. Chem.* **60**, 32 (1956).

G. H. Cartledge, "Electrochemistry of Stainless Steel in Sulfuric Acid," *Nature* **177**, 181 (1956).

G. H. Cartledge, "Studies in Corrosion," *Sci. American* **194**, 35 (1956).

Nonaqueous Systems at High Temperatures

E. R. Van Artsdalen, "Complex Ions in Molten Salts. Ionic Association and Common Ion Effect," *J. Phys. Chem.* **60**, 172 (1956).

M. A. Bredig and E. R. Van Artsdalen, "Zinc and Cadmium Chloride Complexes in Molten Salts," *J. Chem. Phys.* **24**, 478 (1956).

E. R. Van Artsdalen, Duane Brown, A. S. Dworkin, and F. J. Miller, "Self-Diffusion in Molten Sodium Nitrate," *J. Am. Chem. Soc.* **78**, 1772 (1956).

Chemical Physics

M. A. Bredig, "Thermal Expansion and Stability of Layer Structures in Ionic AB Compounds," *J. Chem. Phys.* **24,** 1037 (1956).

D. F. Smith, Duane Brown, A. S. Dworkin, D. J. Sasmor, and E. R. Van Artsdalen, "Low Temperature Heat Capacity and Entropy of Molybdenum Trioxide and Molybdenum Disulfide," *J. Am. Chem. Soc.* **78,** 1533 (1956).

R. Livingston, J. A. Ghormley, and H. Zeldes, "Paramagnetic Resonance Observations on the Condensed Products of Electric Discharges through Water Vapor and Related Substances," *J. Chem. Phys.* **24,** 483 (1956).

CHEMISTRY DIVISION SEMIANNUAL PROGRESS REPORT

SUMMARY

NUCLEAR CHEMISTRY

The effective n capture cross section of U^{236} was found to be 34 ± 6 barns.

Three different methods were used to determine the L/K electron capture ratio for Ce^{139}, namely, 4π scintillation, x-ray and gamma-ray coincidence, and x-ray and conversion electron counting, and good agreement was obtained for a value of 0.36.

Investigations of 13.5-min Tc^{101g} were extended to include gamma-gamma and beta-gamma coincidence spectrometry. Gamma rays of 127 ± 4, 130 ± 3, 183 ± 4, 186 ± 4, 235 ± 5, 307 ± 4, 385 ± 8, 410 ± 10, 545 ± 5, 635 ± 10, 720 ± 8, 846 ± 9, and 939 ± 10 kev energy were detected in various experiments, and their relative intensities were measured. An intense beta-ray group of energy 1.32 ± 0.03 Mev was found in coincidence with the 307-kev gamma ray, and a second group of 1.07 ± 0.05 Mev energy was coincident with the 545-kev gamma ray. These transitions could be fitted into a decay scheme with levels in Ru^{101} at 130, 316, 307, 410, 545, 635, 720, 846, and 939 kev.

The decay of 2.7-min Rb^{90} was studied by scintillation spectrometer methods. Two prominent gamma rays of energy 0.84 ± 0.01 and 1.39 ± 0.02 Mev were found. Other gamma radiations are present and extend to over 5 Mev. One beta-ray group of energy 5.05 ± 0.10 Mev was characterized.

Preliminary measurements on the decay of Cs^{138} showed that gamma rays of energy 0.46, 0.55, and 1.02 Mev exist and are coincident with the known 1.44-Mev gamma ray, while the gamma rays at 2.20 and 2.64 Mev are not in coincidence with the 1.44-Mev transition. A moderately intense gamma ray of 0.83 Mev was found in coincidence with the 1.44-Mev gamma ray.

Scintillation and magnetic spectroscopy measurements on Nb^{90} disclosed gamma rays of energy 2.32, 2.19, 1.96, 1.82, 1.14, 0.1325, 0.1417 Mev, in addition to the positron annihilation radiation. By the coincidence method it was established that the 0.1325- and 2.19-Mev gamma rays are in cascade and that the conversion coefficient of the 0.1325-Mev gamma ray is characteristic of an $E3$ transition. It is proposed that the 0.1325-Mev gamma ray de-excites the 5− level, populating a 2+ level at 2.19 Mev. A 0.142-Mev gamma ray was seen in coincidence with a 1.14-Mev transition. The 0.142-Mev decay is probably $E2$, from its internal conversion coefficient. Also found was a 1.28-Mev gamma ray, believed to be the crossover transition for the 0.142-, 1.14-Mev cascade, and two gamma rays of energy 0.38 and 0.85 Mev. The most energetic positron group was measured as 1.50 ± 0.04 Mev and is coincident with 1.14-Mev gamma rays.

ISOLATION AND CHEMICAL PROPERTIES OF SYNTHETIC ELEMENTS

Heptavalent technetium, present in aqueous solutions as pertechnetate ion, TcO_4^-, was found to be extracted into a variety of organic liquids, including alcohols, ketones, ethers, organo-phosphorus, and tertiary and quaternary amines dissolved in nonpolar solvents. Good extraction from acid but not from neutral nor alkaline solution was observed with the alcohols, esters of phosphoric acid, and tertiary amines. Ketones and quaternary amines extracted technetium efficiently over a wide pH range. The technetium species transferred between phases was shown to be $HTcO_4$ from acid aqueous media, and to be $MTcO_4$ from neutral alkali-metal salt solutions.

The low-temperature heat capacity of potassium hexachlororhenate, K_2ReCl_6, over the temperature range 15 to 320°K was measured. This salt exhibits three anomalies in its heat capacity, with maxima at 76.0, 103.5, and 111.0°K. These anomalies are shown to have a certain degree of irreversibility on cooling, but, given sufficient time to approach equilibrium, reproducible results are obtainable. The entropy at 298.16°K, 87.20 $cal \cdot deg^{-1} \cdot mole^{-1}$, is high compared with that of the corresponding diamagnetic platinum compound, K_2PtCl_6.

RADIATION CHEMISTRY

The addition of formic acid was found to increase the yield for ceric reduction by gamma rays from a value equivalent to $2G_{H_2O_2} + G_H - G_{OH}$ to a maximum value equivalent to $2G_{H_2O_2} + G_H + G_{OH}$. The Ce^{+++}, HCOOH, and H_2SO_4 compete for OH radicals with rate constants in the ratio 650:380:1.

Radiation induces the reduction of chromate by either bromide or chloride ion. The kinetics were studied.

The yield of NO_2^- by "direct action" in the gamma-ray decomposition of concentrated solutions (0.1 to 3.0 *M*) of the alkali-metal nitrates can be expressed by $G_{NO_2^-} = 1.23 \log [NO_3^-] + 1.72$. The cation has little influence on the yield.

A platinum-lined stainless steel autoclave was designed for use in reactor irradiations of aqueous solutions at temperatures up to 300°C.

The 100-ev yield of N_2 from the reactor decomposition of a solution containing 7 *m* $Th(NO_3)_4$, 7 *m* $Be(NO_3)_2$, 0.05 *m* $UO_2(NO_3)_2$ was the same as that for a solution containing 7 *m* $Th(NO_3)_4 \cdot 2HNO_3$, 0.05 *m* $UO_2(NO_3)_2$, namely, $G_{N_2} = 0.15$. There was little or no back-reaction of the N_2 for irradiations at temperatures up to 300°C. The lower vapor pressure of the mixed salt solutions, compared with the nitric-acid-stabilized solution, offers a distinct advantage in their application as a blanket solution in a power-breeder reactor.

Deuterium and tritium were used as tracers to determine the origin of the hydrogen and methane obtained in the radiolysis of ethanol and acetic acid. Little of the hydrogen from ethanol originated from the methyl group. In the formation of hydrogen from ethanol or acetic acid, and in the formation of methane from acetic acid, molecular processes were shown to be unimportant. With a gas phase present, the radiation-induced exchange between hydrogen and ethanol was negligible.

Jortner and Stein reportedly demonstrated a stable bound state of the electron in H_2O, CH_3OH, C_2H_5OH. The evidence for the stable electron in water was based on an absorption peak at about 900 mμ for a solution of potassium dissolved in water at a temperature near 0°C. On repeating this experiment, the results indicated that the peak attributed to absorption by electrons may have been the weak absorption by water itself or the effect of temperature on this absorption.

Amorphous ice prepared by condensing water vapor on a liquid-nitrogen-cooled surface evolves heat to the extent of 8 cal/g when warmed the first time to −125°C, and crystallizes, starting at −120°C, with a heat of crystallization of 15.8 cal/g. Gamma-ray irradiation at −196°C produces more H_2O_2 in amorphous ice than in crystalline ice.

The catalytic activity of gamma alumina for the hydrogen-deuterium exchange reaction at −78°C was found to be increased ninefold by irradiation with Co^{60} gamma rays for 1 hr.

ORGANIC CHEMISTRY

The isotope effect (k_H/k_D) in the rearrangement of triphenylethylene glycol-1-H^2 was determined when the rearrangement was carried out under five separate reaction conditions. The value of k_H/k_D was shown to be constant at 3.0 ± 0.3.

The *p*-tolyl/phenyl and the *o*-tolyl/phenyl migration ratios in the aldehyde-ketone rearrangement were investigated. The *o*-tolyl/phenyl ratio was determined as 3.3.

It was found that one anisyl group is better able to stabilize a carbonium ion than two phenyls in formic, in 50% sulfuric, or in 0.16 *M* perchloric (acetic) acids.

Organo-phosphorus compounds labeled with P^{32} were used to evaluate the losses of solvents from mixtures of di-2-ethylhexyl hydrogen phosphate and tributyl phosphate in kerosene into water. Tributyl phosphate-P^{32} losses were less than 50 mg/liter under all the conditions tested. Di-2-ethylhexyl hydrogen phosphate-P^{32} was synthesized.

CHEMISTRY OF AQUEOUS SYSTEMS

In connection with the previously reported use of ion exchangers for the separation of short-lived daughter elements from their parent activities, the diffusion coefficient of tracer lead in a typical anion exchanger was measured by a shallow-bed technique. It is estimated that in some cases the ion exchange method will permit separation of daughter activities with half lives of the order of milliseconds. In view of their unusual selectivities, certain inorganic adsorbents may also be used for such separations. The separation of 2.6-min Ba^{137} from long-lived Cs^{137}, using zirconium phosphate as a cation exchanger, is discussed.

Detailed studies of the adsorption of Th(IV) from sulfuric acid and ammonium sulfate solutions on a quaternary amine anion exchanger were carried out. Excellent adsorption occurs at low sulfuric acid concentrations and at both low and high ammonium sulfate concentrations. The distribution coefficients are similar to those of U(VI) in the same media though consistently lower for Th(IV). The data strongly suggest existence of negatively charged thorium sulfate complexes.

Earlier reported differences in the degrees of polymerization of Th(IV) in perchlorate and chloride media were shown to be due to differences in rates of polymerization. The differences in degree of polymerization on aging in chloride solutions are not paralleled by large differences in acidities of the solutions at constant degree of hydrolysis.

Preliminary ultracentrifugations of Pb(II) and Sn(IV) in basic solutions showed little evidence for polymerization of these elements in strong base (1 *M* NaOH). Some polymerization was found for Mo(VI) in 3 *M* HCl; there was considerable aggregation in 1 *M* HCl.

Studies on the adsorption of ions in inorganic materials continued. The use of oxides, particularly zirconium oxide, for chromate and other heavy-metal anion recovery and concentration appears promising. Further work on the cation exchange properties of oxides is described; in many cases they may be used for separations, including separation of groups of elements. Oxides containing Bi(III) were found to have excellent adsorptive properties for chloride ions. Heavy-metal salts containing polyvalent anions, for example, zirconium tungstate and similar materials, continued to show interesting cation exchange properties. Zirconium molybdate was utilized for the separation of the alkaline earths from each other as well as of the alkali metals from each other. Zirconium arsenate was demonstrated to be a satisfactory cation exchanger.

Work on the preparation of concentrated Th(IV) polymer solutions is continuing. At low temperature, good stability of concentrated polymer solutions was observed, although no conditions for stabilities at high temperatures were found.

A new method for the measurement of solubilities based on passage of solutions through packed columns was developed. The method appears suitable for measurements of solubilities at high temperatures.

An apparatus was constructed for determining osmotic and activity coefficients of a solute at elevated temperatures by isopiestically measuring relative solvent vapor pressures vs concentration of solute. The unit allows the periodic weighing by remote control of 20 sample dishes on a magnetic balance inside a pressure vessel. Preliminary tests showed that the transferring and weighing of dishes could be carried out satisfactorily up to 140°C and that about eight days was required for NaCl solutions to come to equilibrium at 83°C.

Data were obtained experimentally or from the literature on the solubility of Ag_2SO_4 in aqueous $AgNO_3$, KNO_3, $Mg(NO_3)_2$, $Al(NO_3)_3$, Na_2SO_4, $CuSO_4$, $MgSO_4$, $La_2(SO_4)_3$, $Al_2(SO_4)_3$, and $In_2(SO_4)_3$. Curves for the log of the molality solubility product (on the basis of complete dissociation) vs the square root of the stoichiometric ionic strength were, in spite of the great difference in valence types involved, surprisingly similar, whether or not a common ion was present in the supporting electrolyte. The great change of solubility of AgCl with ionic strength clearly indicates strong complexing, and was interpreted in terms of the complexes $AgCl_2^-$, $AgCl_3^{--}$, $AgCl_4^{---}$, and Ag_2Cl^+, Ag_3Cl^{++}, Ag_4Cl^{+++}, in HCl and $AgNO_3$ media, respectively.

EMF data are presented for the cell Pt, PbO_2, $PbSO_4$, $H_2SO_4(m = 1)$, Ag_2SO_4(sat.), Ag as a function of temperature. It is shown that this information in conjunction with other thermodynamic data can be used to calculate the stoichiometric activity coefficients of H_2SO_4, at least over the range 25 to 150°C.

The vapor pressures of several concentrated salt solutions were measured over the temperature range from 200 to 400°C. Solutions of either $LiNO_3$ or $Ca(NO_3)_2$ show some promise for application as primary heat transfer media for solid-fuel-element reactors as well as for a fuel-bearing material for homogeneous reactors.

A survey study of the temperatures at which phase separation occurs in dilute solutions in the system UO_2SO_4-$CuSO_4$-$NiSO_4$-H_2SO_4-H_2O disclosed the approximate temperature limits of homogeneity as a function of the composition of the solution. The data indicate that operation of the HRT at the design temperature will result in partial or complete precipitation of the uranium.

A stable ThO_2 sol peptized with $Th(NO_3)_4$ was the subject of an intensive study with the objective of elucidating the factors which contribute to the thermal stability of the sol. Its viscosity, pH, refractive index, and electrolytic conductance were measured. An effort is being made to prepare sols with a larger particle size by varying factors during the peptization step.

A complete and rigorous thermodynamic calculation was completed on the bromide-chloride anion exchange equilibrium with variously cross-linked Dowex 2 preparations. Agreement with experimentally measured selectivity coefficient values, D^{Br}_{Cl}, was found within the errors involved in the thermodynamic treatment, except for the most highly (16% DVB) cross-linked exchanger. This latter exchanger, however, possessed a much lower capacity, so that one of the basic assumptions of the theory underlying the calculations was not obeyed.

Selectivity coefficient values for the uptake of tracer bromide ion by various salt-forms of sulfonium-type anion exchanger showed that the greater the water absorption by a given salt-form, X, the greater D_X^{Br}. Measurements on the sodium-hydrogen ion exchange equilibrium with a series of specially prepared variable-capacity polystyrenesulfonic acid cation exchangers, where only *p*-sulfonic acid groups were present, showed that D_H^{Na} decreased with decreasing capacity at constant cross-linking. In addition, a selectivity coefficient inversion (i.e., H^+ ion preferred over Na^+ ion) was observed for the lowest-capacity exchangers.

A study of the details of ionic interactions in organic ion exchangers revealed that the characteristic parameters describing ion exchanger salt mixtures are of the same magnitude as those observed for aqueous electrolyte mixtures, but that no general correlation existed between the two systems. This latter fact was interpreted as an indication that the interactions of the "counter-ions" with the fixed ionic groups are of predominant importance in ion exchangers.

CHEMISTRY OF CORROSION

The normal electrode potential of the osmium(IV)-osmium(VIII) electrode was determined. Osmium(VIII) oxide passivates iron so completely that the iron electrode indicates the thermodynamic potential of the osmium couple. The passivity produced by osmic acid was sensitive to electrolytes, and hence presumably involves a competitive adsorption in the same manner as was observed for other inhibitors of the XO_4^{n-} type. These observations suggest a new interpretation of the passivating (Flade) potential.

The study of the relation between the corrosion rate and potential of a stainless steel in sulfuric acid was extended by potentiostatic measurements. Two maximum corrosion rates show up in the base region of potentials, where only one had been previously observed in similar work elsewhere. The observations are interpreted in terms of the rates of the different processes involved at the electrode surface.

The study of the electrochemical behavior of stainless steel in sulfuric acid was extended to include the effect of gamma radiation.

NONAQUEOUS SYSTEMS AT HIGH TEMPERATURES

The electrical equivalent conductance of molten alkali fluorides as a function of temperature was determined in a new apparatus built of stainless steel. The potential drop across two probes located between two a-c current-carrying electrodes was measured by using a low-resistance transformer bridge. Significantly, CsF was found to have a higher conductivity than LiF, and the order of conductivity as a function of the anion was found to be $F^- > Cl^- > Br^- > I^-$ for potassium and cesium, but $Br^- > Cl^- > I^- > F^-$ for lithium salts. Data for $CaCl_2$, $SrCl_2$, and $BaCl_2$ and for a few rare-earth halides are also reported and briefly discussed in the light of the complex-forming tendencies of the ions.

The self-diffusion coefficients and their temperature dependence (heats of activation) for the ions in fused KNO_3 and $NaNO_3$ were measured by an isotopic tracer method. A comparison with electrical conductances points out the possibility that the Nernst-Einstein equation derived for dilute aqueous solutions is not applicable to fused salts. Measurements of melting-point depressions in $NaNO_3$ were continued for the purpose of determining the state of association and dissociation of the salts dissolved in the molten nitrate.

The results of exploratory measurements of the exchange of fluorine between salts and gases are reported.

The study of the miscibility of potassium metal with each of its four halides in liquid phase was completed. The method of thermal analysis was used both for the liquid-liquid and liquid-solid equilibria and gave considerably higher accuracy than chemical analysis after phase equilibration and separation. The bromide phase diagram was found to be distinguished by the smallest finite area of immiscibility in the liquid phase, the metal and bromide being in all proportions miscible at a temperature as low as 6°C below the melting point of the pure salt. All the potassium systems, like all the sodium systems, exhibit strong positive deviations from Raoult's law in the liquid salt phase near the upper quadruple point (monotectic).

A modification in the apparatus for measuring electric conductivity of alkali-metal solutions in molten halides appears to have accomplished the

desired objective of preventing loss of volatile metal from the solution.

An apparent coloration of liquid alkali metal in the presence of small amounts of salt were demonstrated to be due to the light absorption in the vapor of the metal, above the liquid.

A radial distribution function based on the x-ray scattering from molten cesium iodide showed a single prominent peak at 3.85 Å and a full width at half-height of about 1 Å. The area corresponds to an average coordination number of 4.5, which may be thought of as at least in qualitative agreement with considerations of the large volume increase on melting. It is, however, considerably and somewhat unexpectedly lower than that reported in the literature for KCl, 5.8, which will require checking.

The vapor pressure of solid potassium chloride was measured from 10^{-5} to 10^{-1} mm Hg (730 to 1044°K), utilizing an effusion technique and a surface ionization detector.

CHEMICAL PHYSICS

Molecular hydrogen and oxygen yields from sulfuric acid irradiated with Co^{60} gamma rays at 77°K were measured to see whether there is a correlation with the yields of atomic hydrogen measured by means of paramagnetic resonance under similar radiation conditions. The gas yields depend on whether the acid is frozen to a glassy or crystalline solid.

Several effects were observed in a paramagnetic resonance study of single crystals of calcium hydroxide irradiated with gamma rays at 77°K. An absorption line appears with a strength that indicates a yield of about 2.6 unpaired electrons for every 100 ev of energy absorbed. The unpaired electron is located on a symmetry axis of the crystal. Observations with a crystal containing Ca^{43} show that the electron is not at a calcium atom, while other observations show that it probably is at an OH^- lattice site. Optical absorption studies indicate that the OH radical is present; however, it is considered more likely that the unpaired electron observed is in an *F* center rather than on the OH radical. A very much smaller effect is the appearance of a small amount of atomic hydrogen that resides in ordered lattice sites on symmetry axes of the crystal. A third effect is the appearance of a very small yield of a species that does not show axial symmetry and very possibly is an interstitial formed by an Auger cascade.

The first results of a study, by neutron diffraction, of the crystal structure of diaspore, AlO(OH), are reported.

NUCLEAR CHEMISTRY

CAPTURE CROSS SECTION OF U^{236}

J. O. Blomeke[1] J. Halperin
R. W. Stoughton

A measurement has been made of the effective n capture cross section of U^{236} in highly irradiated MTR fuel elements.[2] An average value of 34 ± 6 barns is reported which is consistent with the large resonance integral deduced from resonance parameters[3] and from measurements of the cadmium ratio of U^{236}.

MEASUREMENT OF L/K ELECTRON CAPTURE RATIOS

B. H. Ketelle A. R. Brosi
H. Thomas

Disintegration energies have been determined for only a relatively few nuclides which decay by electron capture. Presently known decay energies have been obtained from inner bremsstrahlung end points, L/K capture ratios, and threshold energies of nuclear reactions. None of these methods has general applicability. The inner bremsstrahlung and L/K capture ratio measurements are, to a certain extent, complementary. The inner bremsstrahlung measurements are most useful when the decay energy is large compared with the K electron binding energy, whereas the L/K capture ratio gives reliable disintegration energies only when these are of the order of a few times the K binding energy.

Previous L/K capture ratio measurements were made by 4π counting. Gaseous sources have been introduced into proportional counters, and solid sources have been incorporated into activated NaI crystals. In each case the detectors are used with pulse-sorting equipment. Recently a 4π technique has been used in which the source was placed between two NaI crystals. These 4π methods can be used only in special cases where peaks resulting from corresponding L and K capture processes can be resolved in a pulse-height spectrum.

Because of the limited applicability of the 4π electron capture ratio methods, two coincidence methods were checked, by the use of Ce^{139} sources. In one method, proposed by Pruett and Wilkinson, x-ray–x-ray coincidences and x-ray–γ-ray coincidences are measured with scintillation spectrometers.

The ratio of the coincidence counting rates, N_{xx} and $N_{x\gamma}$, and the singles counting rates in one channel, N_x and N_γ,

$$R_3 = \frac{N_{x\gamma}/N_\gamma}{N_{xx}/N_x}$$

can be related to the electron capture ratio as shown in the following equation:

$$1 + \epsilon = \frac{1 + \beta}{2R_3 - 1}\left(\frac{1}{\alpha_K} + \frac{1 + R_1}{R_1}\right) .$$

Here $1 + \epsilon$ is the ratio of all electron captures to the excited state to K electron captures to the excited state, β is the ratio of ground state to excited state K-shell captures, α_K is the K conversion coefficient, and $(1 + R_1)/R_1$ is the ratio of all conversions to K conversions.

If a magnetic-lens spectrometer and a scintillation spectrometer are used, coincidences can be measured between K x rays and conversion electrons. The L conversion electron–x-ray coincidence rate, N_{xL}, the K conversion electron–x-ray coincidence rate, N_{xK}, and the singles conversion electron counting rates, N_L and N_K, are related to ϵ as follows:

$$2 + \epsilon = \frac{N_L/N_{xL}}{N_K/N_{xK}} .$$

The conversion electron–x-ray coincidence counting method has the advantage over other coincidence methods of no additional constants being required in order to solve for ϵ. Both coincidence methods have the disadvantage of a small error in the experimental ratio leading to a large error in ϵ when ϵ is small. Because of this, constant errors resulting from scattered radiation or from improper random coincidence corrections can lead to serious errors. (The random coincidence correction is a function of detection efficiency.)

[1] Chemical Technology Division.

[2] J. O. Blomeke, J. Halperin, and R. W. Stoughton, *HRP Quar. Prog. Rep. April 30, 1956*, ORNL-2096, p 138.

[3] J. A. Harvey and V. E. Pilcher, private communication.

In addition, the equation given above for computing ϵ from x-ray–conversion electron coincidence counting is correct only when the x-ray counting efficiency is very low. At higher x-ray counting efficiencies, coincident K x rays are absorbed in the crystal and give pulses twice the size of a single x-ray pulse. Discrimination against these pulses eliminates some of the coincidences between K conversion electrons and x rays but none between L conversion electrons and x rays. This leads to error in ϵ unless the equation is corrected by terms which are a function of the x-ray counting efficiency.

Several determinations of ϵ for Ce^{139} have been made by each of the methods listed below; the data indicate agreement within the statistical errors:

Method of Measurement	Ce^{139} Electron Capture Ratio, ϵ
4π scintillation counting	0.37 ± 0.02
X-ray and γ-ray coincidence counting	0.35 ± 0.08
X-ray and conversion electron coincidence counting	0.36 ± 0.02

STUDIES ON SHORT-LIVED FISSION PRODUCTS

Energy Levels in Ru^{101} from the Disintegration of 13.5-min Tc^{101g}

G. D. O'Kelley Q. V. Larson
G. E. Boyd

The preliminary investigations of the decay of Tc^{101g} described previously[4] have been extended to include gamma-gamma and beta-gamma coincidence spectrometry, from which it is possible to assign energy levels to Ru^{101}.

Table 1 summarizes the gamma-ray energies and relative intensities derived from a careful analysis of the spectrum measured on a 3 × 3 in. NaI(Tl) scintillation spectrometer, with a source-to-crystal distance of 9.3 cm. Also included are the intensities measured in various coincidence experiments, relative to the intensity of the 307-kev gamma ray, so that they may be compared with the single-crystal data.

[4] G. D. O'Kelley, Q. V. Larson, and G. E. Boyd, *Chem. Semiann. Prog. Rep. Dec. 20, 1955*, ORNL-2046, p 32.

TABLE 1. ENERGIES AND INTENSITIES OF THE GAMMA RAYS FROM THE DECAY OF Tc^{101g}

Gamma-Ray Energy (kev)	Intensity Relative to 307-kev Gamma Ray	
	From Single-Crystal Data	From Coincidence Measurements
127 ± 4		0.011 ± 0.002
130 ± 3	0.037 ± 0.010	
183 ± 4		0.0084 ± 0.0020
186 ± 4	0.033 ± 0.008	
235 ± 5	0.006 ± 0.003	0.011 ± 0.004
307 ± 4	1.00	
385 ± 8		0.0019 ± 0.005
410 ± 10	0.0051 ± 0.0015	
545 ± 5	0.087 ± 0.009	0.091 ± 0.010*
635 ± 10	0.0092 ± 0.0015	
720 ± 8	0.012 ± 0.002	
846 ± 9	0.0039 ± 0.0005	
939 ± 10	0.0030 ± 0.0005	

*Calculated from comparison of ratio of intensity of 127- and 183-kev gamma rays to that of 307- and 545-kev gamma rays, as measured by the coincidence method.

The gamma-gamma coincidence spectrometry results may be summarized as follows: the 720-kev gamma ray was in coincidence with a 127-kev gamma ray; the 545-kev gamma ray was in coincidence with 127-, 183-, and 385-kev gamma rays; the 307-kev gamma ray was in coincidence with 127-, 183-, 238-, and probably 385-kev gamma rays. Although coincidence measurements are difficult with the window of the coincidence spectrometer set below 300 kev, because of the Compton spectrum of the intense 307-kev gamma ray, the 130- and 186-kev gamma rays appear to be in coincidence, as might be expected from their nearly equal gamma-ray intensities in the single-crystal spectrum.

Beta-ray spectra from the decay of Tc^{101} were measured on an anthracene crystal scintillation spectrometer. The most energetic beta-ray group has an energy of 1.32 ± 0.03 Mev and is in coincidence with the 307-kev gamma ray. A second beta group of 1.07 ± 0.05 Mev energy is coincident with the 545-kev gamma ray. Although other beta-ray groups must be present, they could not be resolved in these experiments.

The level scheme shown in Fig. 1 is consistent with the data described above. Except for the level at 939 kev, McGowan and Stelson[5] found the same levels in Ru^{101} by coulomb excitation and, in addition, could definitely assign the 130-kev gamma ray rather than the 186-kev gamma ray to the de-excitation of the first excited state of Ru^{101}. The data on the decay of Tc^{101g} alone cannot establish the order of the 186-, 130-kev cascade.

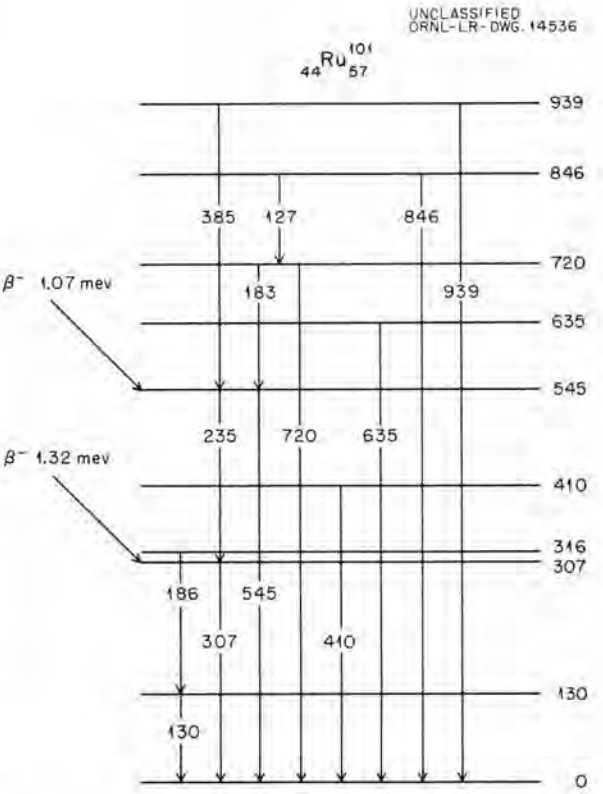

Fig. 1. Level Scheme of Ru^{101} Inferred from the Decay of 13.5-min Tc^{101g}.

Decay of 2.7-min Rb^{90}

G. D. O'Kelley N. R. Johnson, Jr.

Kofoed-Hansen and Nielsen[6] studied the decay properties of Rb^{90} formed in the decay of mass-separated Kr^{90} and found the half life of Rb^{90} to be 2.74 min. By aluminum absorption, the maximum beta-ray energy was measured as 5.7 Mev, with evidence for additional beta-ray groups and gamma radiations. The purpose of the work described below is to make a more detailed study of this complex decay in the hope that a consistent decay scheme can be evolved.

Sources of Rb^{90} were prepared from the decay of 33-sec Kr^{90}. Bare platinum foils coated with U^{235} were irradiated inside air-filled gas cells within Graphite Reactor pneumatic transfer rabbits. The system used for removal of the resulting fission-product gases has been described elsewhere.[7] Once removed from the pneumatic transfer rabbit, the mixed krypton and xenon gases were passed through a charcoal trap at 0°C. The krypton gas, which "breaks through" first, was collected in a gas cell and allowed to decay, collecting the rubidium recoil atoms on a strip of charged aluminum foil. In this way, pure sources of Rb^{90} + Rb^{89} were obtained with negligible radiocesium contamination.

Preliminary measurements of the gamma rays from Rb^{90} were made on a 3 × 3 in. NaI(Tl) scintillation spectrometer used with a 20-channel pulse-height analyzer. Two prominent gamma rays

[5] F. K. McGowan and P. H. Stelson, private communication, June 1956.

[6] O. Kofoed-Hansen and K. O. Nielsen, *K. Danske Videnskab. Selskab Mat.-fys. Medd.* 26, No. 7 (1951).

[7] G. D. O'Kelley, N. H. Lazar, and E. Eichler, *Phys. Rev.* 102, 223 (1956).

were found, one of 0.84 ± 0.01 Mev energy in high intensity, and a less intense gamma ray of 1.39 ± 0.02 Mev energy. Both decayed with a half life of 2.5 to 3.0 min, demonstrating that they follow the decay of Rb^{90} and do not arise from some contaminant such as 32-min Cs^{138}. In fact, careful searches were made in the samples of Rb^{90} + Rb^{89}, after several half lives of Rb^{89}, and the gamma-ray spectrum characteristic of Cs^{138} was never found. It is apparent from these preliminary measurements that the gamma-ray spectrum of Rb^{90} is complex and extends to over 5 Mev. The analysis of the experimental data is made more difficult by the presence of Rb^{89}, with its longer half life and complex gamma-ray spectrum.

A Fermi analysis of the beta-ray spectrum of Rb^{90} as measured on an anthracene scintillation spectrometer yielded an energy of 5.05 ± 0.1 Mev for the most energetic group. If it is assumed that this beta-ray group populates the first excited state, which is probably at 0.84 Mev, the total beta-decay energy is about 5.9 Mev. By use of Levy's empirical mass formula,[8] the Rb^{90}-Sr^{90} mass difference is predicted to be about 6.0 Mev, in agreement with the postulated scheme. Since the ground state of Rb^{90} is probably 2− from Nordheim's rules,[9] it is improbable that the beta decays from this state would populate the 0+ ground state of Sr^{90} in preference to the first excited state, which is almost certainly 2+.

Studies of the decay of Rb^{90} are continuing, with particular attention being given to beta-gamma and gamma-gamma coincidence spectrometry.

Decay of 32-min Cs^{138}

G. D. O'Kelley Q. V. Larson
N. H. Lazar[10]

Preliminary measurements of Cs^{138} gamma rays with 3 × 3 in. NaI(Tl) scintillation spectrometers, both singly and in coincidence, have shown that the gamma rays of energy 0.46, 0.55, and 1.02 Mev exist and are coincident with the known 1.44-Mev gamma ray. Contrary to published decay schemes of this nuclide, the gamma rays at 2.20 and 2.64 Mev are not in coincidence with the 1.44-Mev transition. A number of low-intensity gamma rays were also disclosed in the gamma-gamma coincidence spectra; a moderately intense gamma ray of 0.83-Mev energy was found in coincidence with the 1.44-Mev gamma ray. The investigation of the Cs^{138} decay is continuing; it now seems obvious that the decay of this nuclide is more complex than would be expected from the literature.

Decay of 14.6-hr Nb^{90}

G. D. O'Kelley N. H. Lazar

A study of the decay of 14.6-hr Nb^{90} is interesting because it permits an investigation of the nuclear properties of the "doubly magic" daughter nucleus, Zr^{90}, with 40 protons and 50 neutrons. A number of investigators[11–14] have studied the decay of Nb^{90}. The results obtained indicated that the decay of Nb^{90} proceeded, by positron emission and electron capture, with a half life of 14.6 hr. The most energetic positron group had an energy of 1.50 Mev and was probably complex. Gamma-ray spectra were also complex, with prominent gamma rays at 0.142, 1.14, and 2.20 Mev;[12–14] in addition, Ong Ping Hok[14] found gamma rays of 0.133-, 0.372-, 1.27-, and 1.77-Mev energy, which were assigned to the decay of Nb^{90}. An interpretation of these data is complicated by the presence of the 2.32-Mev metastable state[15] in Zr^{90}, of lifetime 0.83 sec, and a 0+ first excited state[16] at 1.75 Mev.

In the present experiments Nb^{90} was prepared by a (p,n) reaction on 98% enriched Zr^{90} and was chemically purified by extraction with diisopropyl ketone. Gross beta-decay curves for such samples were straight for about nine half lives of Nb^{90}; then some long-lived activity was noted, which was probably due to long-lived isotopes of niobium

[8] H. B. Levy, *A New Empirical Mass Equation: I. Atomic Masses in the Fission-Product Region*, UCRL-4588 (Nov. 30, 1955).

[9] L. W. Nordheim, *Revs. Modern Phys.* 23, 322 (1951).

[10] Physics Division.

[11] D. N. Kundu and M. L. Pool, *Phys. Rev.* 76, 183 (1949).

[12] G. E. Boyd, *Chem. Quar. Prog. Rep. Sept., Oct., Nov. 1948*, ORNL-229, p 31; *Chem. Quar. Prog. Rep. March 31, 1951*, ORNL-1053, p 43.

[13] H. B. Mathur and E. K. Hyde, *Phys. Rev.* 98, 79 (1955).

[14] O. P. Hok, P. Kramer, and G. Meijer, *Physica* 20, 1200 (1954).

[15] E. C. Campbell *et al.*, *Phys. Rev.* 98, 1172 (1955); private communication, 1956.

[16] O. E. Johnson, R. G. Johnson, and L. M. Langer, *Phys. Rev.* 98, 1517 (1955).

that formed in the cyclotron irradiation. The half life measured here is 14.6 ± 0.1 hr.

The gamma rays from Nb^{90} were studied with the use of a 3 × 3 in. NaI(Tl) scintillation spectrometer, two 3 × 3 in. NaI(Tl) spectrometers in coincidence, and a permanent-magnet electron spectrograph.[17] The gamma-ray results are shown below:

Gamma-Ray Energy (Mev)	Relative Intensity
2.32 ± 0.02	1.00
2.19	0.17
1.96	0.076
1.82	0.069
1.14	1.20
0.1325 ± 0.0002	0.054
0.1417 ± 0.0003	0.72
0.511	1.32

Coincidence experiments established that the 0.1325-Mev gamma ray was in coincidence with the 2.19-Mev gamma ray. From the intensity of the 0.1325-Mev gamma ray to that of the 2.19-Mev gamma ray, a total internal conversion coefficient could be calculated for the former. The measured value of 3.0 ± 0.5 may be compared with about 2.4 as calculated from the tables of Rose[18] for an $E3$ transition. It now appears that the 2.19-Mev transition de-excites a 2+ level in Zr^{90} of that energy, and is populated by a 0.1325-Mev, $E3$ transition from the 5− state at 2.32 Mev.

Further coincidence measurements have established that for every 142-kev gamma ray a 1.14-Mev gamma ray is found. The internal conversion coefficient can be calculated from the number of 142-kev gamma rays per 1.14-Mev gamma ray. This measurement yielded an α_T of 0.45, which, in view of the experimental difficulties, is in fair agreement with the theoretical value of about 0.26 for an $E2$ transition.

Not shown in the above tabulation is a 1.28-Mev gamma ray, believed to be the crossover transition for the 1.14-, 0.142-Mev cascade. This transition intensity is about 3% that of the 1.14-Mev gamma ray. Also not shown are two weak gamma rays coincident with the 2.19-Mev transition. These are 0.38 Mev (10% intensity of 2.19 Mev) and 0.85 Mev (5% intensity of 2.19 Mev).

The most energetic positron group was measured as 1.50 ± 0.04 Mev, and is in coincidence with 1.14-Mev gamma rays.

The results presented here permit definite assignments for only a few levels in Zr^{90}. Further work is indicated before some of the weak gamma-ray transitions can be incorporated into a consistent scheme.

[17] The authors are indebted to B. Harmatz for making the measurements with this instrument.

[18] M. E. Rose, *Beta- and Gamma-Ray Spectroscopy*, K. Siegbahn (ed.) Interscience, New York, 1955.

ISOLATION AND CHEMICAL PROPERTIES OF SYNTHETIC ELEMENTS

EXTRACTION AND RECOVERY OF NEPTUNIUM FROM CHALK RIVER URANIUM SOLUTION

G. W. Parker P. M. Lantz
W. J. Martin G. E. Creek

The results of a study of the recovery of neptunium from Canadian uranium solutions are described in the classified section of this report, issued separately as ORNL-2171.

CHEMISTRY OF TECHNETIUM

Heat Capacity of Potassium Hexachlororhenate from 15 to 320°K

R. H. Busey H. H. Dearman
Q. V. Larson

The low-temperature heat capacity of potassium hexachlororhenate, K_2ReCl_6, was measured to provide values of the entropy and free-energy functions in connection with the study of the chemistry of technetium and rhenium. Potassium hexachlororhenate is paramagnetic; its magnetic susceptibility follows the Curie-Weiss law from 400 to 200°K with a Curie-Weiss constant[1] of $\Delta = 57$ deg. The single measurement below 200°K at 78°K shows some departure from this law. These magnetic data indicate the possible existence of a heat-capacity anomaly at low temperatures arising from the transition from the antiferromagnetic to the paramagnetic state. Such an anomaly was found; in fact, this compound shows three anomalies in its low-temperature heat capacity.

No previous heat-capacity data are available for this compound. These measurements constitute some of the first heat-capacity data obtained on any paramagnetic compound of an element of the third transition series and should be of value in interpreting the magnetic behavior of this series.

Potassium Hexachlororhenate Sample. – The K_2ReCl_6 sample was prepared[2] by KI reduction of $KReO_4$ according to the procedure given in *Inorganic Synthesis*.[3] The compound was dried in an evacuated dessicator charged with P_2O_5. The chlorine and rhenium contents were determined gravimetrically[4] to be 44.53 ± 0.04% and 39.06 ± 0.10%, respectively. The theoretical values are 44.58 and 39.04%.

The weight of sample introduced into the calorimeter was 86.915 g (*in vacuo*[5]), which represents 0.18212 mole based upon 477.25 as the molecular weight. One atmosphere pressure of helium was added to ensure rapid thermal equilibrium.

Apparatus and Temperature Scale. – The calorimeter and cryostat have been described previously.[6] Calibration of the gold resistance thermometer–heater was carried out concurrently with the heat-capacity measurements by means of a standard copper-constantan thermocouple. Immediately before the heat-capacity measurements were made, the standard thermocouple and a platinum resistance thermometer were compared in order to check the calibration of the thermocouple. A total of 12 calibration check points was made over the temperature range 14 to 60°K. The temperatures derived from the thermocouple readings agreed with the platinum resistance thermometer to within 0.02 deg.

Heat-Capacity Data. – The heat-capacity observations on K_2ReCl_6 determined by the adiabatic method are given in Table 2. Temperature increments of the individual determinations can be inferred from the mean temperatures. No correction for curvature has been made. The measurements were made in the order of the series given; the measurements in a particular series were continuous in that the calorimeter never cooled overnight by more than 1 to 2 deg. In those series of measurements in which an anomaly in the heat capacity appeared, no interruption in the measurements occurred. The results are expressed in terms of the defined thermochemical calorie equal to 4.1840 j(abs). The ice point was taken to be 273.16°K.

---

[1] C. M. Nelson, G. E. Boyd, and Wm. T. Smith, Jr., *J. Am. Chem. Soc.* 76, 348 (1954).

[2] By D. E. LaValle of the Analytical Chemistry Division.

[3] L. C. Hurd and V. A. Reinders, *Inorganic Synthesis*, H. S. Booth (ed.), p 178–180, vol I, McGraw-Hill, New York, 1939.

[4] Re as $(C_6H_5)_4AsReO_4$: H. H. Willard and G. M. Smith, *Ind. Eng. Chem., Anal. Ed.* 11, 305 (1939); modified by Wm. T. Smith, Jr., and S. H. Long, *J. Am. Chem. Soc.* 70, 354 (1948).

[5] The density of K_2ReCl_6 was determined to be 3.303 g/ml.

[6] R. H. Busey, *A Combination Isothermal-Adiabatic Low-Temperature Calorimeter*, ORNL-1828 (Jan. 26, 1955).

TABLE 2. HEAT CAPACITY (cal·deg^{-1}·mole^{-1}) OF K_2ReCl_6

T_{av} (°K)	C_p
Series 1	
292.98	51.11
300.89	51.34
Series 2	
15.16	4.870
16.74	5.842
18.96	6.919
21.97	8.560
25.36	10.43
28.75	12.22
31.59	13.73
34.55	15.22
38.16	17.04
41.63	18.80
45.29	20.51
49.61	22.48
54.30	24.39
59.18	26.26
64.33	28.15
69.78	30.02
80.46	33.12
86.08	34.60
91.90	36.19
97.92	37.84
119.17	40.23
126.32	41.12
133.51	42.07
140.47	42.90
147.85	43.57
155.49	44.29
163.21	44.99
171.06	45.67
178.88	46.24
186.90	46.94
195.14	47.28
203.51	47.79
211.95	48.22
220.53	48.62
229.23	49.08
238.07	49.37
246.94	49.69
255.95	50.01
265.10	50.29
274.42	50.66
283.22	50.91
292.82	51.16
301.94	51.46
311.30	51.71
320.78	51.97

T_{av} (°K)	C_p
Series 3	
69.35	29.88
83.18	33.82
87.46	35.02
91.49	36.07
95.00	36.99
97.56	37.70
99.61	38.36
101.59	39.27
102.47	39.74
103.09	40.34
103.40	40.53
103.61	40.49
103.88	40.33
104.24	39.92
104.66	39.85
105.25	39.48
106.03	39.48
107.02	39.64
108.26	39.97
109.62	40.47
110.63	41.07
110.82	41.28
111.02	41.02
111.21	40.89
111.48	40.72
111.78	40.46
112.14	40.11
112.67	40.04
113.52	39.94
114.82	39.97
116.73	40.00
119.53	40.24
Series 4	
63.99	28.11
66.03	28.74
68.10	29.42
69.93	30.07
71.55	30.64
72.97	31.17
73.98	31.58
74.60	32.08
75.08	32.49
75.56	33.10
76.02	33.83
76.42	33.01
76.95	32.48
77.42	32.43
77.88	32.48
78.40	32.61
79.11	32.70

T_{av} (°K)	C_p
Series 4	
80.18	33.02
81.90	33.48
84.53	34.19
Series 5	
86.58	34.76
90.13	35.72
93.68	36.66
97.02	37.53
100.02	38.53
102.27	39.68
103.57	40.39
104.21	40.08
104.70	39.69
105.50	39.47
106.71	39.57
108.42	39.94
109.88	40.66
110.61	41.07
111.02	41.19
111.47	40.58
112.00	40.31
112.52	40.08
113.04	40.00
113.70	39.90
114.96	39.91
117.50	40.08
Series 6	
108.85	39.96
109.26	40.07
109.66	40.39
110.03	40.62
110.37	40.98
110.70	41.11
111.02	40.98
111.39	40.69
111.84	40.42
112.50	40.06
Series 7	
101.77	39.18
102.22	39.46
102.66	39.81
103.06	39.91
103.38	39.95
103.64	39.76
103.85	39.72
104.07	39.78
104.30	39.68
104.61	39.52

T_{av} (°K)	C_p
Series 7	
105.07	39.49
105.92	39.39
Series 8	
74.34	31.61
74.89	31.84
75.34	32.15
75.76	32.62
76.14	32.74
76.49	32.41
76.84	32.38
77.22	32.35
77.66	32.35
78.23	32.46
79.24	32.76
Series 9	
71.01	30.44
72.96	31.14
74.58	31.97
75.65	33.16
76.11	33.99
76.31	33.25
76.49	32.98
76.66	32.78
76.83	32.63
77.04	32.51
77.27	32.45
77.56	32.42
78.18	32.57
79.73	32.89
Series 10	
98.21	37.84
99.14	38.13
100.13	38.49
101.11	38.98
101.92	39.46
102.50	40.01
102.86	40.10
103.14	40.26
103.39	40.37
103.61	40.50
103.82	40.31
104.05	40.06
104.31	40.03
104.66	39.73
105.16	39.55
105.86	39.55
106.97	39.61

The measurements given in series 1 and 2 cover the temperature range studied and reveal the possible existence of heat-capacity anomalies between 72 and 78°K and between 100 and 115°K. Results in these intervals obtained in series 2 are not given in Table 2 but are given later. Series 3, 4, and 5 were made to characterize the shape of the heat-capacity anomalies. The other series are discussed below.

Reversibility of the Transitions. – Series 6 through 10 were designed to test the reversibility of the three transitions characterized by the previous measurements. The reversibility of the transitions was studied in the following manner. The day before the measurements of series 6 were made the sample was cooled from room temperature to 116.5°K and maintained at this temperature overnight. The following morning the sample was cooled to 108.5°K at the rate of approximately 0.1 deg/min, and measurements were immediately started. Immediately following the measurements of series 6 the sample was cooled from 113 to 108°K and again maintained at the lower temperature overnight. The following morning the sample was cooled from 108 to 101.5°K at the rate of approximately 0.1 deg/min, and series 7 measurements were begun immediately. Following the series 7 measurements, the sample was cooled to 90°K, allowed to stand at this temperature overnight, and cooled to 73.5°K the following morning at an average cooling rate of 0.25 deg/min; measurements of series 8 were then made.

The object of the cooling technique used for the series 6–8 measurements was to determine whether it is possible to "freeze in" some disorder in cooling rapidly through a particular transition from a temperature a little above to a temperature a little below the maximum in the heat capacity. Figures 2 and 3 present the results of each series of measurements over the temperature ranges of the heat-capacity anomalies. It is evident from the measurements of series 6–8 (represented by the dotted lines) that there is a certain amount of sluggishness in the rate at which thermal equilibrium is established. The anomaly with a maximum at 111°K is apparently more reversible than the other two, because the results of series 6 measurements fall on the smooth curve on the high-temperature side of the anomaly.

The last two series, 9 and 10, were carried out to determine whether the results of series 3, 4, and 5 represented true equilibrium values, since measurements of series 6, 7, and 8 indicate a certain amount of irreversibility: for series 9 measurements the sample was cooled from 185°K – the temperature to which the sample was warmed following series 8 measurements – to 70°K and maintained at this temperature for 42 hr. Measurements of series 9 were then made, and the sample was warmed to 97°K and maintained at this temperature for 114 hr. Series 10 measurements were carried out following this period.

The results of series 9 and 10 agree very well with those of series 3, 4, and 5 (Figs. 2 and 3). It now remains to show that the smooth curves drawn through the data of series 3, 4, 5, 9, and 10 give the same heat content as was obtained in the "large temperature rise" measurements of series 2 and 3. This information is given in Table 3, in which columns 2 and 3 give the temperature interval covered by a single heat-capacity determination made in the series given in column 1, column 4 gives the measured heat content over this interval, and column 5 gives the heat content for the same interval obtained by integration of the smooth curves of Figs. 2 and 3.

TABLE 3. TOTAL HEAT CONTENT THROUGH THE ANOMALOUS REGIONS

Series	T_1	T_2	ΔH (meas) (cal/mole)	$\int_{T_1}^{T_2} C_p\, dT$	Δ
2	72.608	78.470	189.58	189.46	0.12
3	71.944	76.444	143.91	144.03	−0.12
3	76.444	81.064	151.30	151.25	0.05
2	101.086	108.317	287.29	287.26	0.03
2	108.318	115.714	297.69	297.88	−0.19

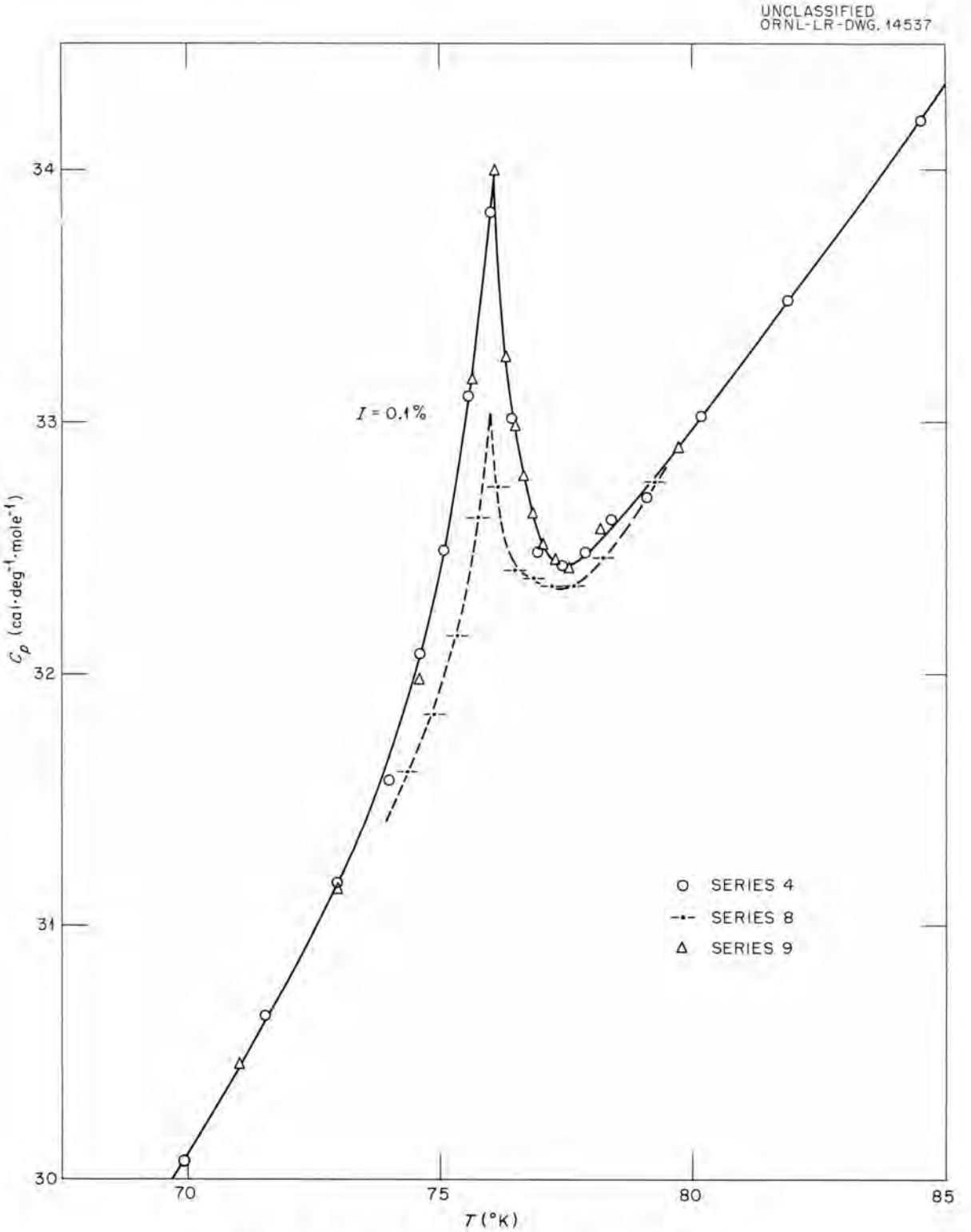

Fig. 2. Heat Capacity of K_2ReCl_6 from 70 to 85°K.

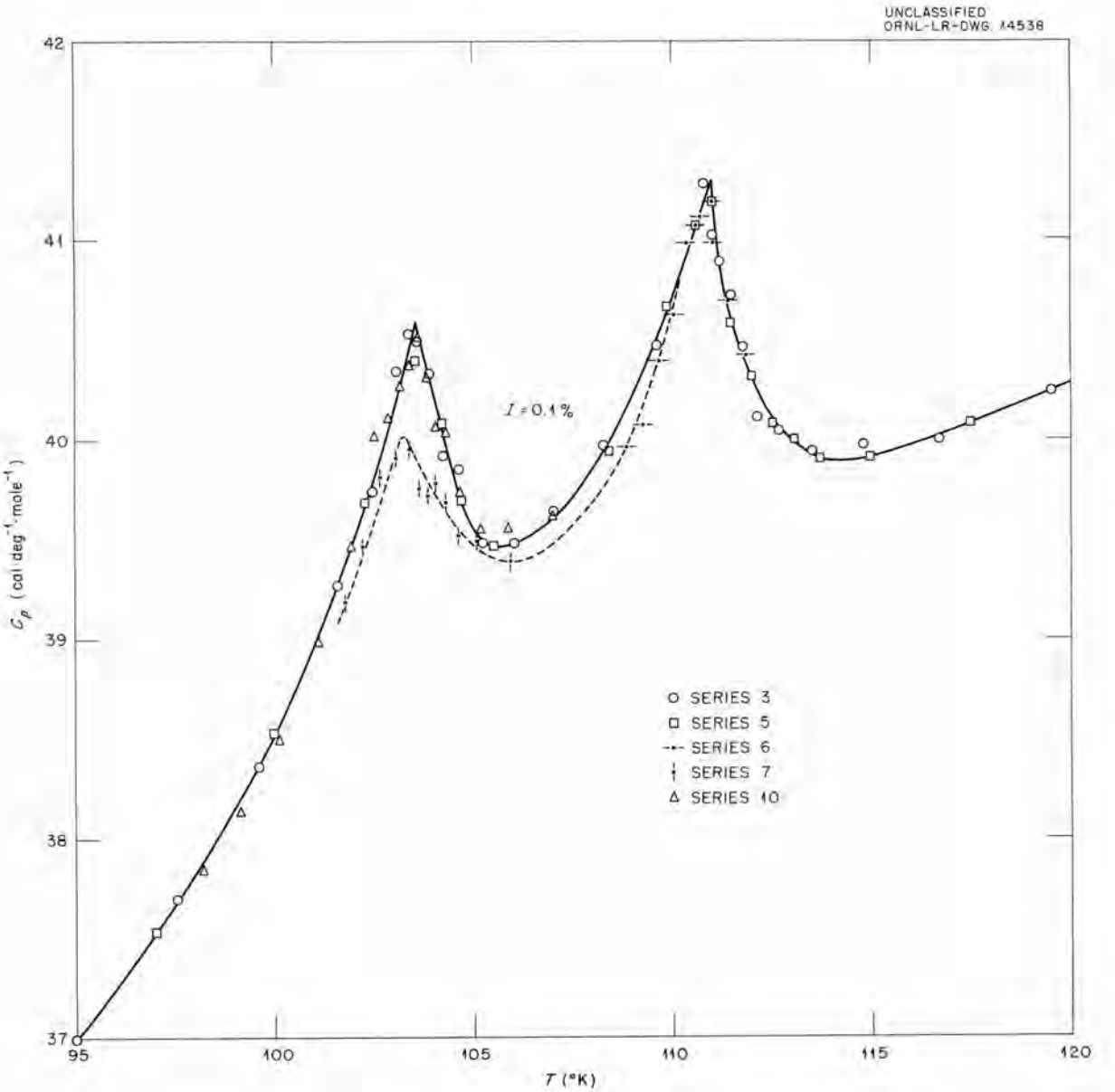

Fig. 3. Heat Capacity of K_2ReCl_6 from 95 to 120°K.

The curves well represent the accurately measured total heat contents.

Entropy of K_2ReCl_6. – The entropy of K_2ReCl_6 is 87.20 cal·deg^{-1}·mole^{-1} at 298.16°K and was obtained by application of the third law of thermodynamics to the heat-capacity data and utilization of the Debye T^3 law for an approximation of the entropy at 15°K, namely 1.75 cal·deg^{-1}·mole^{-1}. It is of interest to compare this entropy with that of the isomorphous, diamagnetic compound K_2PtCl_6, whose entropy at 298.16°K is 79.78 cal·deg^{-1}·mole^{-1}. If the orbital momentum of the Re(IV) is quenched as indicated by the magnetic susceptibility measurements[1] and if the electronic "spin-only" is active, the magnetic entropy at high temperature should be $R \ln (2S + 1) = R \ln 4 = 2.75$ cal·deg^{-1}·mole^{-1} for the K_2ReCl_6. This accounts for only a portion of

the entropy difference of 7.42 cal·deg^{-1}·mole^{-1} between the two compounds.

Discussion of Results. – The magnetic susceptibility data[1] indicate that the anomaly with a maximum at 76.1°K probably arises from the typical second-order transition from an antiferromagnetic to a paramagnetic state.[7,8] The anomalies with maximums at 103.5 and 111.0°K are at present unexplained. They do not have the characteristic shape of a cooperative type of transition, but this might be because of their close proximity to one another. A curve obtained by the summation of two typical lambda-type curves placed close together approximates the curve shown in Fig. 3. The analytical data obtained on the sample of K_2ReCl_6 do not exclude the possibility of a small amount (~1 mole %) of a hydrolysis product such as $K_2Re(OH)Cl_5$ being present in the sample, which might cause anomalous heat-capacity results. To check this possibility a new sample of K_2ReCl_6 that was prepared by an alternate procedure will be measured in the near future.

SOLVENT EXTRACTION OF HEPTAVALENT TECHNETIUM

G. E. Boyd Q. V. Larson

Measurements of the extraction of heptavalent technetium have been undertaken as a preliminary to further studies on the chemical behavior of this element when it is present in solutions at very low concentrations. Hitherto it had been reported[9] that trace quantities of technetium when oxidized with chlorine could not be extracted by diethyl ether from aqueous solutions containing potassium thiocyanate and HCl. Subsequently it was found,[10] however, that a good extraction will occur from this solution into ether if technetium is first reduced with Sn(II) or Hg(I). The extraction of pertechnetate ion into chloroform by the use of tetraphenylarsonium chloride has been reported,[11] as well as the extraction of this same species from 4 *N* NaOH by pyridine.[12] Quite recently, observations on the solvent extraction of technetium from acid, neutral, and alkaline media have been reported,[13] wherein results with several alcohols, ketones, and amines were described. However, many of these results do not agree with earlier findings cited nor with the observations reported below.

The solvent extraction behavior of heptavalent technetium was surveyed at ORNL with the use of the 4.2-day Tc^{96} + 60-day Tc^{95m} gamma-ray-emitting activities produced by molybdenum (d,xn) reactions with 15-Mev deuterons. The chemical procedure to separate, purify, and concentrate the technetium tracer has been described elsewhere.[14] Extraction coefficients, E_a^0, defined by

$$E_a^0 = \frac{\text{Activity in total organic phase}}{\text{Activity in total aqueous phase}} \left(\frac{V_a}{V_o}\right),$$

were measured by shaking initially equal volumes (usually 10 ml) of organic and technetium-containing aqueous phases together for 30 min, effecting a phase separation, and noting the volumes to 0.1 ml, and then assaying the radioactivity in the entire phase with a 4π geometry, high-pressure, argon-filled ionization chamber. Material balances (i.e., activity balances) were obtained for all the data reported below.

A summary of E_a^0 values obtained with a variety of organic liquids and solutions for the extraction of Tc(VII) from 1 *N* H_2SO_4, distilled water, and 1 *N* NaOH is given in Table 4. A number of observations may be made from these data:

1. Oxygen- or nitrogen-containing solvents are required for successful extractions.
2. The value of E_a^0 decreases with increasing size and weight of the organic molecule.
3. As a class, the ketones are the best extractant liquids, while the ethers are the poorest.

---

[7] J. W. Stout and E. Catalano, *J. Chem. Phys.* **23**, 2013 (1955).

[8] R. H. Busey and W. F. Giauque, *J. Am. Chem. Soc.* **74**, 4443 (1952).

[9] C. Perrier and E. Segre, *J. Chem. Phys.* **7**, 155 (1939).

[10] G. E. Boyd, Q. V. Larson, and E. E. Motta, paper presented before the Division of Physical and Inorganic Chemistry, American Chemical Society, Syracuse, N.Y., June 28–30, 1948; see abstract No. 48.

[11] S. Tribalat and J. Beydon, *Anal. Chim. Acta* **8**, 22 (1953); see also, G. W. Parker, *Chem. Quar. Prog. Rep. March 31, 1952*, ORNL-1285, p 33; E. I. Wyatt, *Anal. Chem. Quar. Prog. Rep. June 26, 1951*, ORNL-1113, p 52.

[12] W. Goishi and W. F. Libby, *J. Am. Chem. Soc.* **74**, 6109 (1952).

[13] J. B. Gerlit, *Proceedings of the International Conference on Peaceful Uses of Atomic Energy*, p 145, vol 7, sec. 9B.2, United Nations (1956).

[14] G. E. Boyd and Q. V. Larson, *J. Phys. Chem.* **60**, 707 (1956).

TABLE 4. SOLVENT EXTRACTION OF Tc(VII) FROM VARIOUS AQUEOUS SOLUTIONS

	E_a^0		
	1 *N* H_2SO_4	H_2O	1 *N* NaOH
Alcohols			
n-Amyl	5.9		
Isoamyl	5.9		
n-Hexyl	3.3		
n-Heptyl	1.65		
n-Octyl	1.0		
2-Ethyl-1-hexanol	0.24	0.0075	
Diisobutyl	0.10		
Cyclohexanol	31.7	0.25	
Benzyl	3.1		
Ketones			
Methyl ethyl (MEK)	21.0	1.0	15.1
Diethyl (DEK)	35.0		
Methyl isopropyl (MIPK)	32.7		2.1
Methyl isobutyl (MIBK)	13.6		
Diisopropyl (DIPK)	2.05		
Diisobutyl (DIBK)	0.15		
Cyclohexanone	92.5	8.4	
Ethers			
Diethyl	0.029		
Diisopropyl	0.012		
Dibutyl	0.012		
β,β'-Dichlorodiethyl (DDE)	1.5		0.029
Organo-phosphorus compounds			
Trioctyl phosphine oxide (0.1 *M* in kerosene)	49.0		
TBP (undiluted)	44.0		
Amines			
5% dimethyl octyl (DMOA) in C_6H_6	53.1	18.5	0.66
5% trioctyl (TOA) in C_6H_6	59.8		
0.3 g of cetyl dimethyl benzyl ammonium chloride (CDMBA) in 100 ml of $CHCl_3$	105	10.4	7.9*
Hyamine 10X	52.5		
Hyamine 1622	50		
Miscellaneous compounds			
Benzonitrile	5.1		
Nitrobenzene	1.21		
Nitromethane	3.0		
Benzene	0.017		
Carbon tetrachloride	<0.001		
Chloroform	<0.001		<0.001
Trichloroethylene	<0.001		

*0.1 *N* NaOH.

4. The alcohols show good extraction properties from acid solutions only. Extraction from pure water is small; from 1 N NaOH it is negligible.

5. Trioctyl phosphine oxide and TBP show good extraction properties for acid and neutral, but not for alkaline solutions.

6. The weak-base tertiary amines promote good extraction from acid but not from strongly basic aqueous solutions, while the strongly basic quaternary ammonium compounds show high E_a^0 values over the entire pH range.

Results from a comparative study of the extraction of Tc(VII) from 1 N solutions of a variety of strong acids with the use of the best extractants revealed by Table 4 are summarized in Table 5; the following observations were derived:

1. Extraction of Tc(VII) is most efficient from 1 N H_2SO_4 and least efficient from 1 N $HClO_4$.

2. Cyclohexanol is relatively a better extractant than cyclohexanone from 1 N HI and $HClO_4$, while the latter solvent is distinctly superior for all the other organic liquids examined.

3. Extraction by organo-phosphorus compounds is relatively less from 1 N HNO_3 than it is with the other solvents; TBP appears generally superior to trioctyl phosphine oxide.

4. Extraction by the amines diminishes in the same sequence that the anion-exchange selectivity coefficients for the anions of the acids increases, suggesting that an ion exchange mechanism is involved in the extraction of TcO_4^- ion.

Measurements were also conducted to determine the variations of E_a^0 with acid concentration, with the results shown in Figs. 4 and 5. Curves similar to those in Fig. 4 were observed for the extractions using cyclohexanone and a 5 wt % solution of dimethyl octyl amine (DMOA) in benzene. In all cases the extraction increased rapidly with the acidity of the aqueous phase to a maximum at or below a concentration of 1 N and then diminished exponentially. Owing to the onset of complete phase miscibility, it was not possible to work at the highest acid concentrations with either cyclohexanol or cyclohexanone. The decrease (Fig. 5) in E_a^0 with increasing nitric acid concentration above 1 N was more marked with TBP than with cyclohexanol, while the decrease with 5% DMOA in C_6H_6 was even more pronounced although not exponential.

The dependence of the extraction of Tc(VII) from 1 N H_2SO_4 solutions by trioctyl amine upon the nature of the diluent organic solvent is clearly revealed by the results presented in Table 6, where nearly a fourfold difference between xylene and chloroform was observed.

The dependence of the extraction of technetium from 2 N HNO_3 upon the concentration of pertechnetate ion was investigated with cyclohexanol, cyclohexanone, and DMOA in benzene used as extractant liquids. In these experiments aliquots of a solution containing known amounts of Tc^{99}

TABLE 5. SOLVENT EXTRACTION OF Tc(VII) FROM VARIOUS STRONG ACIDS

Solvent	E_a^0					
	1 N H_2SO_4	1 N HCl	1 N HBr	1 N HNO_3	1 N HI	1 N $HClO_4$
Cyclohexanol	31.7	17	16.5	9.2	5.5	4.3
Cyclohexanone	92.5	50.8	25	14.4	5.1	2.6
β,β'-Dichlorodiethyl ether	1.5	0.40	0.12	0.031	0.074	<0.001
Trioctyl phosphine oxide*	49	24.7	25	0.38	9.2	0.22
Tributyl phosphate	44	85	91	29	69.8	5.6
Dimethyl octyl amine**	53.1	357	106	34	3.3	0.48
Trioctyl amine**	59.8			31	2.3	0.49

*0.1 M in kerosene.

**5% by weight or volume in C_6H_6.

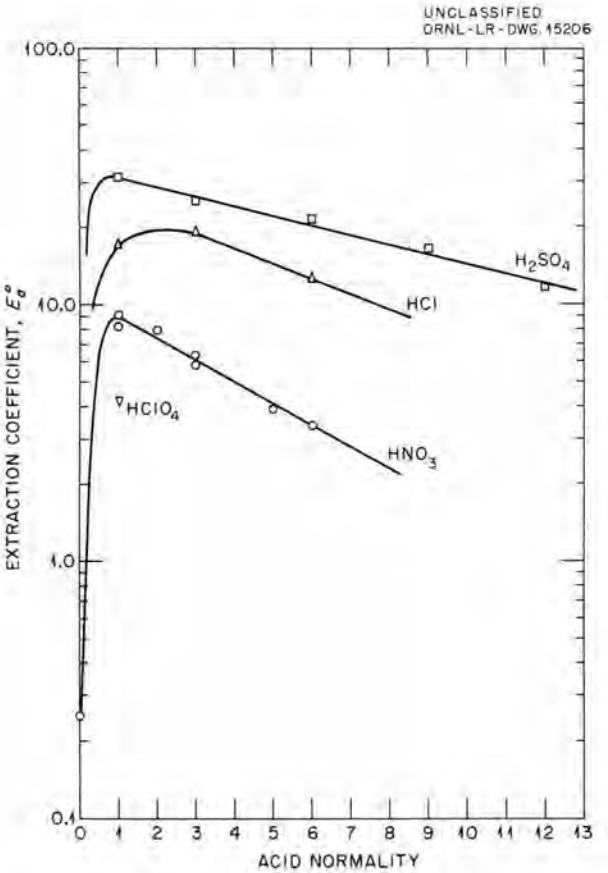

Fig. 4. Variation of Extraction of Tc(VII) by Cyclohexanol with Acid Concentration.

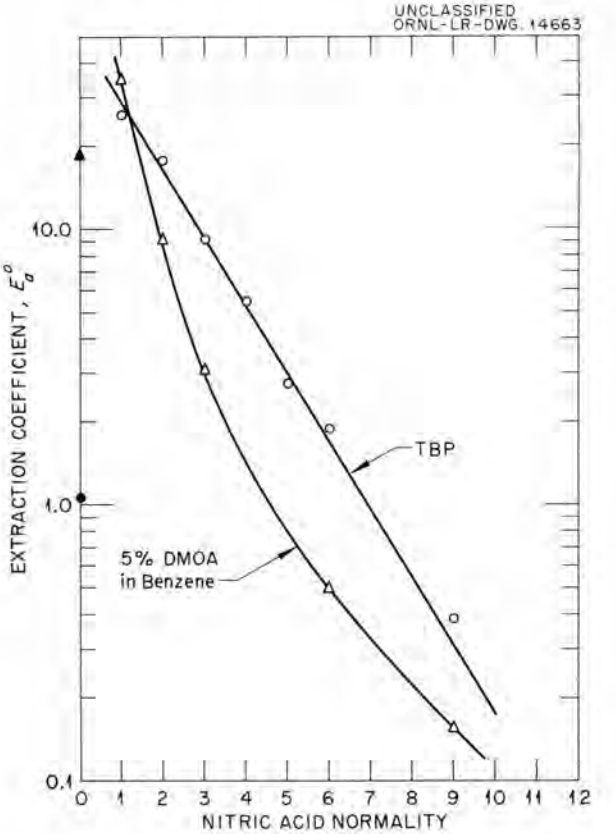

Fig. 5. Variation of Extraction of Tc(VII) with Nitric Acid Concentration.

TABLE 6. EXTRACTION OF Tc(VII) FROM AQUEOUS SOLUTIONS BY TRIOCTYL AMINE (TOA) DISSOLVED IN VARIOUS ORGANIC SOLVENTS (5% TOA by Volume)

Diluent	E_a^0	
	1 *N* H_2SO_4	1 *N* NaOH*
Xylene	110.6	0.027
Benzene	63.5	0.66
Trichloroethylene	52.2	0.69
Carbon tetrachloride	37.5	0.085
Chloroform	30.6	0.169

*DMOA was used.

as pertechnetate were added to nitric acid solutions together with Tc^{96} + Tc^{95m} tracer to give a series of seven mixtures wherein the pertechnetate ion concentration varied from $<10^{-10}$ to 2×10^{-3} mole/liter. Throughout this concentration range the extraction coefficient found with all three extractants was constant and independent of the Tc(VII) concentration present in the aqueous phase within an experimental error of ±2%.

An attempt was made to determine the nature of the technetium species extracted from acid aqueous solutions by measuring the variation of the extraction into cyclohexanol from solutions of varying HNO_3 concentration maintained at constant ionic strength of 1 *M* by the addition of sodium nitrate (Fig. 6). For H^+ ion concentrations less than 0.01 *M*, E_a^0 was independent of the acidity, suggesting that the extracting species may be $NaTcO_4$. At higher concentrations a

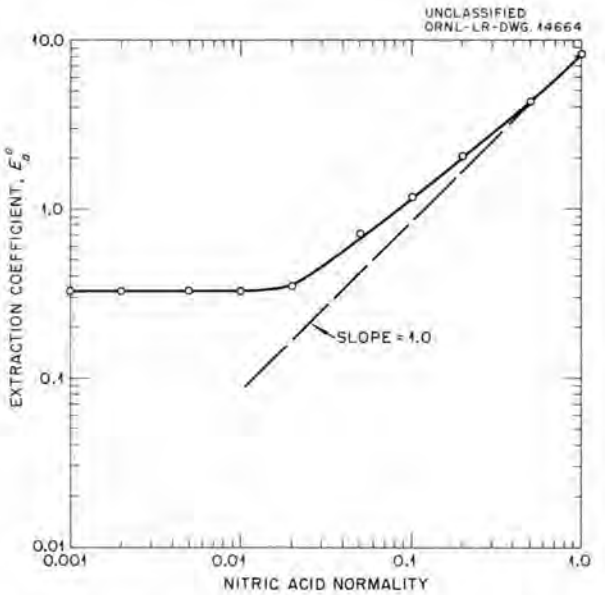

Fig. 6. Variation of Extraction of Tc(VII) into Cyclohexanol with HNO_3 Concentration in HNO_3 + $NaNO_3$ Mixtures at 1 *M*.

limiting slope of unity appeared to be approached, indicating that the acid, $HTcO_4$, was the predominant partitioning technetium species.

Finally, extractions into nitromethane were conducted with tracer technetium present in neutral, 1 *M* solutions of CsCl, RbCl, KCl, NaCl, LiCl, and HCl to determine the role of cation size. Values of E_a^0 were found to increase uniformly with the increasing ionic (e.g., crystal) radius of the cation, as shown below:

Salt	E_a^0
LiCl	0.55
NaCl	1.20
HCl	1.56
KCl	2.14
RbCl	2.45
CsCl	3.66

RADIATION CHEMISTRY

EFFECT OF IONIZING RADIATION ON HETEROGENEOUS CATALYSTS

H. W. Kohn E. H. Taylor

Among the effects of ionizing radiation is an alteration of the catalytic properties of certain solids. The present work concerns the effect of gamma radiation on catalysts for the H_2-D_2 exchange reaction carried out at −78°C to increase the probability of trapping electrons and positive holes.

The previously reported[1] enhancement of the activity of ZnO continues to be observed, but rather erratically. Much more convincing observations have been made on gamma alumina. One sample showed a ninefold increase in activity when irradiated for about 1 hr with Co^{60} gamma rays at about 5000 r/min. The enhanced activity declined slowly at room temperature and perhaps even at −78°C. Reirradiation produced another increase in activity which could again be partially annealed out. Irradiation periods as short as 10 min produced measurable increases in activity. Similar behavior was shown by a separate sample of different initial activity. The reproducibility of the measurements is not yet satisfactory, but the continued observation of enhancement upon irradiation and of decline upon annealing seems to establish the reality of the effect.

AMORPHOUS ICE

J. A. Ghormley

Thermal Behavior

Burton and Oliver[2,3] showed that, by means of x-ray diffraction, amorphous ice is obtained when water vapor is condensed on a surface at low temperature. Pryde and Jones[4] studied the thermal properties of ice prepared by condensation of water vapor on a surface at liquid-air temperature and found that, as the material was warmed, crystallization started at −129°C and evolved heat to the extent of 2 to 7 cal/g. The simple warming experiments described here resulted in a higher and more reproducible value for the heat of crystallization and also indicated that there was heat evolution at lower temperatures.

The apparatus was constructed from two test tubes (12 and 20 mm in diameter) sealed together concentrically, with the tip of the inner tube having been pulled down to a thin-walled capillary. About 1 ml of water was placed in the volume between the two tubes, and air was removed by being pumped through a 50-cm length of 1-mm capillary tubing for about 5 min before the tube was sealed off. Ice on the inner surface of the outer tube was held at a temperature between −40 and −78°C while the vapor was condensed on the inner capillary cooled with liquid nitrogen to −196°C. A thermocouple junction (No. 40 copper, No. 30 constantan) inserted into the capillary served to indicate the temperature of the condensed material. Warming curves were started by pouring the liquid nitrogen out of the inner tube, and they could be terminated at any point by replacing the liquid nitrogen.

A typical series of warming curves for one sample is shown in Fig. 7; the curves were recorded by means of a Brown 10-mv recorder. The sample was prepared by means of an 8-min sublimation, with the outer tube held at −50°C. During

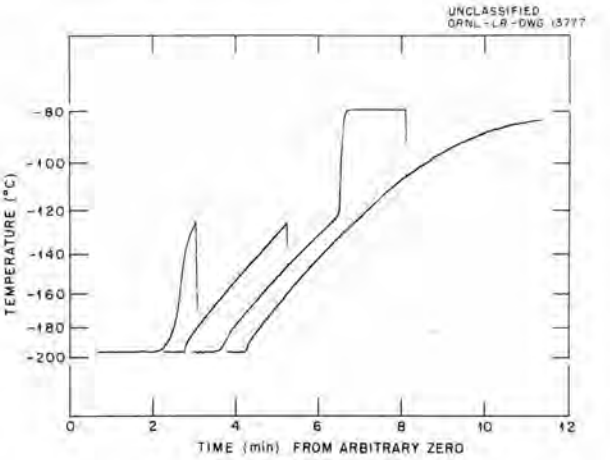

Fig. 7. Photograph of Successively Recorded Warming Curves for a Sample of Ice Condensed from Water Vapor onto a Surface at −196°C.

[1] H. W. Kohn and E. H. Taylor, *Chem. Semiann. Prog. Rep. Dec. 20, 1955*, ORNL-2046, p 66.

[2] E. F. Burton and W. F. Oliver, *Nature* **135**, 505 (1935).

[3] E. F. Burton and W. F. Oliver, *Proc. Roy. Soc. (London)* **A153**, 166 (1936).

[4] J. A. Pryde and G. C. Jones, *Nature* **170**, 685 (1952).

the warming of the material on the inner tube, the outer tube was held at −78°C.

When a sample was warmed the first time to just below the crystallization temperature, the rate of warming was much greater than when the same sample was cooled and allowed to warm again (see Fig. 7). The second warming curve could be obtained repeatedly each time that the sample was cooled before reaching −125°C, as shown by the second and third curves of Fig. 7, and was, within experimental error, identical with that for the same sample after crystallization occurred. If the heat capacity of the materials during the first warming is assumed to be the same as that of crystalline ice,[5] then the amount of heat released may be calculated from the relative slopes of the warming curves. Freshly prepared samples showed a heat evolution of 11 cal/g in the temperature range −185 to −125°C. This heat evolution is probably due to reorientation of water molecules to more stable configurations in the amorphous solid, perhaps with an increase in the number of hydrogen bonds. A sample stored for three days at −196°C showed no heat evolution below −170°C, but the warming curve above this temperature was nearly the same as that for a fresh sample and indicated that 6 cal/g had evolved between −170 and −125°C. The change in only the low-temperature part of the warming curve following annealing at −196°C indicates the occurrence of processes having more than one activation energy.

The rapid temperature rise accompanying crystallization always started at a temperature close to −120°C (slightly higher with faster warming rates) and terminated at a temperature which varied with the ratio of the heat capacity of the condensate to that of the entire system. Under conditions where the heat capacity of the glass and thermocouple wires was negligibly small, the temperature rose from −120 ± 1°C to −75 ± 1°C. When data obtained from a series of warming experiments after sublimation times between 5 min and 3 hr with the outer tube held at −78°C were extrapolated to infinite sublimation time, the same temperature rise of 45°C was indicated. Since the adiabatic crystallization of ice starting at −120°C results in crystalline ice at −75°C, the heat evolved in the transition from amorphous ice at −120°C to crystalline ice at the same temperature would be equivalent to the heat required to raise the temperature of crystalline ice from −120 to −75°C, or 15.8 cal/g.

No indication of a glass transition below −120°C was seen in any of the warming curves. The difference between the 15.8-cal/g heat of crystallization of amorphous ice and the 79.7-cal/g heat of fusion of ice at 0°C must represent the difference between the integral of the heat capacity of "supercooled water" above the temperature of the glass transition and that of crystalline ice in the same temperature range.

Several miscellaneous observations were made in connection with the warming experiments. During warming, the temperature of the ice was highest at the lower tip of the capillary. When the thermocouple junction was raised to a cooler part of the capillary, the sudden temperature rise appeared to start more sharply and at a lower temperature. The temperature rise accompanying crystallization at the warmest part of the capillary obviously triggered crystallization elsewhere in the solid. Samples condensed on a surface of crystalline ice exhibited the same thermal behavior as samples condensed on glass. No change in appearance of the ice was observed at any time during the warming experiments. The condensate remained white and opaque at all temperatures from −196 to 0°C.

Effect of Gamma Rays

Two samples of amorphous ice and another sample prepared in the same manner but allowed to crystallize were irradiated for three days (3.3×10^{21} ev/g) with Co^{60} gamma rays while immersed in liquid nitrogen. The paramagnetic resonance absorption of the irradiated samples was measured by Livingston and Zeldes. The amorphous ice showed strong absorption in a band identical with that observed previously for the condensed product of dissociated water vapor.[6] The absorption by the irradiated crystalline ice was weaker and appeared to be different from that observed in polycrystalline ice prepared by freezing water.[7] No absorption attributable to hydrogen atoms was observed in either crystalline or amorphous ice. The color of the crystalline sample

[5] W. F. Giauque and J. W. Stout, *J. Am. Chem. Soc.* **58**, 1144 (1936).

[6] R. Livingston, J. Ghormley, and H. Zeldes, *J. Chem. Phys.* **24**, 483 (1956).

[7] H. Zeldes and R. Livingston, *Chem. Semiann. Prog. Rep. Dec. 20, 1955*, ORNL-2046, p 49, esp 50.

after irradiation was pale yellow, while that of the amorphous samples was greenish yellow immediately after irradiation and pale blue after the sample was warmed to an undetermined temperature at which the paramagnetic absorption disappeared. Hydrogen peroxide concentrations observed after melting were 0.050 and 0.055 *M* for the amorphous ice and 0.020 *M* for the crystalline sample. In further work it is planned to eliminate the possible effect of ozone produced in the liquid nitrogen.

ELECTRONS IN SOLUTION

C. J. Hochanadel

The existence of a stable bound state of the electron in H_2O, CH_3OH, and C_2H_5OH has recently been reported by Jortner and Stein.[8] The evidence for the stable electron in water was based partially on an absorption peak at about 0.915 μ for a solution of potassium dissolved in water at a temperature near 0°C. The absorption disappeared thermally (with the evolution of H_2) or by admitting O_2. A bluish solution was obtained on dissolving potassium in either CH_3OH or C_2H_5OH at −40°C. The color decayed by the following processes: thermally (with evolution of H_2), by admitting O_2, or by adding H_2O (with evolution of H_2).

An attempt was made to corroborate these extremely interesting observations. Figure 8 shows the near-infrared absorption by liquid water and by 0.1 *N* KOH solution, measured on a Gary, model 14 recording spectrophotometer. Figure 9 shows the effect of temperature on the absorption at 0.975 μ, indicating a weaker absorption at lower temperature. Figure 9 also shows the absorption by a solution of potassium dissolved in water at about 0°C. The solution was prepared according to the following procedure:

1. About 100 ml of specially purified water was thoroughly degassed by alternate freezing, pumping, and melting. The bulb of water was then isolated from the rest of the system by closing the stopcock.
2. Potassium was distilled from bulb to bulb three times, and finally distilled into a 10-cm silica optical cell. The "mirror" contained about 100 mg of potassium.
3. After the silica cell was cooled to −10°C and the water to 0°C, the water (~35 ml) was poured into the silica cell by rotating the bulb on a standard-taper joint.

[8] J. Jortner and G. Stein, *Nature* 175, 893 (1955).

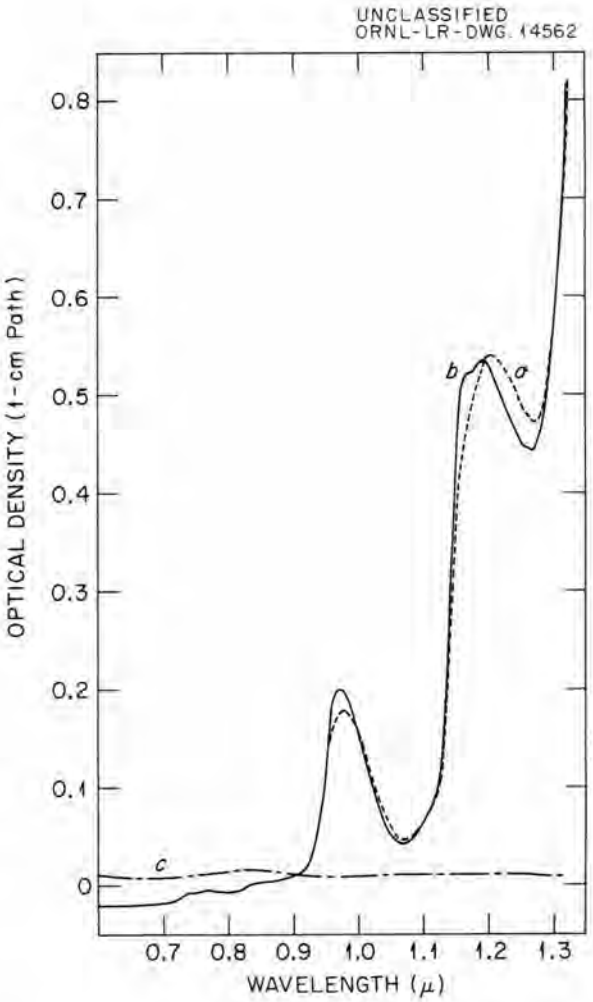

Fig. 8. The Absorption by Liquid Water in the Near Infrared. (*a*) Pure water near 0°C; (*b*) pure water or 0.1 *M* KOH at 25°C; (*c*) empty cell.

The potassium reacted instantly and hydrogen was evolved. There was no visible color produced. The absorption spectrum of the cold solution (curve *c*, Fig. 9), measured within 10 min, was the same as that of cold water. Assuming a molar extinction coefficient, ϵ, of 10^4, the bound electrons could have been detected at a concentration of about 10^{-5} *M* in the presence of the weak absorption ($\epsilon \cong 0.004$) by water at 0.975 μ. The lifetime of the "bound" electrons is apparently much too short to allow spectrophotometric detection within minutes after their formation. The weak absorption peak observed by Jortner and Stein may have been the absorption by water

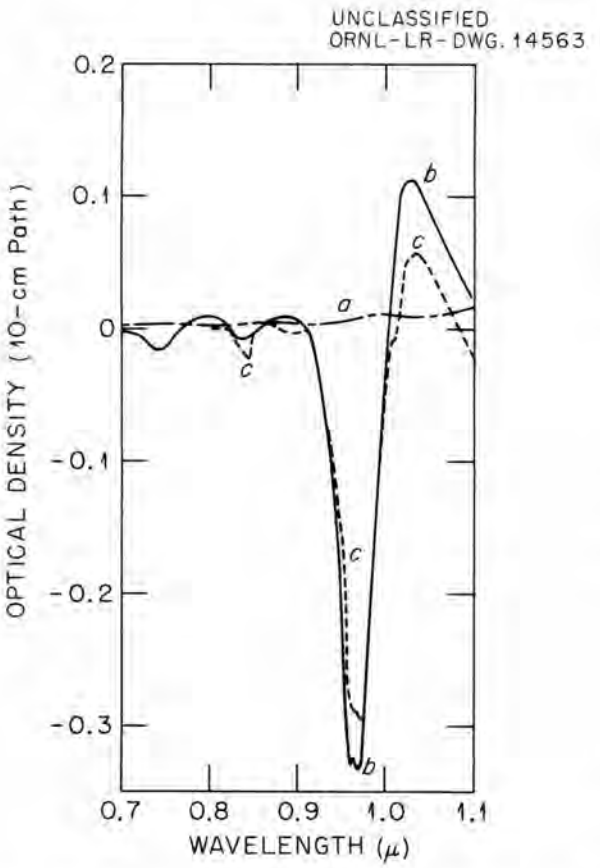

Fig. 9. Comparison of the Optical Absorption of a Solution Prepared by Dissolving Cold Potassium in Water Near 0°C with That of Cold Water Alone. All measurements referred to water at 25°C. (*a*) Pure water or 0.1 *M* KOH at 25°C; (*b*) pure water near 0°C; (*c*) potassium solution near 0°C.

or the effect of temperature on the absorption by water, depending on how the measurement was made.

A solution of potassium in anhydrous methanol was also prepared. A potassium mirror was distilled into the 10-cm silica cell as described above. The cell was then cooled to −80°C, and pure, degassed, anhydrous methanol was vacuum-distilled from Drierite into the cell. The potassium reacted relatively slowly with the liquid, and H_2 was evolved. Both the surface of the wet metal above the liquid level and that immersed under the liquid were bright blue in color, indicating absorption by bound electrons. The bulk liquid itself was colorless, indicating a short lifetime for the bound electrons. The experiment will be repeated at lower temperatures, and optical measurements will be made as soon as the necessary optical equipment is obtained.

A piece of potassium reacting with anhydrous methanol at −80°C, in a test tube purged with helium to eliminate H_2O and O_2, also appeared blue at the surface of the metal. At temperatures above approximately −40°C, the reaction was so rapid that the metal surface showed the usual silver appearance.

RADIATION STUDIES ON NITRATE SOLUTIONS

J. W. Boyle H. A. Mahlman

Two type 347 stainless steel, platinum-lined autoclaves containing 7 *m* $Th(NO_3)_4 \cdot 2HNO_3$ were irradiated in hole 11 of the ORNL Graphite Reactor. The pressure-temperature relations during the runs showed that there was little back-reaction involving N_2 in the temperature range 140 to 240°C.[9] A leak which occurred only at high temperatures prevented investigation of the N_2 back-reaction at 300°C.

The back-reaction at 300°C is now being investigated in an autoclave which was designed for high-temperature studies (see following section for discussion). The indications are that little, if any, back-reaction involving N_2 occurs at 300°C and below.

The material being irradiated in the 300°C experiment is a solution of mixed salts consisting of 7 *m* $Th(NO_3)_4$, 7 *m* $Be(NO_3)_2$, and 0.05 *m* $UO_2(NO_3)_2$. The only water present is the water of crystallization of the salts themselves. The $Be(NO_3)_2$ has a definite advantage over nitric acid as an additive to $Th(NO_3)_4$ breeder-blanket solutions in that it lowers the vapor pressure of the solution below that of pure water, whereas HNO_3 increases the vapor pressure considerably above that of pure water. For example, the vapor pressure at 300°C for pure water is 1246 psi; the vapor pressure for 7 *m* $Th(NO_3)_4 \cdot 2HNO_3$ is approximately 2000 psi; and the vapor pressure for 7 *m* $Th(NO_3)_4 \cdot Be(NO_3)_2$ is approximately 1050 psi. Also, $Be(NO_3)_2$ will prevent hydrolytic precipitation of ThO_2 at temperatures up to at least 300°C in concentrated solutions.

Nitrates of other cations such as lithium, sodium, and calcium have been considered. All have a neutron capture cross section which is higher than that of beryllium, 0.01 barn. Solution of the

[9] J. W. Boyle and H. A. Mahlman, *HRP Quar. Prog. Rep. April 30, 1956*, ORNL-2096, p 136.

$Th(NO_3)_4$-$Be(NO_3)_2$ mixture is effected at a temperature lower – well below 100°C – than that for the other salt mixtures. The ratio of $Th(NO_3)_4$ to $Be(NO_3)_2$ has not been optimized for breeder blanket use. The addition of a nitrate salt, preferably $Be(NO_3)_2$, instead of free HNO_3 is worthy of a thorough investigation because of the pronounced vapor-pressure lowering.

The forward reaction (production of N_2) appears to be the same in the thorium nitrate–beryllium nitrate system as in the thorium nitrate–nitric acid system for comparable nitrate concentrations. It was previously found that the forward reaction was temperature independent from room temperature to 250°C. This temperature independence has now been established up to 300°C. The yield of nitrogen appears to depend only on the concentration of nitrate and on the type of radiation.[10]

AN ALL-PLATINUM SYSTEM FOR HIGH-TEMPERATURE, HIGH-PRESSURE STUDIES

H. H. Stone J. W. Boyle

The use of platinum-lined stainless steel autoclaves has been routine practice at ORNL for several years. Stainless steel capillary tubing has been satisfactorily connected to the platinum lining by using a gland nut to press a 59-deg stainless steel swage welded on the tubing into a 60-deg cone seat in the platinum. The small amount of stainless steel exposed at the swage and connecting tubing has not been a serious handicap.

In the study of properties of homogeneous-reactor solutions at elevated temperatures and also in the study of the radiation chemistry of thorium nitrate solutions, an all-platinum system has become highly desirable. Replacement of the stainless steel capillary and swage with platinum capillary and swage appeared to be the obvious thing to do, but it was found that leaks always occurred when such an assembly was heated between 250 to 300°C. When the temperature was lowered below 250°C, the leak disappeared.

The leaks were apparently due to the difference in the thermal expansion of the platinum swage and the stainless steel autoclave shell and gland nut. Platinum has a linear coefficient of thermal expansion of 9×10^{-6}/°C. Type 347 stainless steel has a coefficient of about 18.5×10^{-6}/°C.

It appeared necessary to find a metal or an alloy with a high coefficient of expansion such that a washer of the material would compensate for the low coefficient of expansion of the platinum swage. Most metals having high coefficients have low melting points or were found to show creep at high temperatures. One alloy consisting of 70% copper and 30% tin looked promising because of its high melting point (870°C) and its hardness. Le Chatelier prepared this alloy in 1889 and reported[11] its coefficient of expansion to be 29.5×10^{-6}. A washer of this alloy, of the calculated thickness, was installed in the platinum autoclave. On retesting, it was found that the autoclave held pressure as the temperature was repeatedly cycled between room temperature and 300°C.

When platinum fittings are pressed together and heated, they often weld so that it is impossible to get them apart without destroying them. To be able to re-use platinum-lined autoclaves with platinum fittings, it is necessary to prevent the two platinum surfaces from welding together. When the platinum surfaces were coated with a very thin layer of silicone stopcock grease before sealing, welding did not take place. No difficulty has been encountered in some dozen runs treated in such a manner.

RADIATION-INDUCED DECOMPOSITION OF CONCENTRATED SOLUTIONS OF THE ALKALI-METAL NITRATES

H. A. Mahlman

The reduction of nitrate to nitrite by various radiations has been reported for almost 50 years. The energy sources used have been the sun, quartz-mercury lamps, x and gamma rays, neutrons, and fission fragments. No attempt has been made to determine the effect of the cation upon the rate of nitrite formation from irradiated aqueous nitrate solutions. The alkali-metal nitrates were investigated because they have a single stable valence, high solubility, and a considerable range of atomic size and atomic weight.

[10] J. W. Boyle and H. A. Mahlman, *Chem. Semiann. Prog. Rep. Dec. 20, 1954*, ORNL-1832, p 69.

[11] C. D. Hodgman (Editor-in-Chief), *Handbook of Chemistry and Physics*, 30th ed., p 1746, Chemical Rubber Publishing Co., Cleveland, 1947.

It has been reported[12] that, when 0.4 *M* sulfuric acid solutions of sodium nitrate containing Ce(IV) ions are exposed to Co^{60} gamma radiation, an enhanced Ce(III) yield is observed. This enhanced yield, dependent upon the nitrate concentration, may be interpreted as evidence for the direct formation of nitrite from nitrate. This may occur by the action of subexcitation electrons or by the transfer of energy from excited water molecules or excited cations.

It was anticipated that, if concentrated aqueous nitrate solutions of a series of cations were subjected to Co^{60} irradiation, significant differences in the nitrite formation rates might be observed. If differences in nitrite formation rates occurred, a correlation with the properties of the cation and/or nitrate salt might be possible. Therefore, 0.4 *M* sulfuric acid solutions containing the desired alkali-metal nitrate and Ce(IV) ions were irradiated with Co^{60} gamma rays. The concentration range of the nitrate was 0.1 *M* to saturation, while the Ce(IV) concentration was about 200 μmoles/liter.

The Ce(IV) ions are reduced rapidly in acid solution by nitrite, hydrogen peroxide, and hydrogen radicals, while the hydroxyl radical oxidizes Ce(III). The use of Ce(IV) ions eliminated the aqueous radical reactions with nitrite and provided a reliable spectrophotometric analytical method for determining the total radiation-induced reducing entities formed. The *G* values (molecules formed per 100 ev of absorbed energy) were based on the total energy absorbed by the solvent and solute. The nitrite yield was taken to be one-half the difference between the observed *G* values for Ce(III) (in 0.4 *M* sulfuric acid) with and without the nitrates present. The data are tabulated in Table 7 and graphically presented in Fig. 10. The semilog plot presents the data adequately and in an easily comparable manner.

It was concluded that the cation exerts an undetectable influence upon the rate of nitrite formation from the alkali-metal nitrates and ammonium nitrate. The nitrite yield by least-squares analysis is given by

$$G_{NO_2^-} = 1.23 \log [NO_3^-] + 1.72$$

for nitrate concentrations between 0.1 and 3.0 *M*.

RADIATION-INDUCED CHEMICAL REACTIONS

T. J. Sworski

Ceric Ion–Formic Acid

The addition of formic acid to sulfuric acid solutions of ceric ion increases[13] the value of

[12] T. J. Sworski, *J. Am. Chem. Soc.* 77, 4689 (1955).

[13] H. E. Spencer and G. K. Rollefson, *J. Am. Chem. Soc.* 77, 1938 (1955).

TABLE 7. NITRATE FORMATION, $G_{NO_2^-}$, FOR Co^{60}-IRRADIATED 0.4 *M* SULFURIC ACID–NITRATE SOLUTIONS CONTAINING Ce(IV)

Molarity	$G_{NO_2^-}$					
	NH_4NO_3	$LiNO_3$	$NaNO_3$	KNO_3	$RbNO_3$	$CsNO_3$
0.10	0.55	0.53	0.50		0.49	0.52
0.14				0.68		
0.20	0.83	0.82	0.87	0.87		
0.30	1.03	1.06	1.03		0.92	1.15
0.34				1.13		
0.50	1.38	1.35	1.39	1.32	1.33	1.38
1.00	1.71	1.78	1.67	1.75		1.73
1.36				1.94		
3.00		2.12				

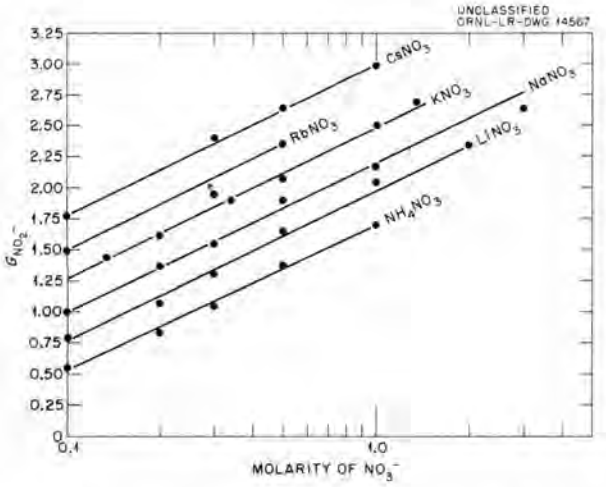

Fig. 10. Nitrite Formation from Nitrate Salts. Each salt successively displaced 0.25 unit from the NH_4NO_3 base line.

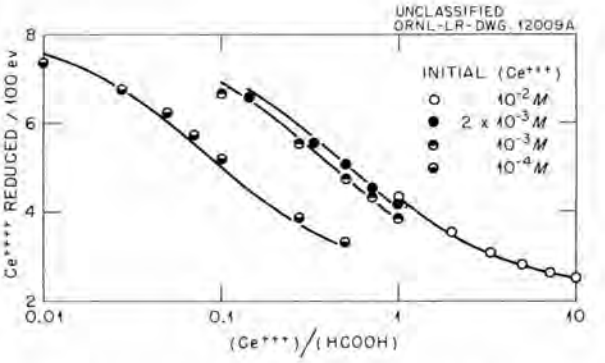

Fig. 11. Reduction of Ceric Ion as a Function of Varying Initial (Ce^{+++})/(HCOOH) Ratio in Air-saturated 0.4 *M* Sulfuric Acid Induced by Cobalt Gamma Radiation.

$G(Ce^{+++})$ from $2G_{H_2O_2} + G_H - G_{OH}$ to a maximum value of $2G_{H_2O_2} + G_H + G_{OH}$. Figure 11 summarizes the data obtained in a kinetic study of the radiolysis of ceric ion–cerous ion–formic acid mixtures in 0.4 *M* sulfuric acid by cobalt gamma radiation. At any constant cerous ion concentration, $G(Ce^{+++})$ increases with decreasing $[Ce^{+++}]/[HCOOH]$ ratio. At any particular $[Ce^{+++}]/[HCOOH]$ ratio, $G(Ce^{+++})$ decreases with decreasing concentration of cerous ion–formic acid mixture.

These data are quantitatively interpreted[14] by the assumption that three solutes compete with each other for reaction with OH radical:

$$Ce^{+++} + OH \longrightarrow Ce^{4+} + OH^-$$
$$HCOOH + OH \longrightarrow HCOO + H_2O$$
$$H_2SO_4 + OH \longrightarrow HSO_4 + H_2O$$

Whether it is H_2SO_4, HSO_4^-, or SO_4^{--} which reacts with OH radical has not been determined, but it will be assumed for kinetic treatment to be H_2SO_4 in 0.4 *M* concentration. In these mixtures, ceric ion is reduced by H, HO_2, HCOO, and H_2O_2, while cerous ion is oxidized by OH and HSO_4. The lines in Fig. 11 are theoretical and are given by the following equation:

$$G(Ce^{+++}) = 2G_{H_2O_2} + G_H - G_{OH} + \frac{2G_{OH}}{1 + \dfrac{k_1[Ce^{+++}] + k_3[H_2SO_4]}{k_2[HCOOH]}}$$

The equation fairly well represents the data with values for k_1/k_2 of 1.70, k_2/k_3 of 380, and k_1/k_3 of 650. Thus, kinetic evidence is presented for an influence of sulfuric acid on reactions of OH radical in 0.4 *M* sulfuric acid.

$K_2Cr_2O_7$–Thallous Ion

Cobalt gamma radiation induces reduction of $K_2Cr_2O_7$ dissolved in 0.4 *M* sulfuric acid solutions with $G(Cr^{+++})$ equal to 0.78 or

$$\frac{1}{3}\left(2G_{H_2O_2} + G_H - G_{OH}\right) \quad .$$

Thallous ion increases[15] $G(Cr^{+++})$ according to the following sequence of reactions:

$$Tl^+ + OH \longrightarrow Tl^{++} + OH^-$$
$$Cr(VI) + Tl^{++} \longrightarrow Cr(V) + Tl^{+++}$$

[14] T. J. Sworski, *J. Am. Chem. Soc.* **78**, 1768 (1956).

[15] T. J. Sworski, *Chem. Semiann. Prog. Rep. Dec. 20, 1955*, ORNL-2046, p 67.

Chromic ion in concentrations up to 10^{-2} *M* has no measurable effect on $G(Cr^{+++})$ either in the presence or absence of thallous ion (10^{-4} to 10^{-3} *M*). The interpretation is that the OH radical does not oxidize chromic ion but must disappear by oxidation of the intermediate Cr(V) or Cr(IV) ions.

$K_2Cr_2O_7$–Halide Ion

In 0.4 *M* sulfuric acid solutions containing $K_2Cr_2O_7$ and NaBr, $G(Cr^{+++})$ increases[15] with increasing $K_2Cr_2O_7$ concentration at constant NaBr concentration, while $G(Cr^{+++})$ decreases[15] with increasing NaBr concentration at constant $K_2Cr_2O_7$ concentration. Similar effects of cobalt gamma radiation are observed in $K_2Cr_2O_7$-NaCl mixtures. A comparison of the effects of NaBr and NaCl on $G(Cr^{+++})$ is shown in Fig. 12.

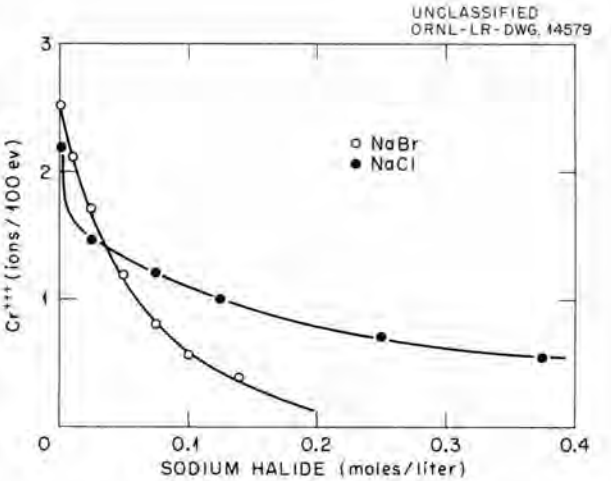

Fig. 12. Effect of Halide Concentration on Initial $G(Cr^{+++})$ at Constant $K_2Cr_2O_7$ Concentration (2.1×10^{-4} *M*).

EFFECT OF RADIATION UPON THE EXCHANGE OF HYDROGEN AND ETHANOL

J. G. Burr, Jr.

Hydrogen gas is one of the major products produced by the action of high-energy radiation upon organic molecules. Irradiation of organic substrates labeled with deuterium or tritium will produce hydrogen gas containing some of the isotopic label. Any subsequent radiation-induced exchange between the molecular hydrogen and the substrate will then redistribute the label in an unpredictable manner. This constitutes a potentially serious handicap to the use of such tracers for the study of organic radiation chemistry.[16]

The possibility of such a radiation-induced exchange between molecular hydrogen and ethanol has been examined briefly. The results of this examination are shown in Table 8. With partial pressures of hydrogen up to 1 atm and a gamma-ray dosage of about 10^{23} ev (4 kcal) per mole of alcohol, the exchange of hydrogen atoms is less than 0.0002% of the hydrogen atoms available for exchange, that is, a yield for exchange of about 0.1 atom per 100 ev of energy absorbed in the heterogeneous system.

The very low rate of any hydrogen exchange which occurs under these conditions can be attributed principally to the physical nature of the system and to the facile reaction of ethanol with hydrogen atoms. The absorption of energy in the gas phase is insufficient to produce an appreciable amount of exchange in that phase, and the concentration of molecular hydrogen in the condensed phase is insufficient to allow the reaction of hydrogen atoms with molecular hydrogen (the reaction essential for over-all ethanol-hydrogen exchange) to compete with the reaction of ethanol with hydrogen atoms. If exchange occurs only in the gas phase, then the sensitivity of these measurements can put an upper limit to that exchange of 10 to 20 hydrogen atoms per 100 ev absorbed in the gas phase. This is sufficient to exclude the possibility of any exchange reaction occurring with a long chain in either gas or condensed phase.

[16] L. M. Dorfman, *J. Chem. Phys.* (in press).

TABLE 8. EXPERIMENTAL DATA ON HYDROGEN-ETHANOL EXCHANGE

Experiment No.	$E^{(a)}$ (ev)	$T^{(b)}$ (°C)	P_{H_2} (mm)	V (ethanol) (ml)	$A_0^{(c)}$ (μc)	$A^{(d)}$ (μc)
1	1.40×10^{20}	−78	117	0.95	5.24	5.23
2	6.38×10^{20}	35	119	0.96	5.33	5.30
3	6.19×10^{20}	35	119	0.96	5.07	5.02
4	0		119	0.96	5.31	5.37

(a) Energy absorbed by the ethanol from Co^{60} radiation. The energy absorbed in the gas phase is negligible.

(b) Temperature of the ampoule during the irradiation.

(c) Amount of tritium introduced into the ampoule.

(d) Amount of tritium found in the hydrogen after irradiation of the ampoules. The volume of hydrogen recovered was in agreement with that calculated from the value of G_{H_2} of 3.66 ± 0.26 measured in this laboratory for the production of hydrogen from ethanol by Co^{60} gamma radiation [cf. W. McDonell and A. S. Newton, *J. Am. Chem. Soc.* **76**, 4651 (1954); W. R. McDonell and S. Gordon, *J. Chem. Phys.* **23**, 208 (1955)]. The activity of the ethanol was found to be indistinguishable from background; complete equilibration of the tritium would have produced ethanol with a specific activity of 0.3 μc/mmole. A 1% loss of tritium from the gas phase (the upper limit set by the above data) would produce ethanol with a maximum specific activity of 0.003 μc/mmole; such an activity level would be indistinguishable from background unless extremely large samples were to be analyzed – a procedure for which the equipment is unsuited.

ORGANIC CHEMISTRY

HYDROGEN-DEUTERIUM ISOTOPE EFFECT IN THE ACID-CATALYZED REARRANGEMENT OF TRIPHENYLETHYLENE GLYCOL

C. J. Collins

The rearrangement of triphenylethylene glycol (I) has been reported previously.[1] By comparing the fates of the chain and ring labels in glycols I*a* and I*c* when these glycols were converted to II and III under the influence of several different acid catalysts, it was possible to calculate the contribution of each of four reaction paths under each set of conditions:

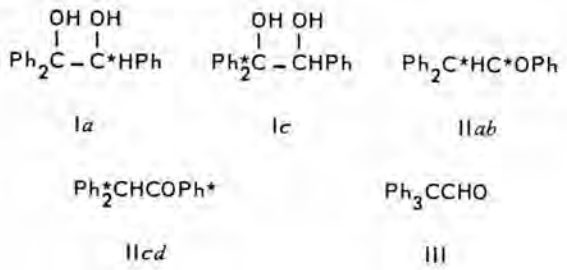

From these data it was possible to determine the relative phenyl/hydrogen migration abilities (k_ϕ/k_H). These studies have now been extended to include the deuterated compounds I*e* and I*g*:

By an experimental technique analogous to that used previously,[1] it was possible to obtain the relative phenyl/deuterium migration abilities (k_ϕ/k_D) under four of the five conditions employed for I*a* and I*c*. The hydrogen/deuterium isotope effect for each reaction was then calculated as follows:

$$\frac{k_H}{k_D} = \frac{k_\phi/k_D}{k_\phi/k_H} .$$

It should be noted that it was not necessary to perform any deuterium assays in the determination of these isotope effects. The ratio of the path occurring with deuterium migration to the paths occurring with phenyl migration was obtained solely by determining the fates of the C^{14} labels during the rearrangement of I*e* and I*g*. The data and results are summarized in Table 9. The hydrogen/deuterium (k_H/k_D) isotope effects are given in the last column. In these calculations the assumption has been made that the fraction of secondary hydroxyl removal from I*e* or I*g* is the same, under the influence of each acid catalyst, as that found[1] for the undeuterated glycol. This assumption is currently being checked with chain-labeled 1,1,2-triphenylethylene glycol-1-H[2]. It will be noted that all the k_H/k_D values lie between 2.5 and 3.4.

p-TOLYL/PHENYL MIGRATION RATIO IN THE REARRANGEMENT OF 1,2-DI-*p*-TOLYL-1-PHENYLETHYLENE GLYCOL

L. W. Kendrick, Jr.[2] C. J. Collins

The *p*-tolyl/phenyl migration ratio in the aldehyde-ketone rearrangement and the correlation of this rearrangement with the pinacol transformation have been discussed previously.[3] It was shown that, contrary to belief, the *p*-tolyl/phenyl migration ratio in these reactions was not inverted, and thus remained greater than 1. Because of the two products obtained in the rearrangement of 2,2-diphenyl-2-*p*-tolylacetaldehyde and related glycols (one was always present in much greater yield than the other), it was not possible to determine the value of the *p*-tolyl/phenyl migration ratio with any great accuracy. Therefore the study of 2,2-di-*p*-tolyl-2-phenylacetaldehyde (IV) and the related glycols V and VI was undertaken, with the hope that the situation would be more favorable

[1] C. J. Collins, *J. Am. Chem. Soc.* **77**, 5517 (1955).

[2] ORINS Fellow from the University of Florida.

[3] B. M. Benjamin and C. J. Collins, *J. Am. Chem. Soc.* 78 (to be issued).

for an accurate p-tolyl/phenyl determination:

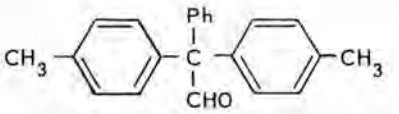

IV

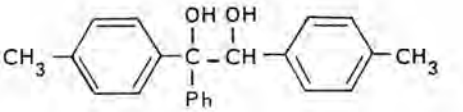

V

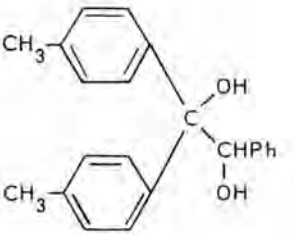

VI

TABLE 9. HYDROGEN-DEUTERIUM ISOTOPE EFFECT (k_H/k_D) IN THE REARRANGEMENT OF 1,1,2-TRIPHENYLETHYLENE GLYCOL-1-H^2

Reactant	Catalyst	Product (%)		C^{14} in $\phi_2^*C=O$ (%)	k_ϕ/k_D	k_ϕ/k_H	k_H/k_D
		II	III				
I	Concentrated H_2SO_4	100	0	67.5	20.6	7.33 [a]	2.82
I$_g$	Concentrated H_2SO_4	100	0	64.0	22.2	7.33 [a]	3.06
III[b]	Concentrated H_2SO_4	100	0	<2			
I$_g$	Boiling HCOOH	100	0	56.5	4.18	1.70 [c]	2.46
III[b]	Boiling HCOOH	100	0	6.9			
I$_e$	HCOOH, 27.6°C	14.5	79.7	100	5.5	1.66	3.3
I$_c$	HCOOH, 27.6°C	37.6	62.4	100		1.66	
I$_g$	31.5% H_2SO_4, boiling	77.4	22.6	29.2	1.35	0.435[a]	3.18
I$_g$	$(COOH)_2 \cdot 2H_2O$, reflux	76.8	23.2	49.8	3.64	1.08 [d]	3.37
I$_c$	$(COOH)_2 \cdot 2H_2O$, reflux	87.4	12.6	83.4		1.08 [d]	

[a]Calculated from data in ref 1.
[b]Labeled in the aldehyde carbon.
[c]Recalculated from ref 1 on the basis of 6.9% scrambling of the chain label of aldehyde III (see line 5 of table).
[d]Recheck of k_ϕ/k_H in which aldehyde yield and per cent phenyl scrambling were determined for same reaction.

Compounds V and VI were synthesized with C^{14} labels in the chain-1 positions. Compound V was synthesized also with a C^{14} label in the 2-tolyl group. Each isotope position isomer of V was subjected to rearrangement in cold, concentrated sulfuric acid, and the yields of the two ketonic products were determined by the isotopic dilution method, and the amount of chain-lable and tolyl-label scrambling was determined in each case by a suitable degradation of the two products. Compounds IV and VI have not yet been subjected to rearrangement conditions. In agreement with expectation, the two ketonic products were obtained in yields of about 55 and 45%, thus offering promise for an accurate calculation of the *p*-tolyl/phenyl migration ratio.[3] The per cent of chain scrambling in the two ketones produced from V was 8.1 and 5.1, respectively, the latter value being for the asymmetric ketone.

o-TOLYL/PHENYL MIGRATION RATIO IN THE REARRANGEMENT OF 1,2-DIPHENYL-1-*o*-TOLYLETHYLENE GLYCOL AND RELATED COMPOUNDS

V. F. Raaen C. J. Collins

Although much attention has been directed toward an understanding of the electrical effects which control the electron-donating or electron-withdrawing abilities of *para*-phenyl-substituted aryl groups,[4] very little is known of the factors which control the reactivities of *ortho*-phenyl-substituted aryl groups. The *p*-tolyl/phenyl migration ratio may vary from 1.1 to about 15 (ref 3), but there seems to be little doubt that this ratio will always be greater than 1. The *o*-tolyl/phenyl migration ratio has been determined as 0.82 in the dehydration[5] of 2-phenyl-2-*o*-tolylethanol-1-C^{14}. The *o*-tolyl/phenyl migration ratio in the acid-catalyzed rearrangement of 2,2-diphenyl-2-*o*-tolylacetaldehyde (VII) has now been determined. The two glycols, VIII and IX, have also been synthesized and subjected to rearrangement. It was shown that compounds VII, VIII, and IX were converted to the ketones X and XI *without scrambling* of the chain label:

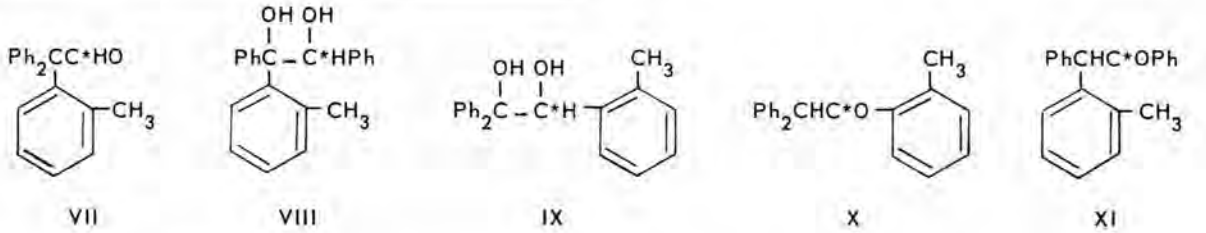

The yields of X and XI from each reactant are given in Table 10. The method employed was similar to that used previously[3] and relies upon the use of the following equation, derived with

[4] See, for example, L. P. Hammett, *Physical Organic Chemistry*, chap. VII, McGraw-Hill, New York, 1940; G. W. Wheland, *Advanced Organic Chemistry*, chaps. 1, 10, and 12, Wiley and Sons, New York, 1949.

[5] B. M. Benjamin and C. J. Collins, *J. Am. Chem. Soc.* 75, 402 (1953).

TABLE 10. *o*-TOLYL/PHENYL MIGRATION RATIO ($2k_T/k_P$) IN THE REARRANGEMENT OF ALDEHYDE VIII IN COLD, CONCENTRATED SULFURIC ACID

Reactant	Product (%)		Mole Ratio	Calculated		
	X	XI	X/XI	k_H/k_ϕ	k_{Tol}/k'_H	$2k_T/k_P$
VII	62.0	38.0	1.63			
VIII	50.0	50.0	1.00	0.241	4.18	3.28
IX	69.3	30.7	2.25			

the aid of the Area Theorem of J. Z. Hearon (see ref 3):

$$\frac{k_T}{k_P} = \frac{k_H}{k_\phi} \cdot \frac{k_{Tol}}{k'_H} \cdot \frac{m_e}{m_d} \cdot \left[\frac{1 + (k'_H/k_{Tol})}{1 + (k_H/k_\phi)} \right].$$

(The ratio m_e/m_d is the ratio, 1.63, of ketones X/XI obtained in cold, concentrated sulfuric acid from the aldehyde VIII.) Also given in Table 10 are the values for k_H/k_ϕ, k_{Tol}/k'_H, and $2k_T/k_P$ of the above equation. From Table 10 it can be seen that the *o*-tolyl/phenyl migration ratio ($2k_T/k_P$) is 3.28. That this ratio is greater than 1, as contrasted with the value[5] of 0.82 in the dehydration of 2-phenyl-2-*o*-tolylethanol-C^{14}, is very simply explained:

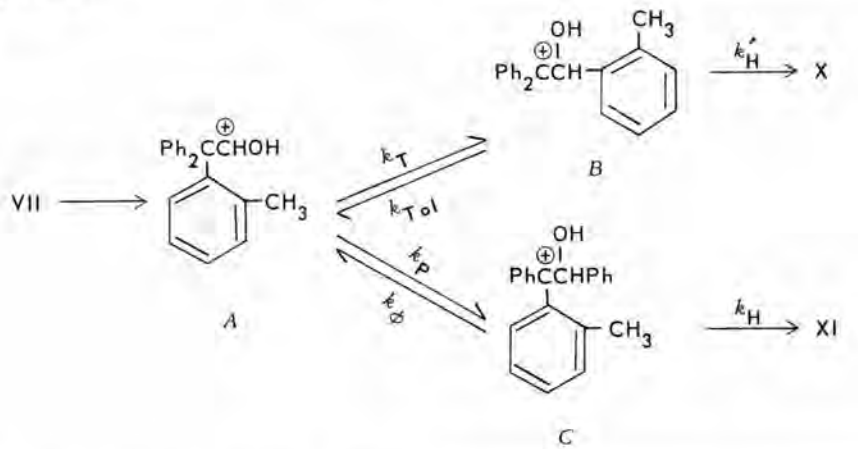

Carbonium ion *A*, upon conversion to ion *B*, does so with the maximum relief of strain, since ion *B* possesses an *o*-tolyl group unencumbered by proximity with other aryl groups. The situation with respect to ion *C*, however, leaves a phenyl and an *o*-tolyl group on the same carbon, in a condition of rather high strain. Further, the stability of ion *C* should be less than that of ion *B* through steric inhibition of resonance by the *o*-tolyl group.

The observation that the *o*-tolyl/phenyl migration ratio in ion *A* is approximately 3 is being checked for the deamination of 2,2-diphenyl-2-*o*-tolylethyl-1-C^{14} amine.

[6] B. M. Benjamin and C. J. Collins, *J. Am. Chem. Soc.* 78 (to be issued).

RELATIVE STABILIZING EFFECTS OF AN ANISYL GROUP AND TWO PHENYLS ON THE FORMATION OF CARBONIUM IONS

C. A. Krauth C. J. Collins

Benjamin and Collins[6] showed that, in weak acids, both glycols XII and XIII undergo rearrangement with a negligible proportion of secondary hydroxyl removal:

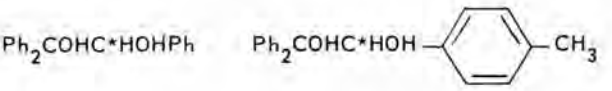

XII XIII

In cold, concentrated sulfuric acid, glycol XII likewise rearranges with essentially no secondary hydroxyl removal, but glycol XIII rearranges with 75% tertiary hydroxyl and 25% secondary hydroxyl removal. This observation is somewhat startling and is of extreme importance to carbonium ion theory.

In the hope that some correlation might be found between the acidity function[7] H_0 and the proportion of secondary hydroxyl removal when the secondary carbon contains a strongly electron-donating[4] group, glycols XIV and XV were synthesized and subjected

[7] L. P. Hammett, *Physical Organic Chemistry*, chap. VII, McGraw-Hill, New York, 1940.

to rearrangement under the influence of various acid catalysts:

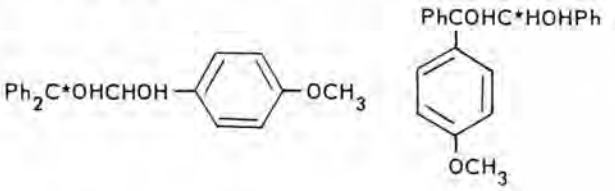

XIV XV

The yields of the ketones XVI and XVII,

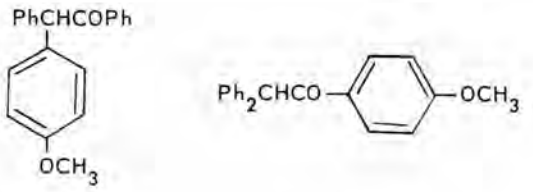

XVI XVII

were determined by the isotopic dilution technique, as were the percentages of scrambling of the chain labels. The results to date are summarized in Tables 11–13.

DISTRIBUTION OF P^{32}-LABELED ORGANO-PHOSPHORUS COMPOUNDS BETWEEN IMMISCIBLE SOLVENTS

W. H. Baldwin C. E. Higgins

Organo-phosphorus compounds that are labeled with P^{32} have proved to be useful analytical tools. Particularly, they have found ready application in the determination of the distribution of the organo-phosphorus compounds between immiscible solvents. The current Dapex process[8] employs a mixture of di-2-ethylhexyl hydrogen phosphate and tributyl phosphate in kerosene for the extraction of uranium from low-grade ores.

[8]Private communication, C. A. Blake.

TABLE 11. YIELDS OF KETONES XVI AND XVII UPON REARRANGEMENT OF 1,1-DIPHENYL-2-*p*-ANISYLETHYLENE-1-C^{14} GLYCOL (XIV)

Acid	Temperature	Yield of XVI (%)	Yield of XVII (%)	Total Yield (%)
HCOOH, 98 to 100%	Reflux	95.3	4.5	99.8
$HClO_4$, 0.82 *M*	Room	99.0	2.0	101.0
$HClO_4$, 0.82 *M*	50°C	102.3*	2.8	105.1*
$HClO_4$, 0.16 *M*	50°C	104.5*	2.5	107.0*
$HClO_4$, 0.005 *M*	50°C	82.0	1.4	83.4

*To be repeated using holdback carrier.

TABLE 12. YIELDS OF KETONES XVI AND XVII UPON REARRANGEMENT OF 1,2-DIPHENYL-1-*p*-ANISYLETHYLENE-2-C^{14} GLYCOL (XV)

Acid	Time (hr)	*p*-Methoxy Benzhydryl Phenyl Ketone Yield (%)	Benzhydryl *p*-Anisyl Ketone Yield (%)	Total Yield (%)
HCOOH	2	81.8	0	81.8
H_2SO_4, 50%	2	79.3	0	79.3
HCOOH	16	98.1	3.26	101.4
H_2SO_4, 50%	40	62.5	1.94	64.5

TABLE 13. PER CENT SECONDARY HYDROXYL REMOVAL UPON REARRANGEMENT OF 1,1-DIPHENYL-2-ANISYLETHYLENE-1-C^{14} GLYCOL (XIV)

Acid	Temperature	Secondary Hydroxyl Removal
HCOOH	Reflux	56.3
$HClO_4$, 0.82 *M*	Room	82.3
$HClO_4$, 0.82 *M*	50°C	93.5
$HClO_4$, 0.16 *M*	50°C	80.4

In studying the solvent losses from the Dapex mixture, tributyl phosphate-P^{32} was tested first. Tributyl phosphate-P^{32} was prepared by the ester exchange between $H_3P^{32}O_4$ and commercial tributyl phosphate.[9] The labeled tributyl phosphate was used to prepare two Dapex solvent solutions: A, containing 0.1 *m* di-2-ethylhexyl hydrogen phosphate, 2.5% tributyl phosphate-P^{32} in kerosene, and B, 0.3 *m* di-2-ethylhexyl hydrogen phosphate, 5% tributyl phosphate-P^{32} in kerosene.

The unlabeled di-2-ethylhexyl hydrogen phosphate, the kerosene, and the aqueous feed solutions were supplied by C. A. Blake. The aqueous feed solutions were typical process solutions representing materials available on the Colorado plateau and, in addition to uranium, contained vanadium, iron, aluminum, sulfate, phosphate, and nitrate.

The kerosene and aqueous phases were equilibrated by tumbling them end over end at 25°C for at least 15 min. The aqueous phase (heavier) was removed by the use of a transfer pipet (that had been drawn to a capillary) after centrifuging. The aqueous phase was centrifuged again; then an aliquot was removed and tumbled end over end with dibutyl ether. An aliquot (15 ml) of the dibutyl ether was counted as previously described.[10]

The kerosene solutions were equilibrated with 10% sodium carbonate until the P^{32} content of the washings was constant. The kerosene solution was then equilibrated with an aqueous feed solution. After separation, the kerosene solution was stripped with either 10% sodium carbonate or first with 1 *m* H_2SO_4 and then with 10% sodium carbonate solution. The cycle of extraction and then stripping was repeated until the P^{32} in the aqueous phases was constant.

Dapex solution A was equilibrated with several aqueous solutions, and the losses to the aqueous phases were found to be 10% Na_2CO_3, 10 mg/liter; 0.2 *m* SO_4^{--} (pH = 1), 43 mg/liter; 0.5 *m* SO_4^{--} (pH = 1), 21 mg/liter; 1 *m* H_2SO_4, 26 mg/liter. The 0.5 *m* SO_4^{--} (pH = 1) solution was chosen as representative of the aqueous feed solutions. The raffinates from the extraction of the feed solutions contained less than 25 mg of tributyl phosphate per liter. The carbonate strip solutions likewise contained no more tributyl phosphate than the 10% aqueous sodium carbonate.

Solution B behaved as expected. Since it contained twice as much tributyl phosphate, more tributyl phosphate was found in the aqueous phases. The 10% Na_2CO_3 solution contained 50% more, the aqueous feed contained 70% more, and the 1 *m* H_2SO_4 contained 100% more than with solution A. Highest losses were found in the 1 *m* H_2SO_4 strip solution from solvent solution B (50 mg/liter).

In conclusion, it can be stated that the losses of tributyl phosphate are sufficiently low to make its use economically feasible.

Preparation of Di-2-ethylhexyl Hydrogen Phosphate-P^{32}

Inasmuch as the second portion of this problem requires data concerning the distribution of di-2-ethylhexyl hydrogen phosphate from similar solutions, this compound has been prepared labeled with P^{32}.

Tri-2-ethylhexyl phosphate obtained from Carbide & Carbon Chemicals Company was exchanged with $H_3P^{32}O_4$ in a modification of the method used for labeling tributyl phosphate (ref 9). The main product from this reaction, tri-2-ethylhexyl phosphate-P^{32}, was de-alkylated by refluxing with excess ethanolamine for 2 hr. The liberated acid was purified by elution from Dowex 2. Distribution studies are continuing with this acid.

[9] W. H. Baldwin and C. E. Higgins, *Chem. Semiann. Prog. Rep. Dec. 20, 1953*, ORNL-1674, p 53.

[10] C. E. Higgins and W. H. Baldwin, *Anal. Chem.* **27**, 1780 (1955).

CHEMISTRY OF AQUEOUS SYSTEMS

RAPID SEPARATION BY ION EXCHANGE

Diffusion Coefficient of Pb(II) in a Strong-Base Anion Exchange Resin

F. Nelson E. C. Campbell[1]

In connection with measurements of the yield in the rapid anion exchange separation of Pb^{207m} ($T_{1/2}$ = 0.8 sec) from its parent, Bi^{207} ($T_{1/2}$ = 8 years), the diffusion coefficient of tracer Pb(II) in a quaternary amine resin (Dowex 1, 10% DVB) was measured by a shallow-bed elution technique similar to that used by Boyd, Adamson, and Myers.[2] The Pb(II) tracer (Pb^{210}, RaD, $T_{1/2}$ = 22 years) was first adsorbed on the resin from 0.5 *M* HCl. The average wet radius, *R*, determined from photomicrographs of the beads[3] in 0.5 *M* HCl, was 3.5×10^{-3} cm. A portion of the Pb^{210}-equilibrated resin was transferred to a small column, 0.12 cm^2 in area, to form a shallow bed about 1 mm in depth. The counting rate of the bed was measured as a function of time during rapid elution with 0.5 *M* HCl. Results of a typical experiment carried out at a solution flow rate of 4.4 cm/sec are shown in Fig. 13. The plot of log counting rate of the resin vs time is approximately linear after a (small) correction for Bi^{210} and room background. The average half-time for removal of Pb(II) from the resin in three separate experiments was 11.0 ± 0.3 sec and was independent of flow rate in the region investigated (0.5 to 6 cm/sec).

According to diffusion theory the concentration of the diffusing species in the resin decreases as $e^{-\lambda_r t}$, where $\lambda_r = D\pi^2/R^2$, *t* is time, and *D* is the diffusion coefficient, after initial transient effects associated with the decay of higher diffusion modes have died out. The average value of λ_r from the three experiments was 0.063 sec^{-1}, corresponding to a diffusion coefficient, *D*, of Pb(II) in the resin of 7.8×10^{-8} cm^2/sec at 25.0 ± 0.3°C.

[1] Physics Division.

[2] G. E. Boyd, A. W. Adamson, and L. S. Myers, *J. Am. Soc.* 69, 2836 (1947).

[3] Measurements made by the Microscopy Section of the Analytical Division.

This value of *D* of Pb(II) in the resin phase, together with diffusion theory and decay rate considerations, was used to calculate the theoretical yield for the separation of Pb^{207m} from Bi^{207} by rapid elution methods, and reasonable agreement was found between the experimental and theoretical values. Further details of the yield experiments and calculations were reported[4] previously.

In the earlier separations of Pb^{207m} from Bi^{207}, the yield was approximately 20%, which at first glance might be considered high for such short-lived activity with the small diffusion coefficient of $\sim 10^{-8}$. However, computations indicate that separations of daughter activities having half lives as short as milliseconds should be possible if diffusion coefficients and distribution coefficients are favorable (see Table 14).

[4] E. C. Campbell and F. Nelson, *Phys. Semiann. Prog. Rep. March 10, 1956*, ORNL-2076, p 37.

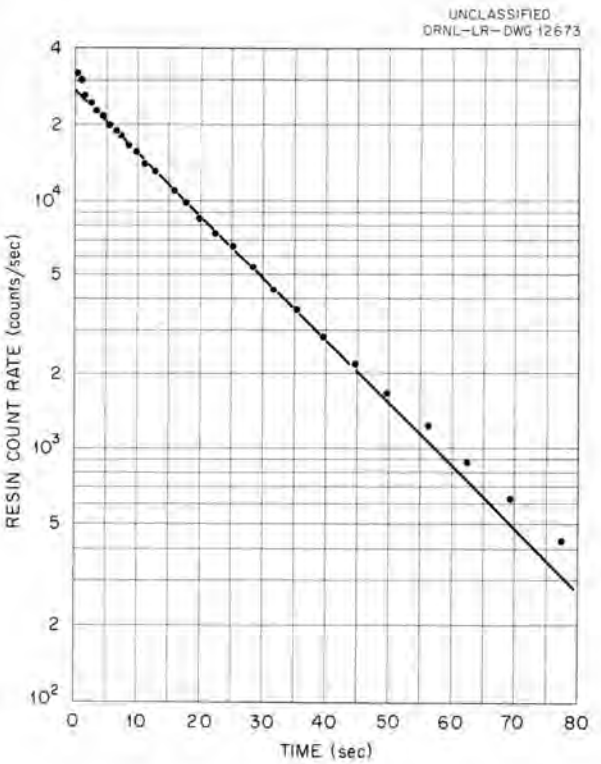

Fig. 13. Elution of Pb^{210} from Anion Exchange Resin. Flow rate, 4.4 cm/sec; 0.5 *M* HCl.

TABLE 14. SEPARATION OF A SHORT-LIVED DAUGHTER ACTIVITY FROM A LONG-LIVED PARENT

Radius $R = 10^{-3}$ cm

Half Life (sec)	Theoretical Yield D (cm^2/sec)			
	10^{-8}	10^{-7}	10^{-6}	10^{-5}
10^{-4}	0.004	0.01	0.04	0.10
10^{-3}	0.01	0.04	0.10	0.32
10^{-2}	0.04	0.10	0.32	0.70
10^{-1}	0.10	0.32	0.70	0.96
1	0.32	0.70	0.96	0.99

Rapid Separation of 2.6-min Ba^{137} from 37-year Cs^{137} with Zirconium Phosphate Used as a Cation Exchanger

H. O. Phillips F. Nelson K. A. Kraus

It has been shown[5] that zirconium phosphate has satisfactory cation exchange properties. In the quoted paper the separation of the alkali metals was discussed. However, many other elements can also be reproducibly adsorbed and eluted with this adsorbent. In particular, it was found that barium can be strongly adsorbed even from fairly concentrated electrolyte solutions at low acidities and can rapidly be eluted by acids. Since in acidic solutions cesium is strongly adsorbed, it appeared possible to separate the short-lived daughter Ba^{137} from the long-lived Cs^{137} by utilizing zirconium phosphate as an adsorbent and ~1 *M* HCl as an eluent.

In a typical experiment, $\sim 2 \times 10^3$ counts/sec of Cs^{137} was adsorbed on the top of a 0.25 cm^2 × 4 cm column of 80- to 170-mesh zirconium phosphate. The column was placed near a sodium iodide (Tl) crystal counter biased at 0.5 kev to count essentially only Ba^{137}, and 1 *M* HCl was passed through the column rapidly. The counter was shielded from the effluent with lead, and the decrease in the counting rate of the solid was determined. As shown in Fig. 14, more than 95% of the activity was removed in 10 sec from the column. After long aging (up to 640 hr) of the column containing the adsorbed cesium, the percentage removal of the barium activity decreased somewhat but was still more than 90% after 10 sec at a flow rate of 5 cm/sec. These results imply that diffusion of barium away from this exchanger is very rapid and that the diffusion coefficients are approximately those normally found in aqueous solutions. After the flow of HCl was stopped, the counting rate in all cases returned to approximately the original values, confirming that Cs^{137} was not removed.

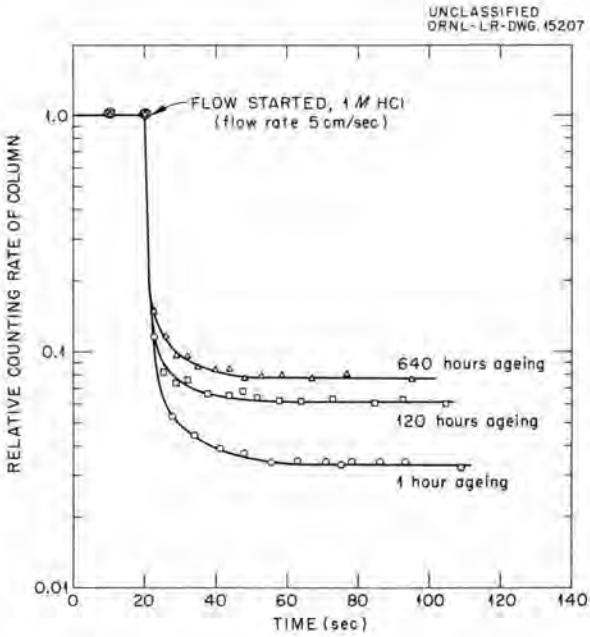

Fig. 14. Rapid Separation of 2.6-min Ba^{137} from Cs^{137} (37-year). Cs^{137} parent adsorbed on 1-ml column of 80- to 170-mesh zirconium phosphate; eluent, 1 *M* HCl.

ANION EXCHANGE STUDIES

Adsorption of Th(IV) from Sulfuric Acid and Ammonium Sulfate Solutions

F. Nelson K. A. Kraus

The anion exchange behavior of Th(IV) in sulfuric acid and ammonium sulfate solutions [adjusted to pH 3 to 4 to avoid hydrolysis of Th(IV)] was investigated with the same strong-base anion exchange resin used in all our earlier work of this

[5] K. A. Kraus and H. O. Phillips, *J. Am. Chem. Soc.* 78, 694 (1956).

type (Dowex 1, 10% DVB). The results are summarized in Fig. 15. At low concentration of both H_2SO_4 and $(NH_4)_2SO_4$ the distribution coefficients, D [(amount per kilogram of dry resin)/(amount per liter of solution)], of Th(IV) are in excess of 100. With increasing sulfate concentration the distribution coefficients decrease to ~1 in 0.6 M H_2SO_4 and ~4 in 4 M $(NH_4)_2SO_4$. Throughout the range investigated, adsorption from ammonium sulfate is considerably better than from sulfuric acid. The adsorption functions are similar to those reported[6] for U(VI); however, at comparable sulfate concentrations, Th(IV) is less strongly adsorbed than U(VI).

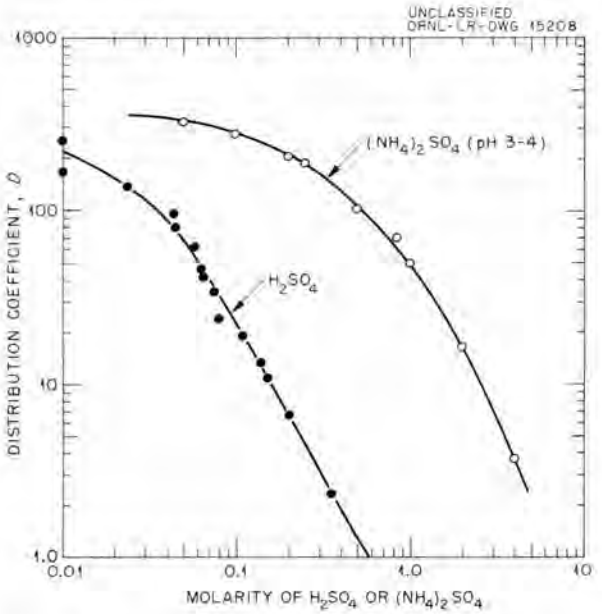

Fig. 15. Adsorption of Th(IV) (Tracer) from Sulfuric Acid and Ammonium Sulfate Solutions.

Since the distribution coefficients of Th(IV) decrease with both sulfuric acid and ammonium sulfate concentration, it can be concluded that the Th(IV) species which exist in the aqueous phase are predominantly negatively charged, at least above ~0.05 M SO_4^{--}. From the slope of the log D vs log M plots, it can probably be concluded that near 0.1 M H_2SO_4 the Th(IV) species has a charge of −2; that is, that it is $Th(SO_4)_3^{--}$. At very high sulfate concentrations a complex of higher negative charge, for example, $Th(SO_4)_4^{4-}$, may be formed.

In view of the large adsorbability of Th(IV) from sulfate solutions, many separations involving Th(IV) should be possible, particularly since a large number of elements, including the rare earths, show negligible adsorbability from such media.

HYDROLYSIS OF Th(IV)

J. S. Johnson R. W. Holmberg K. A. Kraus

It was reported[7] that molecular-weight measurements by the ultracentrifuge of hydrolyzed thorium(IV) perchlorate solutions were in agreement with Hietanen's[8] computation of degrees of aggregation from titration data, based on Sillén's continuous polymerization mechanism.[9] Briefly, the model pictures hydrolytic polymerization as proceeding by the addition of links, here $Th(OH)_3^+$, to chains, the free energy change for the addition reaction being independent of chain length, or varying with it in some simple way. All of Hietanen's titration data [0.001 to 0.020 M Th(IV)] were found to fit such a mechanism up to a hydroxyl number equal to ~2.5. Measurements made here[10] were found to agree well with those of Hietanen's but were carried out over a larger range of Th(IV) concentrations (0.00025 to 0.015 M). The data for Th(IV) concentrations less than 0.002 M and hydroxyl numbers n less than ~0.5 deviated somewhat from those expected from Sillén's continuous polymerization picture, suggesting that if the continuous polymerization picture is accepted, contributions from species of the type $Th(OH)^{+++}$ and $Th(OH)_2^{++}$ in the early stages of hydrolysis must also be included.

It was also reported[7] that for $n \geqq 1.5$, Th(IV) was much more aggregated (a factor of 10 or more) in 1 M NaCl than in 1 M $NaClO_4$. It seemed of interest to see how these large differences in aggregation were reflected in the titration curves in chloride media. Accordingly, titrations were

[6] K. A. Kraus and F. Nelson, *Peaceful Uses of Atomic Energy, Proceedings of the International Conference in Geneva, August 1955*, vol 7, p 113.

[7] J. S. Johnson, K. A. Kraus, and R. W. Holmberg, *Chem. Semiann. Prog. Rep. June 20, 1955*, ORNL-1940, p 5.

[8] S. Hietanen, *Acta Chem. Scand.* 8, 1626 (1954).

[9] L. G. Sillén, *Acta Chem. Scand.* 8, 299 (1954); *Acta Chem. Scand.* 8, 318 (1954).

[10] K. A. Kraus and R. W. Holmberg, *J. Phys. Chem.* 58, 325 (1954).

carried out on 0.002 to 0.050 *M* Th(IV) solutions in 1 *M* NaCl. All curves were found to fit Sillén's mechanism well and were only slightly different from those in perchlorate solutions. If significant, the difference between the curves indicated lower aggregation in chloride than in perchlorate. The titrations were rapidly reversible; the acidity change brought about by the addition of base could be readily reversed by the addition of an equivalent amount of acid. An additional titration in 1 *M* $NaClO_4$, carried out on a 0.05 *M* Th(IV) solution for comparison, again agreed with the Hietanen-Sillén model found for the other perchlorate titrations.

The titration results in chloride were surprising, in view of the high aggregation found by ultracentrifugation. Since the titrations are carried out in a matter of hours, while equilibrium centrifugations require days, it was thought possible that the difference between polymerization in the two media was a matter of the time of observation. This was tested by centrifuging freshly prepared solutions of 0.05 *M* Th(IV), $n = 1.5$, in 1 *M* NaCl and 1 *M* $NaClO_4$ simultaneously in a two-cell rotor. Little difference in the sedimentation of the two solutions was indeed noted at first, but the refractive-index gradient pattern for perchlorate attained equilibrium in about a week, while the pattern for chloride indicated a slow increase in polymerization from day to day during the three weeks of centrifugation.

An attempt was then made to follow changes of acidity in the hydrolyzed thorium chloride solutions corresponding to the polymerization changes. Surprisingly, the degrees of hydrolysis were found to change little, at least for $n \leq 2.3$, over a period of six weeks, and did not reflect the change in aggregation found by ultracentrifugation. The only major difference noted between fresh and aged solutions in chloride was found in the reversibility. If acid is added to a fresh or aged solution in perchlorate, the results are the same; acid addition to an aged chloride solution, however, produces a rapid rise in acidity, greater than would be observed with a fresh solution, followed by a gradual drift back toward the titration curve for a fresh solution.

The insensitivity of acidity to gross changes in polymerization taking place in aging $ThCl_4$ solutions again raises serious questions regarding the legitimacy of molecular-weight estimates obtained from acid-base titration data alone.

ULTRACENTRIFUGATION OF INORGANIC SOLUTIONS

J. S. Johnson K. A. Kraus

The degree of aggregation of a number of metal ions in aqueous solution has been investigated briefly by equilibrium ultracentrifugation during the past six months. A summary of the preliminary observations follows.

Pb(II) and Sn(IV)

Anionic polymers of Mo(VI) and W(VI) are known to exist in solution on the basic side of their isoelectric (precipitation) points, which occur at rather high acidities. It has been suggested that amphoteric metal hydroxides, in general, may be aggregated when they are dissolved even in rather strongly basic solutions. Interest in this phase of chemistry has been sharpened recently by studies of adsorption properties of metal oxides. We have centrifuged 0.02 *M* Pb(II) in 1 *M* NaOH and in 0.5 *M* NaOH, and Sn(IV) in 1 *M* NaOH. There appears to be no appreciable polymerization of lead or tin in 1 *M* NaOH and little, if any, of lead in 0.5 *M* NaOH.

Mo(VI) in Acidic Solutions

The polymerization of Mo(VI) has been investigated by a number of methods on the basic side of its isoelectric point, but little attention seems to have been paid to its aggregation in acidic solution. Polymers have been postulated on the basis of solubility measurements[11] and anion exchange studies.[12]

Solutions 0.05 *M* in Mo(VI), 1 and 6 *M* in HCl, and solutions 0.025 and 0.1 *M* in Mo(VI) and 3 *M* in HCl were centrifuged. In 6 *M* HCl there is apparently no polymerization. In 3 *M* HCl there seems to be a little aggregation, the average degree of polymerization probably being no more than 2. The molecular weight appears to be a little higher in 0.1 *M* Mo(VI) than in 0.025 *M* Mo(VI); this indicates that a concentration-dependent polymerization reaction occurs at this acidity. In 1 *M* HCl the degree of polymerization was much greater than at the higher acidities. Equilibrium was not attained in this

[11] See, for example, M. M. Jones, *J. Am. Chem. Soc.* **76**, 4233 (1954).

[12] K. A. Kraus, F. Nelson, and G. E. Moore, *J. Am. Chem. Soc.* **77**, 3972 (1955).

case, since aggregation was still in progress when the centrifugation was terminated.

Hg(I) and Hg(II) Nitrate

Centrifugations have previously been reported[13] that contradicted inferences (from solvent extraction studies) of dimerization of In(III) in HBr and of Au(III) in HCl solutions. Solvent extraction results for In(III) have since been published.[14] Although there is no reason to doubt that the ultracentrifuge can distinguish between monomers and dimers under these conditions, it seemed appropriate to demonstrate this clearly with measurements on a known system. Accordingly, centrifugations have been carried out with 0.04 and 0.12 *M* Hg(I) in 0.1 *M* HNO_3–1.9 *M* $NaNO_3$ solutions, and of 0.03 and 0.1 *M* Hg(II) in 2 *M* HNO_3. The only available density data applicable to these systems[15] are somewhat open to question, but the results of the centrifugations are clear, nevertheless: The apparent molecular weight for the 0.04 *M* Hg(I) solution was 503 and for the 0.1 *M* solution, 500; the formula weight for $(HgNO_3)_2$ is 525. For 0.03 *M* Hg(II), the observed value is 283, and for 0.1 *M* Hg(II), 266, as compared with the formula weight for $Hg(NO_3)_2$ of 325. The differences between apparent molecular weights and formula weights are essentially as expected for at least partially dissociated electrolytes (charge effect).

ADSORPTION ON INORGANIC MATERIALS

T. A. Carlson D. J. Coombe J. S. Johnson
K. A. Kraus H. O. Phillips

Introduction

The systematic investigation of adsorption of ions from aqueous solutions on various relatively simple inorganic materials has continued. As before, principal interest centered around the anion and cation exchange properties of hydrous oxides and the cation exchange property of insoluble salts containing polyvalent anions such as phosphate, tungstate, molybdate, and arsenate. Detailed discussion of this work does not appear feasible at this time, and the following topics should be considered typical rather than exhaustive.

Adsorption of Chromate by Zirconium Oxide

The hydrous oxides, including zirconium oxide, have earlier been shown to have excellent selectivity for various negative ions, particularly the more highly charged ones. Typical in this connection is the selectivity for chromates. In acidic solutions, tracer chromate may be adsorbed with extremely high distribution coefficients on zirconium oxide, even from solutions of high ionic strength, providing the negative ions carry a charge of −1, for example, Cl^-, NO_3^-. This adsorption of chromate may be utilized for the recovery of this element from various wastes, including waters to which it had been added as a corrosion preventive.

In many instances, uptake considerably in excess of 1 mole of CrO_4^{--} per liter of bed may be realized. For best adsorption the exchanger should be acid-washed (e.g., in the chloride or nitrate forms) or, if the hydroxide form of the exchangers is used, sufficient acid should be present in the chromate-bearing liquor to neutralize the hydroxide ions released in the adsorption process. While small amounts of sulfate do not seriously interfere with adsorption of chromate, very large amounts of sulfate are detrimental and cause an effective decrease in the maximum loading achievable.

Chromate may quickly and efficiently be removed from the exchanger by washing with base (e.g., 1 *M* NaOH). In general, only a few column volumes are necessary for essentially quantitative recovery of chromate.

Since V(V), W(VI), and Mo(VI), as well as many other elements, are also strongly adsorbed by the oxides, their use for recovery and concentration of such elements appears generally to be extremely promising.

Cation Exchange Properties of the Oxides

Zirconium oxide, tin oxide, aluminum oxide, thorium oxide, and many others are anion exchangers in acidic solutions. In less acidic, neutral, or basic solutions, most of them reveal cation exchange properties, the extent depending apparently on the "basicity" of the oxides and their selectivity for the cations to be adsorbed. Detailed investigations of these cation exchange

[13] R. W. Holmberg, K. A. Kraus, and J. S. Johnson, *Chem. Semiann. Prog. Rep. June 20, 1954*, ORNL-1755, p 7; *Chem. Semiann. Prog. Rep. Dec. 20, 1954*, ORNL-1832, p 9.

[14] H. Irving and F. J. C. Rosotti, *J. Chem. Soc.* 1955, 1938.

[15] P. T. Muller and E. Carrière, *Compt. rend.* 154, 695 (1912).

properties are now in progress, particularly with respect to alkaline earths and rare earths. On zirconium oxide, these elements are extremely strongly adsorbed from neutral solutions, even at high ionic strength. Elution may easily be achieved with acids. The differences in selectivity of the oxides for various groups of elements may be utilized for separations. For example, in neutral solutions, the alkali metals (at least sodium to cesium) are readily elutable from zirconium oxide with ammonium chloride solution (e.g., 1 *M* NH_4Cl), while the alkaline earths (at least from magnesium to barium) are retained by the adsorbent. The alkaline earths can then be removed with, for example, 1 *M* HCl. Typical separations of this type may be carried out with columns as short as 1 cm and at reasonable loading of the exchanger with respect to alkaline earths.

Anion Exchange Properties of Oxides Containing Bi(III)

In a search for cation exchangers with unusually high selectivity for chloride ions which might be useful for chloride removal in neutral solutions and at high temperature, compounds containing Bi(III) have been investigated. Bismuth oxide has an enormous "capacity" (or uptake) for acids, and the rates are fast. The end product in these experiments are various oxysalts. Similarly, oxysalts of Bi(III), for example, $BiO(NO_3)$, may be treated with base to convert them to either oxides or hydroxides which, in turn, could be used for the adsorption of negative ions. Unfortunately, the simple bismuth salts investigated tended to disperse in solutions of low electrolyte content and hence did not appear suitable for column operation as initially intended.

For this and other reasons, properties of a number of mixed oxides of Bi(III) have been investigated from the point of view of anion exchangers. Typical examples are fired or dried precipitates containing Bi(III) with Zr(IV), Th(IV), and Sn(IV). Some of these appear promising for column operation. Most of them tend to retain the high selectivity for chloride ions in neutral solutions.

[16]See, for example, K. A. Kraus, T. A. Carlson, and J. S. Johnson, *Nature* 177, 1128 (1956).

Cation Exchange Properties of "Zirconium Molybdate" – Separation of the Alkaline Earths

It had been found[16] that mixed precipitates of Zr(IV) and W(VI) have excellent cation exchange properties which may be used in separations. Similar experiments have now been carried out with precipitates containing Zr(IV) and Mo(VI). After drying and sizing, these materials show satisfactory cation exchange properties, good capacities, and rates suitable for column operations. In fact, the particular "zirconium molybdates" thus far prepared give elution bands at least as sharp as the "zirconium tungstates" and in some cases, for example, the alkaline earths, may even be better. The separation of the alkali metals and alkaline earths, summarized in Figs. 16 and 17, illustrates what may be done with these materials. While the experiments shown refer to separation of tracers, it is expected that similarly good separations could be achieved at macro concentrations.

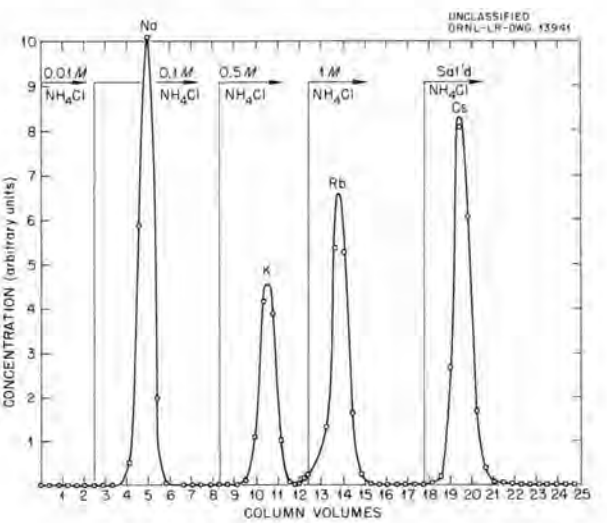

Fig. 16. Separation of the Alkali Metals ("Zirconium Molybdate"). Drying temperature, 25°C; flow rate, 1.1 cm/min; column, 6.4 cm × 0.19 cm^2.

Cation Exchange Properties of Zirconium Arsenate

In continuation of the systematic investigation of cation exchange properties of salts containing polyvalent anions, precipitates of Zr(IV) and

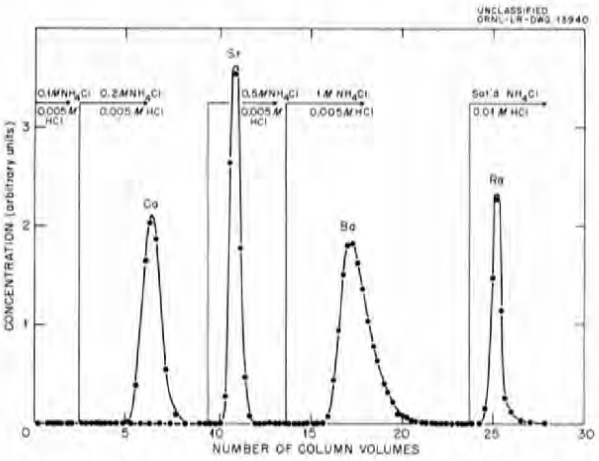

Fig. 17. Separation of the Alkaline Earths ("Zirconium Molybdate"). Drying temperature, 25°C; flow rate, 1.1 cm/min; column, 10 cm × 0.19 cm^2.

arsenate were investigated in a manner similar to the work with tungstates, molybdates, and phosphates. After the precipitates were dried at moderate temperatures, apparent capacities were found to be reasonably high (in excess of 1 mole of Cs^+ per kilogram), and selectivities, as in the case of the other salts mentioned, were high, at least for the alkali metals. Unfortunately, the materials thus far prepared were not so successful for column separations because of considerable tailings of the elution bands.

CONCENTRATED POLYMER SOLUTIONS OF Th(IV)

T. A. Carlson K. A. Kraus
J. S. Johnson H. O. Phillips

It has been reported[17] that precipitates of Th(IV) with base ("hydroxides") dried in the general vicinity of 250 to 300°C become dispersible in water. Solutions containing 1 kg of the solid per kilogram of water may be readily prepared, and in some cases concentrations as high as 3 kg of solid per 1000 g of water have been achieved. The dispersions have relatively low viscosity and appear to have indefinite stability at room temperature. Even at elevated temperatures they show remarkable stability, but at very high temperatures, for example, at 250 to 300°C, precipitation or gel formation occurs fairly rapidly.

As earlier reported, the polymeric particles have degrees of aggregation of the order of 1000 [i.e., 1000 Th(IV) ions per particle]. Recent crystallographic investigation on the solids and the dispersions indicated that they have a typical thorium oxide structure with a particle size[18] (diameter) of the order of 33 Å, in general agreement with the earlier ultracentrifugations and light-scattering work.

Work is continuing in the direction of searching for methods to make these polymeric solutions stable at high temperatures, as well as investigating the kinetics of growth and of depolymerization of the particles.

MEASUREMENT OF SOLUBILITIES WITH PACKED COLUMNS

K. A. Kraus D. J. Coombe

Solubilities of solids in solution are generally determined by shaking a small amount of the solid and the solutions in closed vessels for considerable periods of time. While this method yields excellent results, it is not readily adaptable to the measurement of solubilities at high temperatures and to systems in which the salts show low solubilities. If the rate of equilibration is principally determined in these experiments by the efficacy of stirring and the length of the necessary diffusion path, it is to be anticipated that passage of the liquid through a packed bed of the solid phase, whose solubility is to be determined, should in many cases rapidly and conveniently yield accurate measurements of solubility. In packed beds with relatively small particles, the necessary diffusion paths become of the order of 0.01 mm, which would yield equilibrium in most cases in seconds or less. If the packed columns are jacketed, they can easily be thermostatted and should, with a minimum of machinery, permit measurements of solubilities at very high temperatures.

To test this scheme, the solubility of Ag_2SO_4 in various sulfuric acid solutions was determined by means of a radiometric method of analysis for silver. The results were in good agreement with

[17] K. A. Kraus *et al.*, *HRP Quar. Prog. Rep. Jan. 31, 1956*, ORNL-2057, p 139; *HRP Quar. Prog. Rep. April 30, 1955*, ORNL-1895, p 197.

[18] We are indebted to R. D. Ellison for the x-ray determinations.

those reported earlier by Åkerlöf and Thomas.[19] Equilibrium was reached with columns only a few centimeters high at the maximum flow rates used, 20 cm/min. It is contemplated to use the method for the determination of the solubility of a number of salts in electrolytes, both at room and elevated temperatures, and to determine activity coefficients in these media. The method should be readily adaptable to measurement of solubilities in nonaqueous systems, including fused salts.

FUNDAMENTAL STUDIES ON ION EXCHANGE RESINS

G. E. Boyd G. E. Myers S. Lindenbaum

Thermodynamic Calculation of Anion Exchange Selectivities

The thermodynamic calculation of selectivity coefficients, D, in the exchange of singly charged anions makes use of the basic equation that was employed in the recently reported[20] calculation of cation exchange selectivities:

$$(1) \quad \log D = \frac{P(\bar{v}_1 - \bar{v}_2)}{2.3RT} + \log\left(\frac{\gamma_1}{\gamma_2}\right)_r - 2\log\left(\frac{\gamma_1}{\gamma_2}\right)_w ,$$

where P is the swelling pressure, $\bar{v}_1$ and $\bar{v}_2$ are the partial molar volumes of the exchanger salts formed with anions 1 and 2, and γ_1 and γ_2 are the mean molal activity coefficients for salts 1 and 2 in the exchanger, r, and aqueous mixed electrolyte phase, w, respectively. The swelling pressure in a given cross-linked anion exchanger may be estimated[21] by comparing its water activity, a'_w, with that, a_w, for a very weakly cross-linked exchanger of the same water content (where $P = 0$, effectively). Then,

$$(2) \quad P = \frac{2.3RT}{\bar{v}_w} \log \frac{a'_w}{a_w} ,$$

where $\bar{v}_w$ is the partial molar volume of water. The partial molar volume difference, $\bar{v}_1 - \bar{v}_2$, may be estimated by the use of density measurements on dry and on partially hydrated anion exchangers in their pure and mixed salt-forms by means of the equation[20]

$$(3) \quad \bar{v}_1 - \bar{v}_2 = V_1 - V_2 - \int_0^{x_w} \left(\frac{\partial \bar{v}_w}{\partial x_2}\right)_{x_w} dx_w ,$$

where V_1 and V_2 are the molar volumes of the pure, dry resinates, 1 and 2, respectively. To evaluate the integral in Eq. 3 it is necessary to measure the variation of the equivalent volumes, V_{equiv}, of a series of exchanger salt-forms with their water contents, x_w, so that the partial molar volume of water can be estimated according to $\bar{v}_w = (\partial V_{equiv}/\partial x_w)_{x_1}$; to derive the differential quotient, $(\partial \bar{v}_w/\partial x_2)_{x_w}$, from the variation of $\bar{v}_w$ with composition; and to integrate this quotient with respect to x_w between the limits zero and the value of x_w appropriate to the cross-linked exchanger under question.

Pycnometric density measurements were made on the pure and mixed fluoride, chloride, bromide, and iodide salt-forms of weakly cross-linked (i.e., 1% DVB) strong-base anion exchanger (Dowex 2) containing varying amounts of water, with an inert organic liquid used as a displacing medium. A representative portion of the data is plotted in Fig. 18. All the data were fitted to an empirical equation of the form

$$(4) \quad V_{equiv} = a + \bar{v}^0_w x_w + be^{-cx_w} ,$$

where $\bar{v}^0_w$ is the partial molar volume of pure water (i.e., 18.069 ml/mole). This equation attempts to reflect the facts that for large water contents, x_w, the partial molar volume of water approaches its molar value and that for small x_w there are negative deviations from simple volume additivity.

Differentiation of Eq. 4 gives

$$(5) \quad \bar{v}_w = \bar{v}^0_w - bce^{-cx_w} ,$$

from which the curves in Fig. 19 were computed for the bromide-chloride anion exchange by use of the constants in Table 15. For this latter pair of anions, $\bar{v}_w$ appeared to increase linearly with increasing equivalent fraction of bromide salt-form,

[19] G. Åkerlöf and H. C. Thomas, *J. Am. Chem. Soc.* **56**, 593–601 (1934).

[20] G. E. Myers and G. E. Boyd, *J. Phys. Chem.* **60**, 521 (1956).

[21] G. E. Boyd and B. A. Soldano, *Z. Elektrochem.* **57**, 162 (1953).

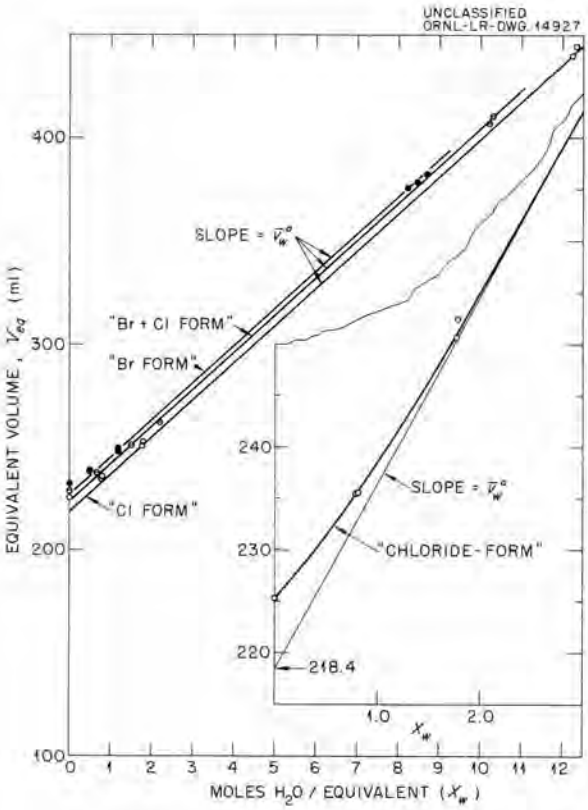

Fig. 18. Variation of Equivalent Volume of Chloride and Bromide Salt-Forms of Dowex 2 with Water Content.

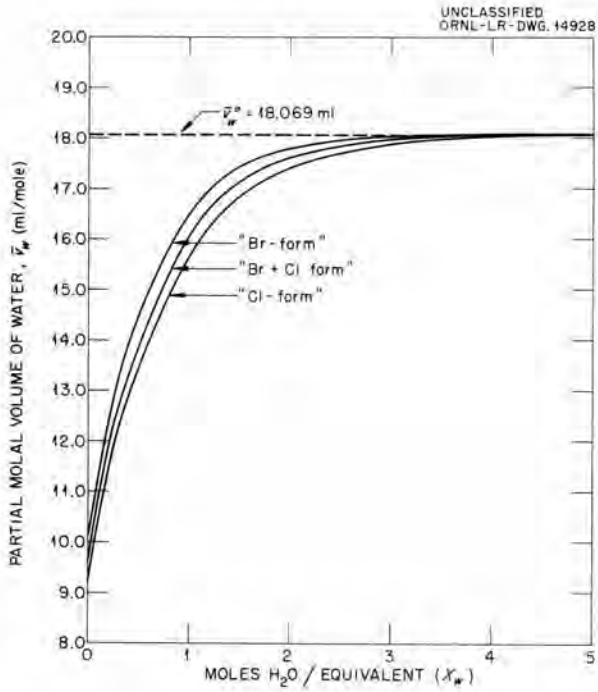

Fig. 19. Variation of the Partial Molal Volume of Water with Degree of Anion Exchanger Hydration.

x_{Br}, from its value for pure chloride salt to that for the pure bromide form, so that Eq. 3 could be integrated analytically to yield

$$(6) \quad \bar{v}_{Cl} - \bar{v}_{Br} = -8.4 + 6.9e^{-1.29x_w} - 5.0e^{-1.69x_w}$$

From Eq. 6 it is seen that $\Delta\bar{v}$ for the bromide-chloride exchange approaches −8.4 ml/mole for large values of x_w. This result may be compared with the difference between the partial molar volumes of chloride and bromide ions at infinite dilution in water, $\bar{v}^0_{Cl} - \bar{v}^0_{Br} = -6.9$ ml/mole, and with the computed value for the difference, $\bar{v}_{Cl} - \bar{v}_{Br} = -6.0$ ml/mole from the values of $\bar{v}_{Cl}$ and $\bar{v}_{Br}$ in pure 9 m cesium chloride and bromide solutions. The general reliability of the ion-exchange volume data would appear to be confirmed by these concordant values.

The second term of the right-hand member of Eq. 1 may be estimated by use of the equation[20]

$$(7) \quad \log\left(\frac{\gamma_1}{\gamma_2}\right)_r - \log\left(\frac{\gamma_1^*}{\gamma_2^*}\right)_r = -\int_0^{\log a_w}\left(\frac{\partial x_w}{\partial x_2}\right)_{a_w} d\log a_w \, .$$

TABLE 15. CONSTANTS IN Eq. 4 FOR THE EQUIVALENT VOLUMES (ml/equiv) OF ANION EXCHANGER SALT-FORMS

Salt-Form	Constants		
	a	b	c
Fluoride	198.7	15.9	0.79
Chloride	218.4	6.9	1.29
Bromide	226.8	5.0	1.69
Iodide	238.8	3.4	2.06
Fluoride-bromide	213.6	6.7	0.91
Chloride-bromide	223.6	5.9	1.46
Iodide-bromide	233.5	4.8	1.68

The evaluation of the integral appearing in Eq. 7 may be effected by using water content measurements taken in isopiestic experiments, as has been described recently.[20] This work with anion exchangers, however, differed from that with cation exchangers in that water contents for $a_w = 1.0$ were determined with the use of a centrifugation technique so that extrapolations of $(\partial x_w/\partial x_2)_{a_w}$ to $\log a_w = 0$ were avoided.

Finally, the third term in Eq. 1, $\log (\gamma_1/\gamma_2)_{w'}$ for the ratio of the anionic activity coefficients in a dilute external (i.e., 0.1 *M*) mixed aqueous electrolyte solution may be estimated to the required accuracy by using Guggenheim's equation.[22]

Results from the calculation of $\log (\gamma_1/\gamma_2)_r$ for the bromide-chloride exchange equilibrium at $x_{Br} = 0$ are shown in Fig. 20, which also shows the relative importance of the various terms in Eq. 1 to the selectivity coefficient, D^{Br}_{Cl}, for this system. The agreement between the calculated and the measured D^{Br}_{Cl} values at $x_{Br} = 0$ (also shown in Fig. 20) for variously cross-linked anion exchangers appears to be within the errors involved in evaluating the right-hand side of Eq. 1. What is believed to be a significant departure occurs with the most highly cross-linked (i.e., 16% DVB) exchanger. The exchange capacity of this preparation, however, is markedly lower than 3.90 meq per gram of dry Cl-form, and therefore one of the fundamental assumptions in the thermodynamic treatment is not satisfied.

[22]E. A. Guggenheim and J. C. Turgeon, *Trans. Faraday Soc.* **51**, 747 (1956).

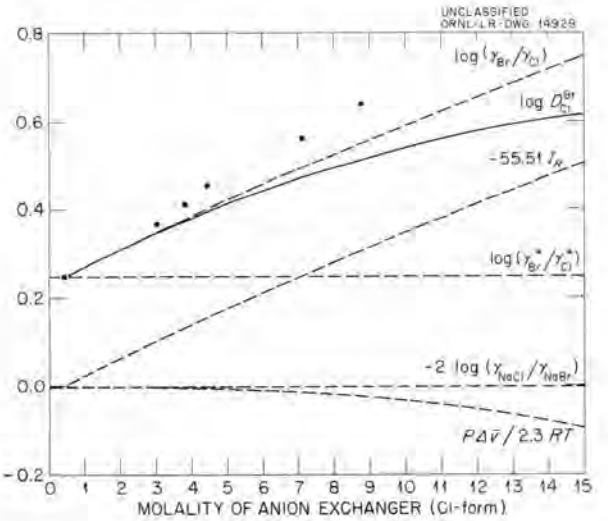

Fig. 20. Summary of Calculations of Terms in Eq. 1 for the Bromide-Chloride Ion Exchange, $x_{Br} = 0.0$.

Selectivity of a Sulfonium Type of Strong-Base Anion Exchanger

The moisture absorption isotherms of several salt-forms of a new phenol-formaldehyde sulfonium strong-base anion exchange resin, Stamex S-44, have been reported.[23] To further characterize this exchanger, a scale of selectivities was determined by measuring the uptake of trace quantities of bromide ion by 12 anion salt-forms. A comparison of the order of affinities with the water uptake at unit activity is given in Table 16.

The data show that the greater the water uptake by a given salt-form, the greater the bromide-ion affinity. The order of selectivity is approximately that observed with Dowex 1 and Dowex 2.[24]

[23]G. E. Myers and G. E. Boyd, *Chem. Semiann. Prog. Rep. June 20, 1955*, ORNL-1940, p 50.

[24]R. M. Wheaton and W. C. Bauman, *Ind. Eng. Chem.* **43**, 1088 (1951).

TABLE 16. SELECTIVITY OF STAMEX S-44 FOR MONOVALENT ANIONS

Resin Salt-Form	Selectivity Coefficient, D^{Br}_{anion}	Millimoles of H_2O per meq of Resin at $a_w = 1$
F^-	37.5	30
IO_3^-	23.2	29
Ac^-	19.3	27
Cl^-	4.98	18
BrO_3^-	3.35	19
NO_2^-	1.67	17
Br^-	1.00	14
ClO_3^-	0.51	14
NO_3^-	0.42	12
I^-	0.07	11
ClO_4^-	0.03	7
SCN^-	0.02	10

Selectivity of Cation Exchange Resins of Variable Capacity

Cation exchange resins of variable capacity prepared by the hydrolysis of *p*-sulfonamidostyrene and styrene copolymers have recently become available.[25] Cross-linking in these exchangers is obtained by the addition of *bis*-(*p*-vinylphenyl) sulfone to the reaction mixture, and the capacity can be controlled by varying the ratio of styrene to *p*-sulfonamidostyrene. This method of synthesis appears to ensure that only *p*-sulfonic acid exchange groups occur in the exchanger. Sodium-hydrogen ion selectivity coefficients, D_H^{Na}, for preparations with three different degrees of cross-linking, each prepared with four different capacity values, have been measured. These D_H^{Na} values are plotted in Fig. 21 as a function of the composition of the exchanger. The graph shows that D_H^{Na} decreases with capacity for a given degree of cross-linking, in agreement with earlier findings[26] on the same ion exchange with desulfonated Dowex 50 preparations.

[25] R. H. Wiley and S. F. Reed, *J. Phys. Chem.* 60, 533 (1956).

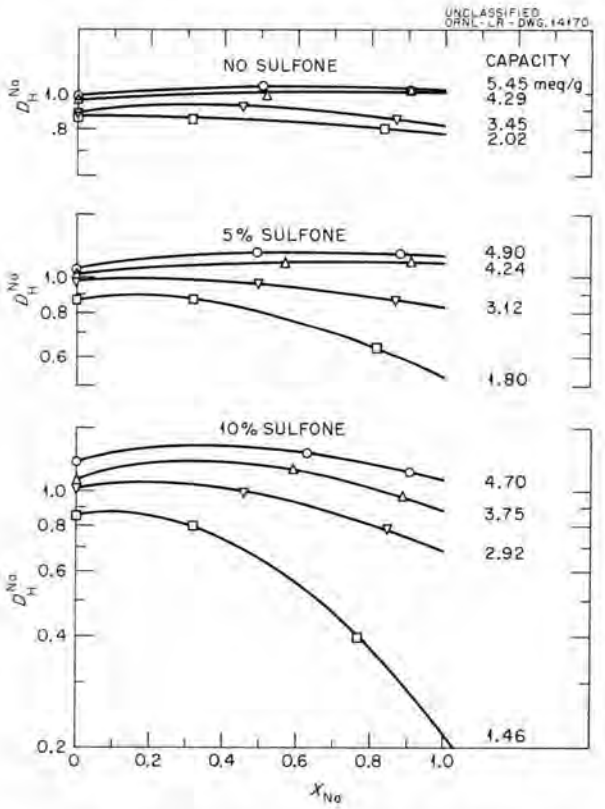

Fig. 21. Selectivity Coefficients for the Sodium-Hydrogen System on Sulfostyrene Copolymer of Variable Capacity.

Ionic Interactions in Organic Ion Exchangers

In general, the selectivity exhibited by an ion exchange resin is governed primarily by the activity coefficient ratio of the two exchanging ions within the resin. The actual magnitude of that ratio reflects, first, the interactions between the exchanging ions and the fixed ionic groups of the resin and, second, how those interactions are affected by the presence of a second counterion. As yet no theoretical investigation of the latter problem appears to have been made. However, it is known experimentally that a considerable number of mixed inorganic salt solutions obey relationships of the type

$$(8a) \qquad \log \gamma_{1(2)} = \log \gamma_{1(0)} - \alpha_{12} x_2 m - \beta_{12} x_2^2 m^2 ,$$

$$(8b) \qquad \log \gamma_{2(1)} = \log \gamma_{2(0)} - \alpha_{21}(1 - x_2)\, m - \beta_{21}(1 - x_2)^2 m^2 ,$$

where $m = m_1 + m_2 =$ constant; $x_2 = m_2/m = 1 - x_1$; α_{12}, α_{21}, β_{12}, and β_{21} are constants at any particular total molality, m. Further, $\gamma_{1(2)}$ represents the mean molal activity coefficient of salt (1) in the presence of salt (2), and $\gamma_{1(0)}$ represents the activity coefficient of salt (1) in the absence of salt (2) at the same total molality. Equations analogous to Eqs. 8 without the squared term describe the so-called "Harned rule" for mixed electrolytes.

Although a simplified Harned rule has previously been employed[27] in attempting to relate observed selectivities with osmotic coefficients of pure resinates, no a posteriori determination of the validity of the more general Eqs. 8 by means of measurements upon mixed resinates appears to have been attempted. Such a determination has now been made with the use of the previously reported[20] water contents of mixed salt-forms of

[26] G. E. Boyd, B. A. Soldano, and O. D. Bonner, *J. Phys. Chem.* 58, 456 (1954).

[27] E. Glueckauf, *Proc. Roy. Soc. (London)* 214, 207 (1952).

0.5% cross-linked Dowex 50 and Dowex 2 resins in the following manner: From the resin water content, values of log $[\gamma_{1(2)}/\gamma_{2(1)}]$ have been calculated[20] as a function of resin molality, m, and loading, x_2. In addition, values of the osmotic coefficient, ϕ_{x_2}, may be calculated from the same data by the definition

$$(9) \qquad \phi_{x_2} = -\frac{127.8}{m} \log a_w \ .$$

With these values, the coefficients of Eqs. 8 may be determined by applying Eqs. 10 and 11, which are derivable from Eqs. 8:

$$(10) \qquad \phi_{x_2} = \phi_{1(0)} - 2.30m\alpha_{12}\, x_2 + 4.60m[(\alpha_{12} + \alpha_{21}) - 2m(\beta_{12} - \beta_{21})]\, x_2^2 + 1.535m^2(\beta_{12} - \beta_{21})\, x_2^3 = a + bx_2 + cx_2^2 + dx_2^3 \ ,$$

$$(11) \qquad \log \frac{\gamma_{1(2)}}{\gamma_{2(1)}} = \left[\log \frac{\gamma_{1(0)}}{\gamma_{2(0)}} + \alpha_{21}m + \beta_{21}m^2\right] - m[(\alpha_{12} + \alpha_{21}) + 2\beta_{21}m]\, x_2 + m^2(\beta_{12} - \beta_{21})\, x_2^2 = a' + b'x_2 + c'x_2^2 \ .$$

Furthermore, the calculated values of the α's and β's may be tested for self-consistency by means of Eq. 12, which results from the application of Cauchy's cross-differentiation condition upon Eqs. 8:

$$(12) \qquad \frac{d(\alpha_{12} + \alpha_{21})}{dm} + \frac{md(\beta_{12} + \beta_{21})}{dm} = -2(\beta_{12} + \beta_{21}) \ .$$

The final results of the calculations are given in Table 17, where literature values for inorganic salt mixtures in water are also included for comparison. The sequence of steps employed in the calculation, once the coefficients of Eqs. 10 and 11 were determined by least squares, was the following: The value of α_{12}, of course, resulted directly from the linear coefficient of Eq. 10, and that of $\alpha_{12} + \alpha_{21}$ from the quadratic coefficient, since $\beta_{12} - \beta_{21}$ was zero in all cases. The value of β_{12}, however, resulted from a combination of the linear coefficient in Eq. 11 and the value of $\alpha_{12} + \alpha_{21}$ already calculated for that same molality. Finally, substitution of the concentration (total molality) dependence of $\beta_{12} + \beta_{21}$ into Eq.. 12 gave an equation for the concentration dependence of $\alpha_{12} + \alpha_{21}$ which may be compared with that obtained directly.

From Table 17 it can be seen that a general inconsistency appears between the $\alpha_{12} + \alpha_{21}$ values determined by the two methods. However, as shown above, the calculation of β_{12} is rather indirect and is particularly so considering that it is based upon the log (γ_1/γ_2) values, which themselves are rather far removed from the original data. Furthermore, the strong concentration dependence of the β's in itself seems inconsistent with the behavior both of the α's calculated here and of α's and β's for ordinary electrolytes and with the fact that $\beta_{12} - \beta_{21}$ is apparently zero.

TABLE 17. INTERACTION COEFFICIENTS OF MIXED RESINATES

System	Molality Range	α_{12}	$\alpha_{12} + \alpha_{21}$ Observed	β_{12}	$\beta_{12} - \beta_{21}$	$\alpha_{12} + \alpha_{21}$ Calculated from β's and Eq. 12
Na-Li polysulfonates	1 → 25	$0.059 - 0.0014m$	$0.015 + 0.0005m$	$0.012/m^{1.26}$	0	$(\alpha_{12} + \alpha_{21})_{m=1} - 0.071(1 - 1/m^{0.26})$
Na-Li chlorides	2 → 6	0.035	$-0.013 + 0.004m$	~−0.001	~0	
K-Na polysulfonates	1 → 25	$0.024 - 0.0006m$	0	$0.023/m^{1.79}$	0	$(\alpha_{12} + \alpha_{21})_{m=1} - 0.0121(1 - 1/m^{0.79})$
K-Na chlorides	2 → 5	0.025	0.017	0	0	
Cs-Na polysulfonates	1 → 25	0.033	0.028	$0.044/m^{1.7}$	0	$(\alpha_{12} + \alpha_{21})_{m=1} - 0.049(1 - 1/m^{0.67})$
Cs-Na chlorides	0.5 → 6	0.056 → 0.044	0.021 → 0.040	(0.0012)		
Dowex 2 Br-Cl	1 → 12	$0.047 \exp(-0.082m)$	0	?	0	
KBr-KCl	2 → 6	0.0033 → 0.0015	0	0	0	

Consequently, it seems reasonable to consider the observed inconsistency a reflection upon the validity of the β's and not upon the validity of the observed α's.

The values of the α's for the resin systems are of the same magnitude as those in analogous electrolyte solutions, but there appears to be no general correlation between the two systems. The latter may be taken presumably as an indication that the interactions between the oppositely charged ions strongly influence the behavior of the α's. In such concentrated solutions, of course, there must also be effects of ion volume and of ion-solvent interactions.

The observed differences in interaction coefficients between exchangers and ordinary electrolyte solutions obviously indicate the inadequacy of the coefficients for the latter to calculate resin selectivities in conjunction with data from pure resinates only.

SOLUBILITY OF Ag_2SO_4 IN VARIOUS ELECTROLYTE MEDIA

M. H. Lietzke R. W. Stoughton

Introduction

Previous work[28] has indicated that the Ag, Ag_2SO_4(sat.) electrode offered considerable promise as a reference electrode for high-temperature emf studies in aqueous solutions. The increasing solubility of Ag_2SO_4 in H_2SO_4 media with increasing acid concentration and temperature,[29] on the other hand, would appear to put upper limits on the values of these variables at which useful thermodynamic data can be obtained with the use of the Ag, Ag_2SO_4 electrode. Because of the moderately high solubility of Ag_2SO_4 in water (about 0.03 m over a rather large temperature range), any appreciable reaction of this salt with an electrolyte in solution may be expected to complicate significantly the interpretation of thermodynamic data. In this connection it was anticipated that a study of the solubility of Ag_2SO_4 in a variety of electrolytes of different valence types even at room temperature would elucidate the general problem of such interpretations.

Data for the solubility of Ag_2SO_4 in $AgNO_3$, $Al(NO_3)_3$, $Al_2(SO_4)_3$, and $La_2(SO_4)_3$ solutions at 25°C were obtained experimentally for this study, while data for the solubility of Ag_2SO_4 in $Mg(NO_3)_2$ (ref 30), Na_2SO_4 (ref 31), $MgSO_4$ (ref 32), $CuSO_4$ (ref 32), and $In_2(SO_4)_3$ (ref 33) solutions were obtained from the literature. The determinations in $AgNO_3$ solutions were made because, as will be shown later, the literature values for this system[30] appeared to be inconsistent with the other data.

Experimental

The Ag_2SO_4 used in the solubility measurements was prepared according to the method described by Archibald.[34] The $La_2(SO_4)_3$ was prepared from Fisher $La(NO_3)_3 \cdot 6H_2O$ by treating the nitrate with Baker's analyzed concentrated H_2SO_4, fuming off the excess H_2SO_4, and igniting the $La_2(SO_4)_3$ in a muffle furnace at 500°C. The $Al(NO_3)_3$, $Al_2(SO_4)_3$, and $AgNO_3$ were all Baker's analyzed reagent-grade chemicals. In each case a series of stock solutions was prepared covering the desired concentration range. Ten-milliliter aliquots of the stock solutions along with an excess of Ag_2SO_4 crystals were sealed in 15-ml centrifuge tubes and rotated at 25 deg for five days. The equilibration was carried out in the dark to prevent photodecomposition of the Ag_2SO_4.

After equilibration, the solutions and the solid phase, as well as the original stock solutions, were analyzed to determine exact concentrations. In all cases included in the present work, Ag_2SO_4 was the stable solid phase in equilibrium with the solution.

Results and Discussion

Values of the apparent solubility product, S, of Ag_2SO_4 were calculated for each system on a molality basis on the assumption of complete dissociation of the Ag_2SO_4 and of the supporting electrolyte. In making the calculations the solubility data from the literature were converted,

[28] M. H. Lietzke and R. W. Stoughton, *J. Am. Chem. Soc.* 75, 5226 (1953).

[29] M. H. Lietzke and R. W. Stoughton, *J. Am. Chem. Soc.* (in press).

[30] W. D. Harkins, *J. Am. Chem. Soc.* 33, 1807 (1911).

[31] M. Barre, *Compt. rend.* 150, 1321 (1910).

[32] G. Åkerlöf and H. C. Thomas, *J. Am. Chem. Soc.* 56, 593 (1934).

[33] M. H. Lietzke and R. W. Stoughton, *J. Am. Chem. Soc.* (in press).

[34] E. H. Archibald, *The Preparation of Pure Inorganic Substances*, Wiley and Sons, New York, 1932.

where necessary, to molalities by means of the density data from the *International Critical Tables.*[35] Log S was then plotted against the square root of the ionic strength, I, as shown in Fig. 22. The curves were all drawn to go through the value of the log of the solubility product of Ag_2SO_4 in pure water[32] (represented by the lowest point). The data obtained in the course of the present study are also given in Table 18.

As can be seen in Fig. 22, the apparent solubility products on a molality basis vary in a surprisingly similar manner with the stoichiometric ionic strength whether or not the "supporting electrolyte" contains sulfate ions. The solubility data of Ag_2SO_4 in $AgNO_3$ solutions obtained in this study appear to be generally consistent with the other data, while the values obtained by Harkins[30] fall considerably above the limiting slope. It is interesting to note that the ionic strength in this case is essentially independent of $AgNO_3$ concentration.

For purposes of comparison, plots of log $\gamma_{\pm}^3$ for Na_2SO_4 (ref 36) and a generalized average activity coefficient function are also shown in

[35] *International Critical Tables*, 1st ed., McGraw-Hill, New York, 1936.

[36] R. H. Stokes, *Trans. Faraday Soc.* 44, 295 (1948).

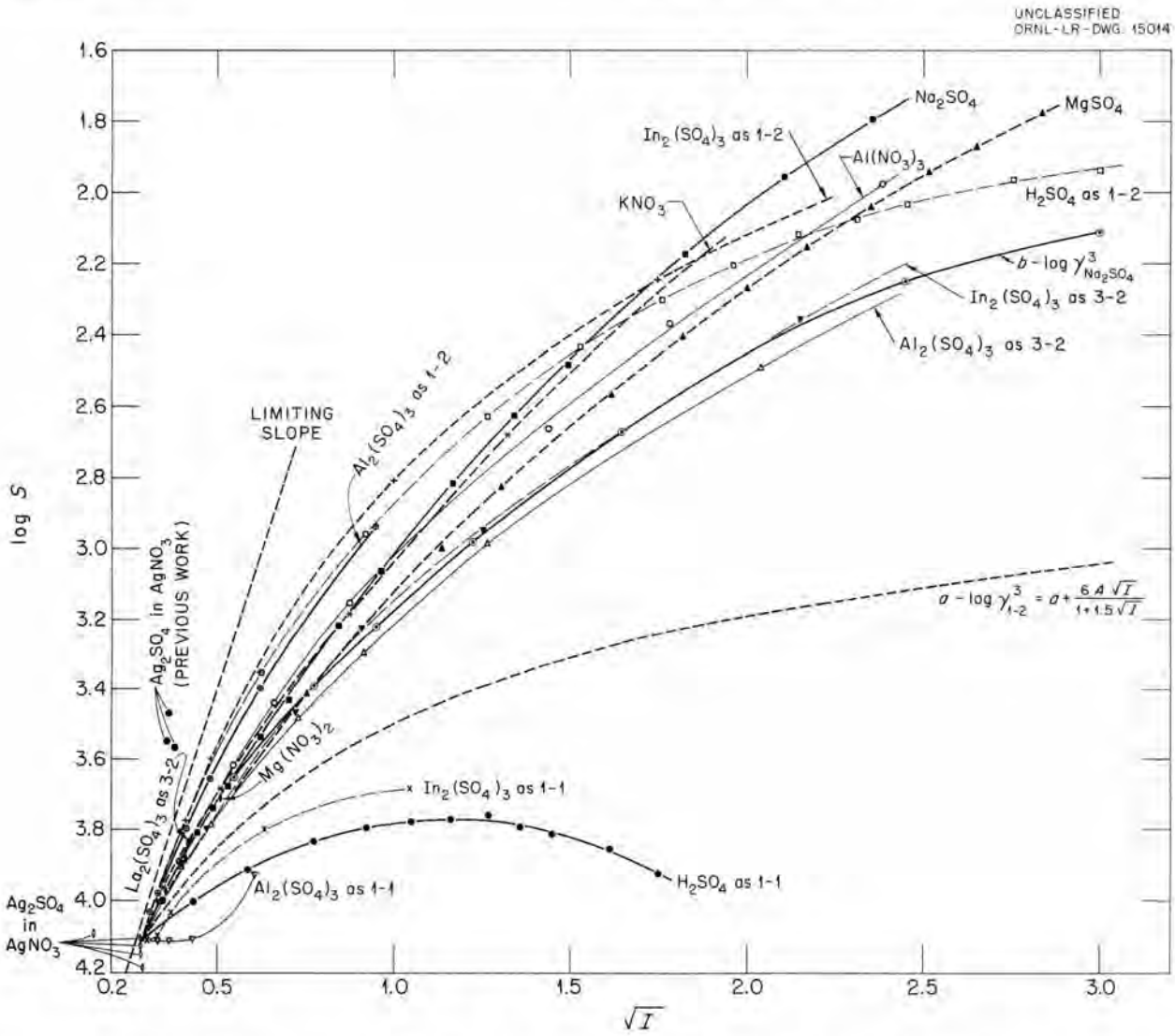

Fig. 22. Apparent Solubility Product of Ag_2SO_4 in Various Electrolyte Media.

TABLE 18. SOLUBILITY OF Ag_2SO_4 IN $AgNO_3$, $Al(NO_3)_3$, $Al_2(SO_4)_3$, AND $La_2(SO_4)_3$ SOLUTIONS AT 25°C

Added Electrolyte	Molality of Added Electrolyte	Molality of Ag_2SO_4
$AgNO_3$	0.00983	0.0238
	0.0174	0.0211
	0.0268	0.0180
	0.0448	0.0130
$Al(NO_3)_3$	0.00527	0.02950
	0.01029	0.03180
	0.03014	0.03923
	0.05035	0.04493
	0.1005	0.05595
	0.3044	0.08166
	0.4787	0.1022
	0.8774	0.1382
$Al_2(SO_4)_3$	0.00221	0.02741
	0.00531	0.02692
	0.01030	0.02664
	0.03048	0.02644
	0.05072	0.02672
	0.1010	0.02785
	0.2712	0.03091
$La_2(SO_4)_3$	0.001999	0.02733
	0.004938	0.02747
	0.009819	0.02769

Fig. 22. These plots were shifted vertically to make them go through the point representing the solubility product of Ag_2SO_4 in pure water. The generalized average activity coefficient function was obtained by calculating log $\gamma_\pm^3$ for a 1-2 electrolyte from Eq. 1, which relates log γ of an ion to the ionic strength, I, the charge of the ion, Z_i, and the Debye-Hückel limiting slope, A:

$$\log \gamma_i = -\frac{AZ_i I^{1/2}}{1 + 1.5I^{1/2}} . \tag{1}$$

For a 1-2 electrolyte

$$\log \gamma_\pm^3 = -\frac{6AI^{1/2}}{1 + 1.5I^{1/2}} . \tag{2}$$

As can be seen, the activity coefficient of Na_2SO_4 varies with its stoichiometric ionic strength in a manner very similar to that in which the activity coefficient of Ag_2SO_4 varies with the stoichiometric ionic strength in the various mixed electrolyte solutions. The activity coefficient plots of both these electrolytes remain much closer to the line representing the limiting law slope than does the activity coefficient plot of the hypothetical "average" 1-2 electrolyte given by Eq. 2.

Originally it had been hoped that some qualitative agreement concerning the degree of dissociation of electrolytes such as the 3-2 sulfates would result from inspection of the curves in Fig. 22. For this reason the 3-2 sulfates were assumed to dissociate "completely" on three separate bases:

$$\text{3-2} \quad M_2(SO_4)_3 = 2M^{+++} + 3SO_4^{--}$$

$$\text{1-2} \quad M_2(SO_4)_3 = 2MSO_4^{+} + SO_4^{--}$$

$$\text{1-1} \quad M_2(SO_4)_3 = MSO_4^{+} + M(SO_4)_2^{-} .$$

Values of S and I were then determined on each of these three bases. As can be seen from Fig. 22, basis 3-2 gives the best agreement with the other curves. Basis 1-2 causes deviations from the other curves in a direction consistent with greater association or complexing of either the Ag^+ or SO_4^{--} (or both) up to an ionic strength of about 2.3. Basis 1-1 shows effects entirely unlike those of the 1-1 salt KNO_3. In the case of $In_2(SO_4)_3$, at least, it is surprising that the three different bases do not cause more widely differing curves. Apparently the ionic strength effect and the common ion effect approximately cancel each other when a comparison of the three bases is made. The fact that basis 3-2 gives best agreement with the other curves should not, it is believed, be interpreted as indicating that the principal species in solution are M^{+++} and SO_4^{--}. For example, in a previous paper,[33] evidence was presented to show that $In_2(SO_4)_3$ is by no means completely dissociated into In^{+++} and SO_4^{--} ions.

In the case of the solubility of Ag_2SO_4 in H_2SO_4 media, two bases of dissociation were considered:

$$\text{1-2} \quad H_2SO_4 = 2H^+ + SO_4^{--}$$

and

$$\text{1-1} \quad H_2SO_4 = H^+ + HSO_4^-$$

It is known that the second equation more nearly represents the principal species in H_2SO_4 solutions in the concentration range of interest than

does the first. According to Fig. 22, basis 1-2 indicates an activity coefficient for Ag_2SO_4 which varies with ionic strength almost exactly like it does in $Al_2(SO_4)_3$ and $In_2(SO_4)_3$ media on basis 1-2. Such a close similarity in these three different cases is surprising. When H_2SO_4 is treated as a strong 1-1 electrolyte, the plot of the Ag_2SO_4 activity coefficient varies with ionic strength in a manner distinctly different from that for the other curves in Fig. 22 and similar to that for some of the 1-1 halide curves.

It would be interesting to calculate S and I for the Ag_2SO_4-H_2SO_4 systems on an actual ionic basis, using the data of Young[37] for the values of the concentration quotient K for HSO_4^- dissociation as a function of ionic strength calculated from the actual ionic concentrations in pure H_2SO_4 solutions. However, both the calculation and its interpretation would be complicated, since the ionic strength on this basis must be calculated by a reiterative process; the equilibrium quotients vary, in general, with species in solution as well as with ionic strength (especially at higher values of the latter), and, as shown in Fig. 22, log S appears to be, to a good approximation, a function of the stoichiometric ionic strength alone. The calculation may be even further complicated by the existence of Ag^+-SO_4^{--} complex ions.

A calculation similar to the one just discussed was carried out in an attempt to determine Ag_2SO_4 solubilities in H_2SO_4 media more accurately than was done previously.[29] The previous calculation involved the assumptions that (1) only the species Ag^+, H^+, HSO_4^-, and SO_4^{--} existed in solution, (2) that S and K varied with ionic strength (calculated from actual ionic concentrations) in a manner predictable by Eq. 1, and (3) that only A in Eq. 1 varied with temperature or dielectric constant. In the current calculation, assumption 2 was altered in that log S was assumed to vary with I (in this calculation, I being determined by the actual ionic concentrations) in a manner represented by the average of the curves in Fig. 22, where the supporting electrolytes were assumed to dissociate completely into their simple ions, that is, basis 1-2 for H_2SO_4, basis 3-2 for $Al_2(SO_4)_3$, etc. The log S curve at any other temperature was assumed to be given in terms of that at 25°C by Eq. 3:

$$(3) \quad \log S(t,I) = \frac{A(t)}{A(25°C)} \log S(25°C,I) \ .$$

The variation of K with I (on an ionic concentration basis) at 25°C was obtained from the data of Young,[37] and the relation given by Eq. 3 was also assumed to hold for log K; that is,

$$(4) \quad \log K(t,I) = \frac{A(t)}{A(25°C)} \log K(25°C,I) \ .$$

These calculations were carried out for 25 and 150°C and for 0.1, 0.5, and 1.0 m H_2SO_4 based on the solubilities in pure water. Contrary to expectation, the agreement with the experimental values was not noticeably better than in the previous calculations.

In contrast with the Ag_2SO_4 system, where possible complexing of Ag^+ or SO_4^{--} with ions of the supporting electrolyte cannot be deduced definitively from the solubility data, the solubility of AgCl in electrolyte solutions containing a common ion shows a dramatic behavior. From the data of Forbes,[38] Pinkus and Timmermans,[39] Pinkus, Frederic, and Shepmans,[40] and Pinkus and Shepmans[41] for the solubility of AgCl in HCl, in $AgNO_3$, and in HNO_3 the solubility products were calculated on a molality basis and on the basis of complete dissociation into simple ions. A plot of log S was then made against the square root of the stoichiometric ionic strength as shown in Fig. 23. In the case of HNO_3 media, log S approaches the Debye-Hückel limiting slope at low ionic strengths and deviates at higher ionic strengths in a manner expected from the behavior of strong 1-1 electrolyte activity coefficients. In the cases of HCl and $AgNO_3$ media the deviations from the limiting low slope clearly show strong complexing. Further, the two curves are almost coincident, which strongly implies complexing (with excess Ag^+ or Cl^-) that is symmetrical and that takes place to the same degree in both cases.

[37] T. F. Young, private communication.

[38] G. S. Forbes, *J. Am. Chem. Soc.* **33**, 1937 (1911).

[39] A. Pinkus and A. M. Timmermans, *Bull. soc. chim. Belges* **46**, 46 (1937).

[40] A. Pinkus, S. Frederic, and R. Shepmans, *Bull. soc. chim. Belges* **47**, 304 (1938).

[41] A. Pinkus and R. Shepmans, *Bull. soc. chim. Belges* **47**, 337 (1938).

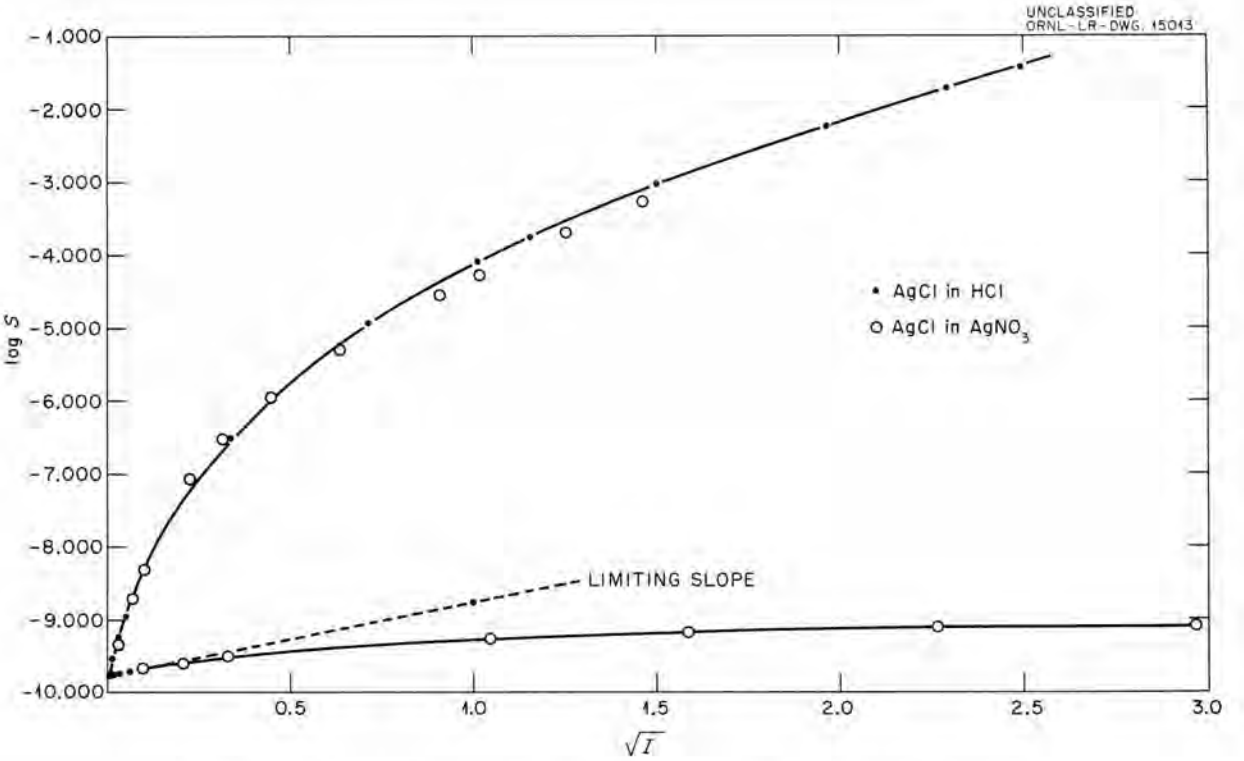

Fig. 23. Apparent Solubility of AgCl in HCl, HNO_3, and $AgNO_3$ Media.

Some idea of the extent of complexing may be obtained in the AgCl-HCl system by making the assumption that only mononuclear complexes exist and then plotting the data in the form of log S vs log m_{HCl}. On the basis of this assumption the observed S in terms of the molal solubility s and the species assumed to exist is given by

(5) $$S = (m + s)\, s \ .$$

When $m >> s$,

(6) $$S = ms = m\left(\left[Ag^+\right] + \left[AgCl\right]_{aq} + \left[AgCl_2^-\right] + \left[AgCl_3^{--}\right] + \ldots\right) .$$

If the molality solubility quotients S_i (where $i = 1, 2, \ldots n$) represent the assumed ionic equilibria

$$\underline{AgCl} = Ag^+ + Cl^- \qquad S_0$$

$$\underline{AgCl} = AgCl_{aq} \qquad S_1$$

$$\underline{AgCl} + Cl^- = AgCl_2^- \qquad S_2$$

$$\ldots \qquad \ldots$$

$$\underline{AgCl} + (n - 1)Cl^- = AgCl_n^{-n+1} \qquad S_n$$

Eq. 6 becomes

(7) $$S = S_0 + mS_1 + m^2S_2 + \ldots + m^nS_n$$

If a single silver species predominates in any HCl concentration range, then the slope of a log S vs log m curve in that region gives the number of chlorides in the predominant species, and an extrapolation of that slope to $m = 1$ gives the appropriate log S_i. For an accurate treatment of the data, corrections would have to be made for activity coefficient changes throughout the region under consideration. However, for a qualitative interpretation it may be assumed that activity coefficient changes are of the order of magnitude of the changes in the AgCl-HNO_3 curve with ionic strength and hence may be neglected.

In general, more than one species may exist to an appreciable extent in any region, and hence the slope will give an average value of i. The simplest interpretation where the slope lies between i and $i + 1$ is to assume that $AgCl_i^{-i+1}$ and $AgCl_{i+1}^{-i}$ are the principal species. If such an interpretation is made, it appears that $AgCl_2^-$, $AgCl_3^{--}$, and $AgCl_4^{---}$ become significant

species above about 0.002, 0.1, and 1 *m* HCl, respectively. Since there is no extended region where the slope is equal to a single integral value of *i*, it appears that more than one species is important throughout the whole range studied except perhaps at the lowest ionic strength values. Consistent with the interpretation given here is that of Barney, Argersinger, and Reynolds,[42] who interpreted their solubility data to give an $Ag^+/AgCl_2^-$ ratio of about unity at 0.0015 *m* KCl.

The similarity between the AgCl-HCl and AgCl-$AgNO_3$ curves suggests the existence of species like Ag_2Cl^+, Ag_3Cl^{++}, and Ag_4Cl^{+++} in the presence of excess Ag^+ at approximately the same ionic strength values where $AgCl_2^-$, $AgCl_3^{--}$, and $AgCl_4^{---}$ appear to exist in the presence of excess Cl^-. Actually, in either system or in both systems polynuclear complexes may exist. Additional information is needed to settle the question definitively.

Berne and Leden[43] interpreted solubility data for AgCl in chloride media and in $AgNO_3$ media in a manner consistent with that given above.

PREPARATION OF A LEAD DIOXIDE ELECTRODE FOR USE AT HIGH TEMPERATURES

J. V. Vaughen[44] M. H. Lietzke

Introduction

The study of the Pt, PbO_2, $PbSO_4$ electrode has been motivated by two factors: it is used as one component of the lead storage battery, and it offers a means of measuring the activity of H_2SO_4 solutions. However, various authors seem to differ in their estimation of the electrode: some credit it with erratic behavior,[45] while others have used it for thermodynamic measurements.[46,47] The present work was undertaken in an effort to develop a stable Pt, PbO_2, $PbSO_4$ electrode that could be used as an indicator electrode in systems at elevated temperatures not compatible with the hydrogen electrode. It was hoped that through the use of the Pt, PbO_2, $PbSO_4$ electrode in conjunction with a suitable reference electrode the activity of H_2SO_4 and of various other sulfate solutions could be measured at elevated temperatures.

Experimental

Two types of Pt, PbO_2, $PbSO_4$ electrodes were prepared and studied in the present work. One type was an electrode prepared according to the method suggested by Vosburgh and Craig[47] and used by Hamer.[46] Essentially, this type of electrode consisted of a platinum wire covered with a slurry of PbO_2 and $PbSO_4$. The PbO_2 was prepared by electrolysis of a solution of $Pb(NO_3)_2$ in HNO_3. After being treated in hot H_2SO_4, the PbO_2 was mixed with $PbSO_4$ and slurried in H_2SO_4 of the concentration to be studied.

The other type of electrode was prepared by plating onto platinum a hard, tightly adhering deposit of PbO_2 from a 35% HNO_3 solution saturated with $Pb(NO_3)_2$. The electrodeposition was carried out at reflux temperature (~111°C). In the course of the investigation the time of deposition was varied from a few seconds to several hours, and the current from 10 ma to 1 amp. In all cases the electrode base consisted of a spatula of platinum made by flattening a 25-mm length of 18-gage wire on one end. The platinum was sealed in a soft glass tube for support so that the average dimensions of the exposed part were $15 \times 2 \times 0.25$ mm. Connection to the platinum was accomplished by soldering stranded insulated copper wire to the end within the glass tube. The electrode was surrounded with $PbSO_4$ slurried in H_2SO_4 of the concentration to be studied. The slurry was held in place with a sleeve of Fiberglas or a wad of glass wool.

The Ag, Ag_2SO_4 reference electrode consisted of a spiral of silver wire spotted to a platinum wire which was sealed into a soft glass tube. Connection with the silver electrode was accomplished in the same fashion as with the PbO_2, $PbSO_4$ electrode. The silver spiral was surrounded with crystals of Ag_2SO_4 prepared by the method described by Archibald.[48] It was observed that the presence of $PbSO_4$ throughout the cell

[42] J. E. Barney, II, W. J. Argersinger, Jr., and C. A. Reynolds, *J. Am. Chem. Soc.* **73**, 3785 (1951).

[43] E. Berne and I. Leden, *Svensk Kem. Tidskr.* **65**, 88 (1953).

[44] Temporary summer employee (1955) from Stetson University, DeLand, Florida.

[45] D. J. Brown and J. C. Zimmer, *J. Am. Chem. Soc.* **52**, 1 (1930).

[46] W. J. Hamer, *J. Am. Chem. Soc.* **57**, 9 (1935).

[47] W. C. Vosburgh and D. N. Craig, *J. Am. Chem. Soc.* **51**, 2009 (1929).

[48] E. H. Archibald, *The Preparation of Pure Inorganic Substances*, Wiley and Sons, New York, 1932.

shortens the useful life of the Ag, Ag_2SO_4 electrode. The electrodes and solution were sealed into a Fischer and Porter tube provided with the necessary flanges to hold the Teflon ends in place. This type of apparatus was suitable for use to about 140°C; above this temperature it was no longer pressure-tight.

The electrode assembly was heated in an electric oven provided with a circulating fan. The temperature was controlled to ±1°C and was measured by means of an iron-constantan thermocouple. Electrode and thermocouple potentials were measured by means of a Rubicon portable precision potentiometer.

Results and Discussion

Since the primary purpose of the present study was to use the Pt, PbO_2, $PbSO_4$ electrode at elevated temperatures, an attempt was first made to use the type of electrode described by Hamer (the first type described above). It was observed, however, that different emf values were obtained from two different platinum wires immersed in the same PbO_2, $PbSO_4$ slurry when measured against an Ag, Ag_2SO_4 electrode. Although new platinum wires were used which showed no difference in potential between each other in H_2SO_4 solutions, they showed a difference of at least 100 mv when immersed in the PbO_2, $PbSO_4$ slurry. The same phenomenon was observed with old platinum wires that had been in contact with lead solutions. No explanation for this behavior is available, although it may be due in some way to adsorption of lead or a lead compound on the platinum.

It was possible to bring two platinum electrodes in PbO_2, $PbSO_4$ slurry to the same emf vs an Ag, Ag_2SO_4 electrode by connecting them together for a short time. The agreement was temporary, however, and an emf between them returned on standing. A pair of platinum wires sealed in glass and left for several weeks in a PbO_2, $PbSO_4$ slurry still showed a difference in potential of 1.5 mv. Because of the difficulty of obtaining reproducible results with this type of PbO_2, $PbSO_4$ electrode, attention was directed to a study of the electrode made by plating PbO_2 on platinum (the second type described above).

Hard, mechanically resistant PbO_2 for electrode purposes has been prepared by others.[49] While not all these modifications have been investigated in the present work, the method of preparation described as the second type seemed to offer the most promise. Merely plating PbO_2 onto platinum by electrolysis of $Pb(NO_3)_2$-HNO_3 solutions without regard to the concentrations and temperature given did not produce a satisfactory electrode. Besides variability in initial potential from sample to sample, the electrodes tended to suffer a decrease in potential with age.

Figure 24 shows the emf values obtained with the cell Pt, PbO_2, $PbSO_4$ (type 2), H_2SO_4(1 *m*), Ag_2SO_4(sat.), Ag as a function of temperature. The various points on the graph were obtained in the course of six different runs, each made with a new Pt, PbO_2, $PbSO_4$ electrode. The mean values of the emf (in millivolts) for the system as a function of temperature are given by the equation

$$E = 891.9 + 0.3406t \ , \tag{1}$$

obtained by the method of least squares.

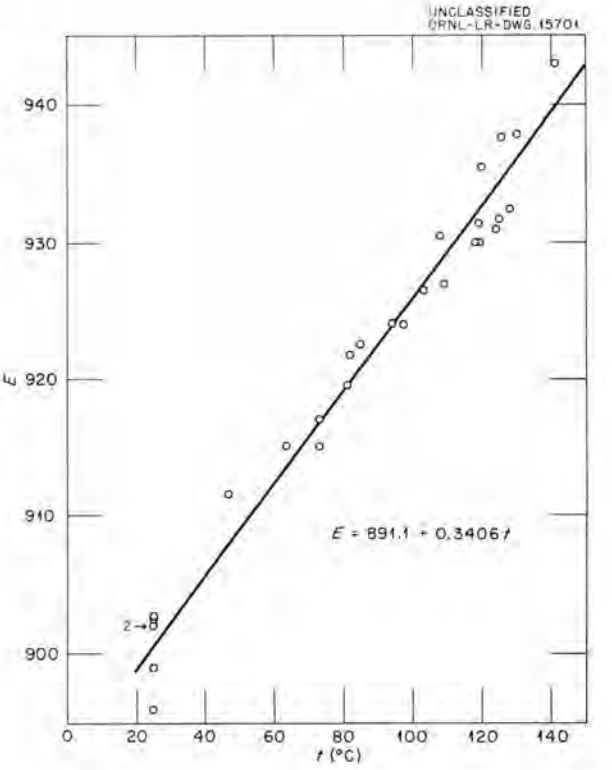

Fig. 24. The EMF of the System Pt, PbO_2, $PbSO_4$(1 *m*), Ag_2SO_4(sat.), Ag as a Function of Temperature.

[49] K. Sugino, *Bull. Chem. Soc. Japan* 23, 115 (1950).

When the Ag, Ag_2SO_4 electrode is measured against the Pt, PbO_2, $PbSO_4$ electrode in H_2SO_4, the cell reaction is

$$(2) \quad 2Ag + PbO_2 + 2H_2SO_4 = Ag_2SO_4 + PbSO_4 + 2H_2O$$

The ΔF^0 for this reaction is −47,420 calories; hence $E^0 = 1.028$ v. The $\Delta S^0 = 69.62$ e.u.; hence dE^0/dt at 25°C is 1.51 mv/deg. In order to obtain a value of E^0 at any other temperature it is necessary to integrate the expression

$$(3) \quad \left(\frac{\partial \frac{\Delta F^0}{T}}{\partial T}\right)_p = -\frac{\Delta H}{T^2},$$

where $\Delta H = \Delta H^0 + \int \Delta C_p \, dT$. The equations giving $C_p(T)$ for each substance are:

$$C_p\,(Ag) = 5.09 + 2.04 \times 10^{-3}T + 0.36 \times 10^5(T^{-2}) \text{ (ref 50)},$$

$$C_p\,(PbO_2) = 12.7 + 7.80 \times 10^{-3}T \text{ (ref 50)},$$

$$C_p\,(Ag_2SO_4) = 23.1 + 27.9 \times 10^{-3}T \text{ (ref 50)},$$

$$C_p\,(PbSO_4) = 10.96 + 31.00 \times 10^{-3}T + 4.20 \times 10^5(T^{-2}) \text{ (ref 50)},$$

$$C_p\,(H_2SO_4) = 4.0 \text{ (ref 51)},$$

$$C_p\,(H_2O) = 17.996 \text{ (ref 51)}.$$

When ΔC_p is expressed with these equations and the integration performed on the assumption that the C_p equations hold throughout the temperature range 25 to 150°C, the following equation is obtained for the free energy of the reaction as a function of temperature:

$$(4) \quad \Delta F^0 = -40{,}147 - 99.42T \log T - 23.51 \times 10^{-3}T^2 - \frac{2.28 \times 10^5}{T} + 231.2T.$$

Then E^0 may be evaluated at any desired higher temperature, since $E^0 = -\Delta F^0/nF$. At 50°C, $E^0 = 1.067$; at 100°C, $E^0 = 1.153$; and at 150°C, $E^0 = 1.248$.

In the case of the electrode system H_2, $H_2SO_4(m)$, $PbSO_4$, PbO_2, Pt studied by Hamer,[46] $dE^0/dt = 0.33$ mv/deg at 25°C, computed from entropy data, while the experimentally observed value at 25°C was 0.35 mv/deg.

The emf of the cell Pt, PbO_2, $PbSO_4$, $H_2SO_4(m)$, Ag_2SO_4(sat.), Ag can be expressed by the Nernst equation in the form

$$(5) \quad E = E^0 - \frac{RT}{2F} \ln \frac{a_w^2}{a^2_{H_2SO_4}}.$$

Therefore

$$(6) \quad E = E^0 - \frac{RT}{F} \ln a_w + \frac{RT}{F} \ln 4m^3\gamma^3,$$

where $4m^3\gamma^3 = a_{H_2SO_4}$. When $m = 1$ and $T = 298.16$°C, $a_w = 0.9620$ from vapor pressure measurements.[52] By substituting these values, the E^0 value calculated above, and the value $E = 0.9004$ from the present work into Eq. 6, it is found that $\gamma_{H_2SO_4(1m)} = 0.119$.

At $m = 1$ and $T = 323.16$°C, $a_w = 0.9627$ (ref 53) and $E = 0.9089$. The value of E was obtained by solving Eq. 1 at 50°C. When these values and the value $E^0 = 1.067$ calculated above are substituted into Eq. 6, it is found that $\gamma_{H_2SO_4(1m)} = 0.094$. When values of a_w based on a linear extrapolation of the values measured between 0 and 60°C (ref 53) are used at 100 and 150°C, it is found that $\gamma_{H_2SO_4(1m)} = 0.060$ at 100°C and $\gamma_{H_2SO_4(1m)} = 0.039$ at 150°C.

Table 19 shows a comparison of the values of $\gamma_{H_2SO_4(1m)}$ obtained in the present work and the values based on the work of Hamer[46] from 0 to 60°C. The values $\gamma_{H_2SO_4(1m)}$ (ref 46) at 100 and 150°C were calculated by using the equation for the partial molal heat content ($\bar{L}_2$) derived from Hamer's emf measurements. The equation relating

[50] K. K. Kelley, Bulletin 476, U.S. Department of the Interior, Bureau of Mines, U.S. Government Printing Office, Washington, 1949.

[51] F. D. Rossini *et al.*, *Selected Values of Chemical Thermodynamic Properties*, Circular of the National Bureau of Standards 500, U.S. Government Printing Office, Washington, 1952.

[52] S. Shankman and A. R. Gordon, *J. Am. Chem. Soc.* 61, 2370 (1939).

[53] H. S. Harned and B. B. Owen, *The Physical Chemistry of Electrolyte Solutions*, p 436, Reinhold, New York, 1950.

TABLE 19. COMPARISON OF $\gamma_{H_2SO_4(1m)}$ VALUES AS A FUNCTION OF TEMPERATURE

Temperature (°C)	$\gamma_{H_2SO_4(1m)}$*	$\gamma_{H_2SO_4(1m)}$**
25	0.119	0.130
50	0.094	0.101
100	0.059	0.065
150	0.038	0.043

*Present work.

**From work of Hamer (see ref 46).

the activity coefficient and the partial molal heat content is

$$(7) \qquad \nu\left(\frac{\partial \ln \gamma}{\partial T}\right)_m = \frac{-\bar{L}_2(T)}{RT^2} ,$$

where $\nu = 3$ for H_2SO_4 and

$$(8) \qquad \bar{L}_2(T) = \bar{L}_2(0) + \alpha(T - 273.16) + \beta(T - 273.16)^2 .$$

When Eq. 8 is substituted into Eq. 7 and the integration performed between the limits of 273.16 and T, Eq. 9 is obtained:

$$(9) \qquad \nu \ln \frac{\gamma_T}{\gamma_{273.16}} = \left[\frac{\bar{L}_2(0)}{273.16RT} + \frac{273.16\beta - \alpha}{RT} + \frac{\beta}{R}\right](273.16 - T) + \left[\frac{2(273.16)\beta - \alpha}{R}\right] \ln \frac{T}{273.16} .$$

When the appropriate values of the constants[46] are substituted into Eq. 9, the values of $\gamma_{H_2SO_4(1m)}$ (ref 46) at 100 and 150°C can be calculated.

In order to check the slope of Eq. 1 it was observed that, for the cell whose reaction is described by Eq. 2,

$$(10) \quad \frac{dE}{dT} = \frac{S^0_{Ag_2SO_4} + S^0_{PbSO_4} - 2S^0_{Ag} - S^0_{PbO_2}}{nF} - \frac{2\left(\partial\bar{F}_{H_2O}/\partial T\right)}{nF} + \frac{2\left(\partial\bar{F}_{H_2SO_4}/\partial T\right)}{nF} ,$$

where S^0_i is the molal entropy of each substance in its standard state and $\bar{F}_i$ is the partial molal free energy of the substances indicated.

When the appropriate values are substituted into Eq. 10, it is found that $dE/dT = 0.50$ mv/deg. This compares with the observed value of 0.34 mv/deg. These values may be within experimental error due to uncertainties in the entropy and activity values. (In the calculation the term $\partial \ln a_{H_2SO_4}/\partial T$ was computed by using Hamer's γ values, while the entropy values were taken from the Bureau of Standards compilation.[51]

A similar calculation applied to the system H_2, $H_2SO_4(m)$, $PbSO_4$, PbO_2, Pt used by Hamer shows a calculated slope of −0.16 mv/deg in 1 m H_2SO_4, against a measured slope of −0.12 mv/deg.

ISOPIESTIC EQUIPMENT FOR THERMODYNAMIC STUDIES AT ELEVATED TEMPERATURES

B. A. Soldano R. W. Stoughton

In recent years the isopiestic method for investigating the thermodynamic properties of solutions has gained prominence and has been shown to be a method of intrinsic flexibility and simplicity. The technique is essentially one in which a salt solution is equilibrated with a standard solution of fixed solvent activity. At equilibrium the solvent activity in both solutions will be equal; hence, by a series of weight measurements on standard and unknown solutions, data may be obtained from which the osmotic coefficients and the activity coefficients of the solute may be calculated.

The interest of the Laboratory in high-temperature solution behavior naturally raised the question of the feasibility of the isopiestic technique at elevated temperatures. Previous attempts to apply the method at elevated temperatures had not met with success, since the equilibration vessel had to be opened in order for the samples to be weighed. In the current attempt the program undertaken was the design, development, and construction of an

isopiestic unit which would permit the equilibration of 20 dishes at elevated temperatures and pressures in a vacuum-tight system and which would allow the transfer and weighing of the dishes periodically inside the equilibration vessel by remote control. The unit has now been constructed, and preliminary tests have been made on the operability of the design up to 140°C and in the presence of high water-vapor pressure.

The essential features involve weighing with a magnetic balance, which is constructed of titanium and the deflections of which are monitored by means of a microformer pickup. The weight is obtained, in principle, by reading the current required to create a field just sufficient to keep a permanent magnet attached to the balance pan from moving downward. In actual practice the potential drop across a standard resistance is read with a Rubicon B potentiometer. The dishes after equilibration on a copper block are weighed by bringing them around in a circle one space at a time as each one, in turn, is lowered onto the balance pan. Each movement of the dishes involves raising them all on a wheel, turning the wheel one space by a torsional motion, and then lowering the wheel again. The vertical and torsional motions are conducted by means of a bellows and rotating vacuum seal.

The equilibration vessel is made of stainless steel. The head is held in place with some 20 bolts and sealed vacuum-tight with a 16-in.-dia Teflon gasket. This seal was found to enable the maintenance of a vacuum of 200 μ over extended periods of time and is believed to be adequate for isopiestic measurements at elevated temperatures. The equilibration vessel rests inside an insulated thermostatted tank. A brief diagram of the unit is given in Fig. 25.

The sensitivity of the balance is indicated by the following tabulation, in which are listed the voltages required to balance the corresponding weights; the voltages should be linear with test weights.

Volts (× 10)	Weight (mg)
0.00347	5
0.01320	20
0.03280	50
0.06527	100
0.13151	200
0.32819	500
0.65630	1000

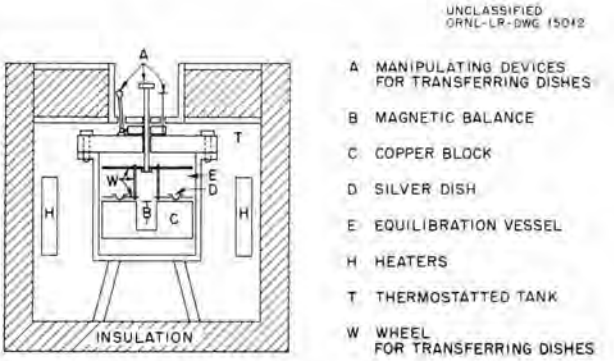

Fig. 25. Simplified Diagram of High-Temperature Isopiestic Unit.

It can be seen that the balance in its present form is sensitive to milligram changes in weight and is fairly linear in its response.

The reproducibility of the balance was then tested at elevated temperatures (i.e., up to 140°C). The actual operational reproducibility of the unit at 140°C is shown below:

Number of Weighings and Transfers of Same Dish	Volts (× 10)	Deviations (mg)
1	0.27190	0.0
2	0.27200	+ 0.2
3	0.27185	− 0.1
4	0.27190	0.0
5	0.27190	0.0

These tests at elevated temperatures also give a measure of the reproducibility of the mechanical transfer equipment in the unit, since the weight read from the balance is very sensitive to the exact positioning of the dish. In order to decrease the energy put into the equilibration vessel during weighing and in order to increase the accuracy, most of the weight of the dishes is balanced by a tare, and therefore the readings show only the difference.

An examination of the reproducibility data reveals that the balance remains sensitive to milligram weight changes at elevated temperatures and that the small irreproducibilities in the positioning system introduce no serious deviations. These data, however, do not test long-time effects concerning reproducibility.

The real test of the over-all operability and corrosion stability could be accomplished only by

measuring the water pickup of salt solutions in an atmosphere of high water-vapor pressure at elevated temperatures. To make the test a rigid one, some samples were placed in the chamber in a relatively concentrated form; others, along with a standard reservoir, were in a relatively dilute form, and one dish was left empty. The purpose of this run was to test whether difficulties might arise resulting from thermal fluctuations inherent in the unit through faulty design (e.g., undesirable condensation onto "cold spots") and whether the dishes containing the more concentrated solutions would come to equilibrium in a satisfactory manner. It is well known in isopiestic work that, although the same equilibrium concentration must be attained either by dilution or concentration of a solution, in practice it is far easier to attain equilibrium by weight loss than by weight gain.

Into each of two dishes was put 1 cc of a 2.45 *N* NaCl solution, and into each of three others was put 1 cc of 0.49 *N* NaCl solution. Into a standard reservoir was put 200 cc of the 0.49 *N* solution. All these vessels were placed in the unit, and the temperature was adjusted to 83.35°C.

At equilibrium the solution in each of the dishes originally containing 1 cc of the standard 0.49 *N* NaCl now weighed approximately 0.7750 g. This indicated that the normality of the standard had increased to about 0.63 *N* by loss of water. This loss is consistent with the water required to saturate the chamber and dilute the other salt solutions. In any case, since there was exactly 5 times more NaCl in the 2.45 *N* NaCl solution than in the 0.49 *N* NaCl, at equilibrium the weights of the solutions in the two sets of dishes should differ by a factor of 5.

With a weight of 0.7752 g used for the contents of one of the dishes containing the 0.63 *N* NaCl standard solution at equilibrium, a value of 3.876 g was calculated for the contents of each of the dishes which originally contained 2.45 *N* NaCl. This weight is only about 1% or so different from the actual weight of about 3.820 g contained by three separate dishes (see Table 20).

Thus, it appears that the system approached equilibrium in about eight days. Triplicate dishes placed in different positions in the unit agreed well to within 1%.

In this test the air had not been evacuated initially from the chamber. It is reasonable to expect that the reduction in the mean free path of the water molecules in the presence of air may have reduced the rate of attaining equilibrium, and hence initial evacuation in future work may reduce the time required for equilibration. On the other hand, the slowest step in the over-all process may occur in solution, in which case the elimination of air may not be important.

The fact that the weight of the empty dish (Table 20) showed no change over this period strongly suggests that any thermal fluctuations did not result in condensation of the vapor even at the high water activities obtaining during the run. The occurrence of "rain" or condensation due to thermal fluctuations is known to be a serious problem in isopiestic work.

After three weeks of continuous operation, with the standard weights showing no change in weight reading (a good indication that the unit was operating properly), minor difficulties due to a faulty connection in an electrical circuit were noted. This afforded an opportunity to examine the inside

TABLE 20. RATE AND REPRODUCIBILITY CHARACTERISTICS OF ISOPIESTIC UNIT AT 83.35°C

Days Equilibrated	Weight (g) of 1 cc of Original 0.49 *N* NaCl Standard Solutions		Weight (g) of 1 cc of Samples of 2.45 *N* NaCl Solutions			Empty Silver Dish (in Excess of Tare)
	I	II	1	2	3	
0			~1.0	~1.0	~1.0	1.7360
3	0.7745	0.7760	2.4944	2.5306	2.6533	1.7363
4	0.7752	0.7750			3.0156	1.7450
7	0.7750		3.8793	3.7444	3.7402	1.7506
8	0.7753	0.7750	3.8237	3.818	3.8043	1.74050

of the unit. None of the inner workings (electrical and mechanical) showed any evidence of corrosion or related breakdown save for a small nickel-plated alnico magnet used in the balance. This component could be used in a slightly eroded condition if the operating clearances were enlarged. However, a magnet which will not corrode significantly is preferred. New materials are now being tested for this purpose. No perceptible breakdown has been noted in the electrical system which operates with microampere currents; it appears to be stable under the rather severe operating conditions.

In summary, the high-temperature isopiestic unit appears to be stable and operational within milligram accuracy. Changes are being effected which should increase the sensitivity of the system.

STABILIZATION OF ThO_2 SOLS

F. H. Sweeton

Previous to this period a ThO_2 sol designated as "Sol E" had been prepared and studied as a first step in evaluating the use of ThO_2 sols for blankets in nuclear reactors. This particular preparation, with $Th(NO_3)_4$ used as a peptizing agent, had been shown to have a thorium concentration of 2.5 moles/liter, a nitrate concentration of 0.9_7 mole/liter, and an average ThO_2 crystallite diameter of about 56 Å according to x-ray data. The sol had been found to flocculate in a matter of minutes when heated to 200°C.

During the present period the study of Sol E was continued with measurements of its viscosity, pH, refractive index, and electrolytic conductance. The relative viscosity was found to be 1.4_8 at 25°C. The pH as determined by both a methyl orange indicator and a standard pH meter with glass and calomel electrodes was about $3._0$ units. The refractive index at 25°C was found to be 1.389. The electrolytic conductivity measured at the same temperature was 0.0125 mho, which is about one-fourth the conductance of a $Th(NO_3)_4$ solution having the same nitrate concentration as the sol. These conductance results indicate that there is considerable interaction between the ThO_2 and the $Th(NO_3)_4$ in the sol.

According to the theory of sol stability as given by Verwey and Overbeek,[54] increasing the particle size should increase the stability; therefore an effort is being made to prepare sols with large particles. Since it appears that the crystallites are formed during the peptization step, the temperature, rate of ThO_2 addition, and concentration of $Th(NO_3)_4$ during peptization are being correlated with the resulting crystallite size.

This interest in crystallite size has resulted in a simultaneous study of the feasibility of studying particle size by means other than x rays. Use of a spectrophotometer is being tried, in spite of the disadvantage that loss in light passing through the sample can be due to absorption as well as to scattering by particles. However, the simplicity of the measurement makes further study worthwhile. In addition, plans are being made to try a sensitive light-scattering instrument.

[54] E. J. W. Verwey and J. T. G. Overbeek, *Theory of the Stability of Lyophobic Colloids*, Elsevier, New York, 1948.

CONCENTRATED SALT SOLUTIONS FOR REACTOR FUEL MEDIA OR HEAT EXCHANGER FLUIDS

W. L. Marshall F. J. Loprest
C. H. Secoy

It has been suggested that aqueous salt solutions might be of interest as heat transfer agents for use in atomic power reactors. Presumably, by dissolving a salt in water, the vapor pressure of water could be lowered sufficiently for power removal operations to be carried out at higher temperatures and still not exceed a particular maximum pressure limitation. The higher operating temperature would result in greater thermodynamic efficiency, provided other properties of the water-salt system were favorable or, if unfavorable, were offset by the higher available temperature.

It is perhaps possible that concentrated aqueous salt solutions could be adapted for use in homogeneous reactors utilizing either solutions or slurries. For example, soluble uranium salts could be dissolved in a high-concentration aqueous salt solution to produce a final solution of low vapor pressure. Such a system might also alleviate the problem of hydrolytic precipitation characteristic of very dilute uranyl salt solutions. As another alternative, concentrated aqueous salt solutions could well provide stable media for the suspension of insoluble UO_3 or ThO_2 to form slurries capable of fueling a reactor. These slurries would possess considerably lowered vapor pressures compared with pure water-solid slurries. In addition, the higher viscosities and the electrolytic character of the aqueous salt solution—

solid suspension might possibly tend to stabilize the suspension, thereby reducing over-all settling rates. Also, the higher viscosity of the mixture compared with water might tend to reduce erosion effects caused by the suspended solid particles. In other words, the solid particles might be "cushioned."

There is a good possibility that aqueous salt heat transfer systems will be radiation and thermally stable as contrasted with the radiation and thermal decomposition of organic liquids, that is, diphenyl and others, at high temperature. In comparison with fused salt systems, which are solids at room temperature, aqueous salt solutions can be selected which are liquid from 25°C to temperatures above 400°C. In addition, an appreciable concentration of moderator is present as hydrogen or deuterium constituents of water, thus providing suitable conditions for thermal reactors.

The purpose of this investigation was to select and explore several aqueous salt systems with respect to vapor-pressure lowering. Several factors were considered in their selection:

1. The salt selected must show sufficiently high solubility in water throughout the high temperature range.

2. A high solubility is necessary in order to obtain a sufficient vapor-pressure lowering. Several salts, which otherwise appear attractive, have not been studied because they almost certainly undergo sufficient hydrolysis to yield precipitates at elevated temperatures; among these are zirconium and beryllium compounds.

3. It is desirable, but not necessary, that the water-salt system be liquid at room temperature.

4. The salt must have sufficient thermal and radiation stability in water, and the nuclide components of the salt must have low neutron absorption cross sections and must not produce highly radioactive daughter nuclides.

5. In addition, the usual properties of heat exchanger fluids such as viscosity, heat capacity, thermal conductivity, and density, must be considered.

With these factors in mind, the following aqueous salt systems were selected for vapor-pressure measurements: 3.8 m Li_2SO_4 plus 3.8 m UO_2SO_4 (combined solution); Li_2SO_4 (sat.); $MgSO_4$ (sat.); 50.0 wt % $LiNO_3$; and several $Ca(NO_3)_2$ solutions.

The experimental data were obtained by direct measurement of vapor pressure by the use of, in most of the runs, a precision Heise pressure gage. Data for all systems studied are comparatively shown in Tables 21 and 22 and in Fig. 26. Experimental data were obtained at every 2- to 5-deg interval; however, in Fig. 26 and in the tables, only the data at approximately 10-deg intervals are given. The actual vapor pressure can be obtained by multiplying the ratio p/p_0, where p = experimental pressure and p_0 = saturated steam pressure, by the vapor pressure of saturated steam at the particular temperature.

The data indicate no large changes of p/p_0 as a function of temperature, at least up to 400°C. It is not certain at this time whether the small changes of p/p_0 with temperature for each particular curve are significant or whether they are due to inaccuracies arising from experimental techniques. The solution concentrations are those at room temperature and do not represent the true concentration at the high temperature. The high-temperature concentrations, however, should not differ from the room-temperature value by more than several per cent at the highest temperature.

In Fig. 27, p/p_0 measured at 350°C is plotted as a function of the mole fraction of $Ca(NO_3)_2$. A mole fraction of 0.2 corresponds to the stable solid hydrate, $Ca(NO_3)_2 \cdot 4H_2O$, at room temperature. This solid melts at 42.7°C to form a liquid which is apparently stable to above 400°C. A slight orange-red vapor phase coloration is observable in sealed silica tubes in the temperature range 450 to 500°C, thus indicating some decomposition of the nitrate to nitrogen oxides. Lithium nitrate–water solutions apparently are as stable as $Ca(NO_3)_2 \cdot H_2O$. A 50.0 wt % $LiNO_3$ solution is liquid from room temperature to above 400°C.

Figure 28 indicates the possible increase in operating temperature for $Ca(NO_3)_2 \cdot 4H_2O$ liquid over that of pure water at a particular temperature and pressure. For example, at 350°C at a saturated steam pressure of 2398 psi, $Ca(NO_3)_2 \cdot 4H_2O$ liquid could be used at 412°C (i.e., 350 + 72°C) at the same vapor pressure. Since the line in Fig. 28 is essentially straight, it can be represented by the equation $\Delta t = 0.1875t + 7.00$.

In conclusion, favorable vapor-pressure lowering could be achieved by using concentrated aqueous salt solutions which might indicate possible advantages to be attained over pure water, organic, and fused salt heat transfer agents. It would remain to be seen how the other heat transfer

TABLE 21. VAPOR-PRESSURE DATA OF SEVERAL SALT-WATER SYSTEMS

50.0 wt % $LiNO_3$ (14.5 *m* or 0.207 mole fraction)		3.8 *m* Li_2SO_4 + 3.8 *m* UO_2SO_4		Li_2SO_4 (sat.)		$MgSO_4$ (sat.)	
t (°C)	p/p_0*	*t* (°C)	p/p_0	*t* (°C)	p/p_0	*t* (°C)	p/p_0
214	0.407	220	0.71	240	0.97	225	0.92
220	0.407	225	0.70	245	0.90	235	0.92
225	0.405	230	0.73	248	0.88	245	0.91
230	0.402	240	0.72	250	0.91	256	0.98
234	0.401	245	0.73	252	0.94	260	0.96
238	0.399	250	0.74	260	0.95	262	0.97
243	0.399	255	0.75	265	0.96	267	0.95
250	0.399	260	0.75	270	0.97	275	0.94
254	0.405	270	0.78	275	0.98	281	0.96
259	0.403	275	0.79				
270	0.407	280	0.81				
275	0.406	285	0.81				
280	0.408						

*p_0 = pressure of saturated steam (Osborne and Myers, U.S. Bureau of Standards); p = experimental pressure of the solution.

factors and the radiation stability would compare with those of the other liquid media mentioned above after the differences in allowable operating temperatures and in the other factors were considered.

A STUDY OF DILUTE SOLUTIONS IN THE SYSTEM UO_2SO_4-$CuSO_4$-$NiSO_4$-H_2SO_4-H_2O

F. E. Clark R. Slusher
J. S. Gill C. H. Secoy

The purpose of the study on the system UO_2SO_4-$CuSO_4$-$NiSO_4$-H_2SO_4-H_2O was to ascertain the maximum temperature at which solutions of specified compositions could be held without the appearance of a nonhomogeneity. A nonhomogeneity might involve the formation of a second liquid phase or the formation of one or more solid phases. The composition variables were limited to selected values for each of the components in the range of HRT interests. The nominal values chosen were:

	Molality
UO_2SO_4	0.04
$CuSO_4$	0, 0.005, 0.01, 0.02, 0.03, 0.04
$NiSO_4$	0, 0.01, 0.02, 0.03, 0.04
H_2SO_4	0.01, 0.02, 0.03

Ninety stock solutions representing all combinations of these values were prepared. The analysis of these solutions has not been completed, but in all completed cases the analytical values agree with the nominal concentrations within a few per cent.

The method of determining the phase transitions points consisted in sealing samples of the solution in 1-mm quartz tubing and observing the solution with a 6X telemicroscope while the tube was being heated in an aluminum block furnace. Agitation was obtained by intermittent vibration of the tube with a Burgess Vibra-Tool.

TABLE 22. VAPOR PRESSURES OF $Ca(NO_3)_2$-H_2O SOLUTIONS

Concentration of $Ca(NO_3)_2$ (wt %)											
69.5 (13.8 *m* or 0.20 mole fraction)		61.6 (9.80 *m* or 0.15 mole fraction)		50.3 (6.17 *m* or 0.10 mole fraction)		37.7 (4.50 *m* or 0.075 mole fraction)		32.4 (2.92 *m* or 0.05 mole fraction)		Pure Water	
t (°C)	p/p_0	t (°C)	p/p_0	t (°C)	p/p_0	t (°C)	p/p_0	t (°C)	p/p_0	t (°C)	p/p_0
200	0.413	200	0.622	201	0.622	204	0.898	200	0.942	200	1.000
212	0.417	211	0.603			217	0.888	212	0.930	210	1.014
222	0.432	222	0.571	212	0.656	228	0.869	222	0.943	225	1.000
234	0.411	234	0.569			239	0.832	230	0.953	235	1.004
250	0.407	246	0.575	222	0.657	247	0.848	238	0.959	245	1.007
264	0.420	250	0.575	228	0.665	257	0.838	246	0.968	250	1.009
278	0.421	258	0.589	238	0.672	271	0.838	250	0.967	260	1.013
297	0.435	266	0.593	245	0.679	283	0.819	258	0.974	270	1.006
313	0.436	274	0.600	250	0.679	292	0.810	266	0.973	280	1.010
322	0.437	282	0.604	260	0.687	313	0.810	278	0.972	290	1.002
330	0.434	290	0.608	273	0.695	319	0.804	286	0.963	300	1.005
336	0.434	298	0.609	280	0.706	334	0.802	294	0.961	310	1.008
340	0.434	306	0.607	290	0.701	340	0.806	300	0.951	320	1.002
347	0.433	314	0.606	300	0.699	354	0.790	308	0.948	330	1.007
350	0.434	322	0.602	310	0.699	360	0.783	318	0.935	345	0.999
355	0.428	330	0.600	321	0.696	370	0.783	324	0.927	350	1.002
360	0.425	338	0.577	330	0.691			332	0.922	360	1.006
365	0.428	348	0.573	340	0.692			340	0.911	370	1.012
370	0.426	358	0.542	350	0.686			348	0.901	374	1.018
		368	0.545	360	0.683			356	0.891		
		370	0.544	370	0.678			365	0.883		
		380	0.54*	380	0.67*			372	0.879		
		388	0.54*	390	0.68*			380	0.88*		
				400	0.67*			390	0.88*		
								400	0.88*		

*Using extrapolated values for p_0.

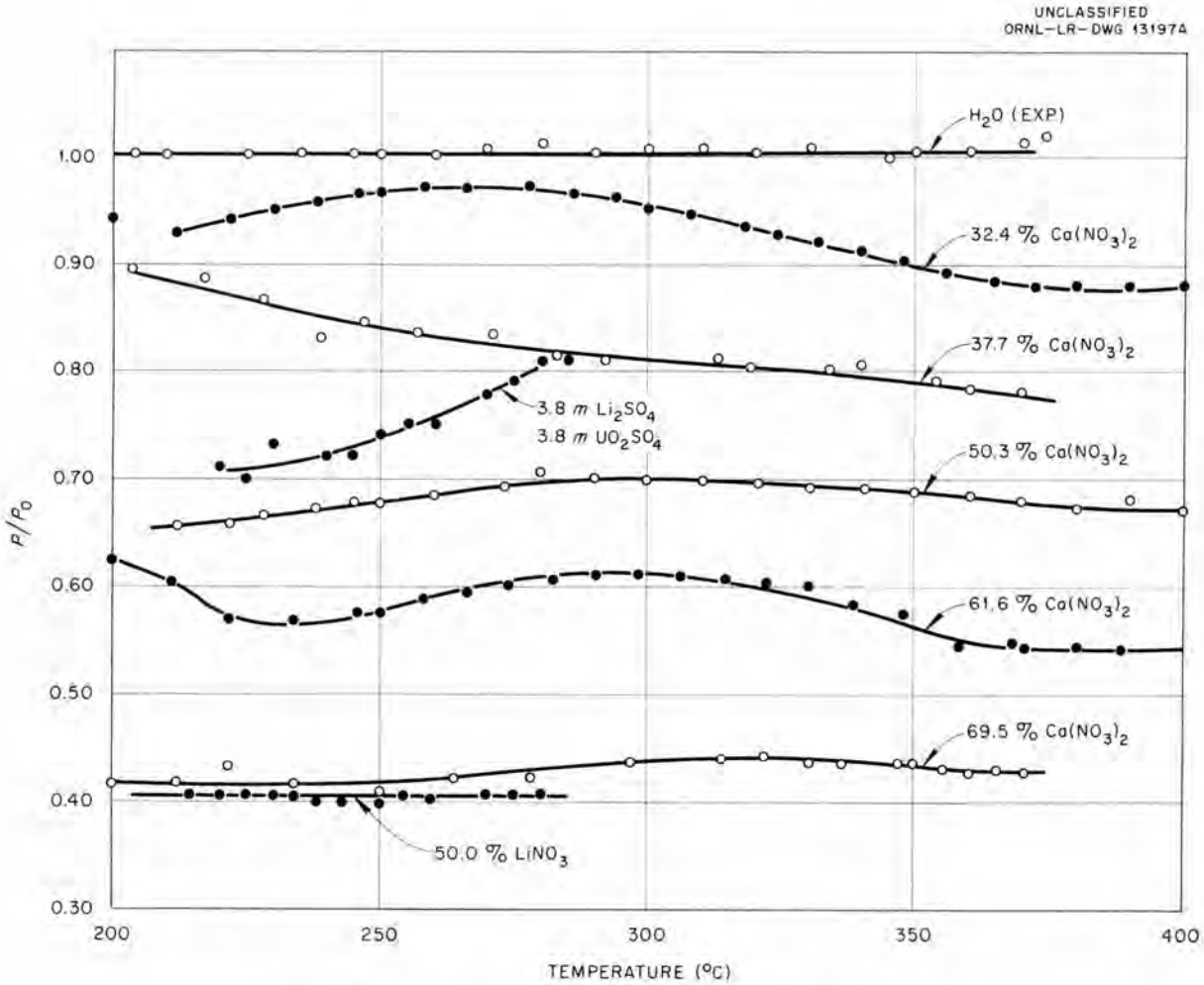

Fig. 26. Vapor Pressures of Several Aqueous Salt Solutions.

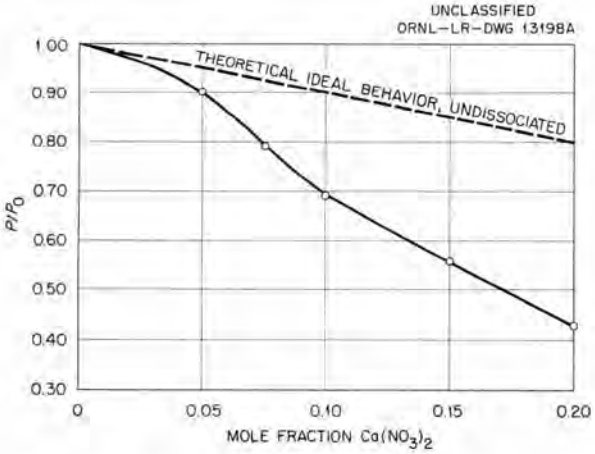

Fig. 27. Vapor Pressures of $Ca(NO_3)_2$ Solutions at 350°C.

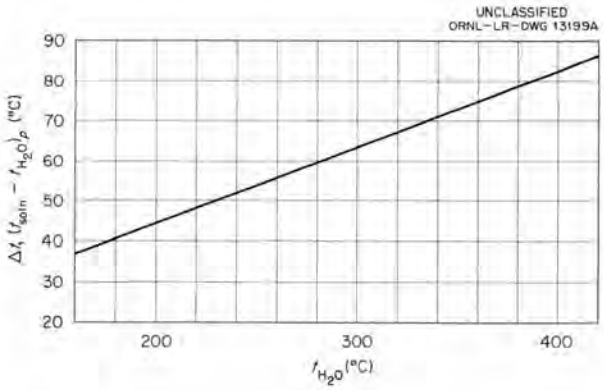

Fig. 28. Comparison of $(t_{soln} - t_{H_2O})$ at Constant Pressure.

Early in the work some indication of attack on the quartz was observed after 30 min or more of heating. Therefore all tubes were arbitrarily limited to not more than 15 min in the hot furnace. For each solution a series of tubes was employed, the first being used to determine the approximate temperature of transition and the succeeding tubes used to fix the temperature more accurately and to verify the observation by duplication. The short duration of the equilibration and the rather limited stirring obtainable introduce doubt as to whether equilibrium was really established. This fact, as well as uncertainty as to the amount of corrosion of the quartz, makes the data presented in Table 23 of only qualitative value. Further doubt as to the validity of the temperatures as given arises from the fact that, even though the phase transitions in all cases were sharp and reversible, the amount of material involved is very small. The initial appearance of the solids was usually very difficult to detect, and redissolving of the crystals upon lowering the temperature was usually too slow for the arbitrarily imposed time limit.

TABLE 23. OBSERVED TEMPERATURES OF THE APPEARANCE OF NONHOMOGENEITY IN THE SYSTEM UO_2SO_4-$CuSO_4$-$NiSO_4$-H_2SO_4-H_2O

Solution No.	$CuSO_4$ (m)	$NiSO_4$ (m)	New Phase*	Temperature (°C)
	0.04 m UO_2SO_4; 0.01 m H_2SO_4			
4001	None	None	2 LP	335
4011	None	0.01	2 LP	325
4021	None	0.02	YS	295
4031	None	0.03	YS	<288
4041	None	0.04	YS	247
4501	0.005	None	2 LP**	318
4511	0.005	0.01	2 LP	323
4521	0.005	0.02	YS	287
4531	0.005	0.03	YS	265
4541	0.005	0.04	YS	231
4101	0.01	None	2 LP	318
4111	0.01	0.01	2 LP	317
4121	0.01	0.02	YS	280
4131	0.01	0.03	YS	<273
4201	0.02	None	2 LP	316
4211	0.02	0.01	2 LP	313
4221	0.02	0.02	YS + GS	277
4231	0.02	0.03	GS	255

TABLE 23 (continued)

Solution No.	$CuSO_4$ (m)	$NiSO_4$ (m)	New Phase*	Temperature (°C)
	0.04 m UO_2SO_4; 0.01 m H_2SO_4			
4301	0.03	None	2 LP	308
4311	0.03	0.01	GS	255
4321	0.03	0.02	GS	238
4331	0.03	0.03	GS	220
4401	0.04	None	GS	256
4411	0.04	0.01	GS	226
4421	0.04	0.02	GS	215
4431	0.04	0.03	GS	208
	0.04 m UO_2SO_4; 0.02 m H_2SO_4			
4002	None	None	2 LP	345
4012	None	0.01	2 LP	328
4022	None	0.02	2 LP	313
4032	None	0.03	YS	279
4042	None	0.04	YS	268
4502	0.005	None	2 LP**	327
4512	0.005	0.01	2 LP	323
4522	0.005	0.02	2 LP	316
4532	0.005	0.03	YS	291
4102	0.01	None	2 LP	330
4112	0.01	0.01	2 LP	332
4122	0.01	0.02	2 LP	315
4132	0.01	0.03	YS	272
4202	0.02	None	2 LP	322
4212	0.02	0.01	2 LP	323
4222	0.02	0.02	2 LP	314
4232	0.02	0.03	2 LP	315
4302	0.03	None	2 LP	320
4312	0.03	0.01	2 LP	314
4322	0.03	0.02	YS	311
4332	0.03	0.03	YS	283
4402	0.04	None	2 LP	324
4412	0.04	0.01	YS	260
4422	0.04	0.02	GS	313
4432	0.04	0.03	GS	241

*2 LP indicates appearance of second liquid phase; YS indicates appearance of white, yellowish-white, or orange-yellow solid; GS indicates appearance of green or bluish-green solid.

**Produced finely divided red solid upon quenching.

TABLE 23 (continued)

Solution No.	$CuSO_4$ (m)	$NiSO_4$ (m)	New Phase*	Temperature (°C)
	0.04 m UO_2SO_4; 0.03 m H_2SO_4			
4003	None	None	2 LP	352
4013	None	0.01	2 LP	333
4023	None	0.02	2 LP	322
4033	None	0.03	YS	311
4043	None	0.04	YS	291
4503	0.005	None	2 LP	332
4513	0.005	0.01	2 LP	335
4523	0.005	0.02	2 LP	323
4533	0.005	0.03	2 LP + YS	335
4103	0.01	None	2 LP	335
4113	0.01	0.01	2 LP	334
4123	0.01	0.02	2 LP	323
4133	0.01	0.03	YS	290
4203	0.02	None	2 LP	328
4213	0.02	0.01	2 LP	328
4223	0.02	0.02	2 LP	323
4233	0.02	0.03	2 LP	323
4303	0.03	None	2 LP	326
4313	0.03	0.01	2 LP	324
4323	0.03	0.02	2 LP	328
4333	0.03	0.03	2 LP	320
4403	0.04	None	2 LP	328
4413	0.04	0.01	2 LP	325
4423	0.04	0.02	2 LP	<331
4433	0.04	0.03	YS	299

*2 LP indicates appearance of second liquid phase; YS indicates appearance of white, yellowish-white, or orange-yellow solid; GS indicates appearance of green or bluish-green solid.

**Produced finely divided red solid upon quenching.

No effort has been made to identify any of the solid phases. In the table they have been placed in one of two groups designated as "YS" (yellow solid) and "GS" (green solid), respectively. All species in the YS group probably contain uranium, and members of the GS group may contain uranium. Two of the solutions, Nos. 4501 and 4502, yielded a finely divided red solid upon quenching from temperatures above about 250°C. The red solid could not be obtained without the quench, and it slowly redissolved. It appears to be the same as a red solid obtained in earlier work as an equilibrium phase in solutions of lower excess acid concentration and which was tentatively identified as a copper uranate. Other possible solid phases which have previously been identified include the following:

$NiO \cdot 2.5UO_3 \cdot SO_3 \cdot xH_2O$	Yellow
$NiO \cdot 4UO_3 \cdot 2SO_3 \cdot yH_2O$	Orange-yellow
$3CuO \cdot SO_3 \cdot 2H_2O$	Green
$4CuO \cdot SO_3 \cdot 3H_2O$	Green
$CuO \cdot 2UO_3 \cdot 2SO_3 \cdot 7H_2O$	Dark green

Several general conclusions appear to be valid from an inspection of the data. At low copper or nickel concentrations the initial phase separation is the appearance of the second liquid phase. Increasing either the copper sulfate concentration or the nickel sulfate concentration lowers the temperature of phase separation slightly. Increasing the acid concentration elevates the temperature, it being more effective in the absence of copper and nickel than in their presence. At higher nickel or copper concentrations a solid phase appears at temperatures lower than two-liquid-phase phenomena, and, as either of these ion concentrations increases further, the temperature of precipitation drops rapidly. Increasing the excess acid alleviates this effect somewhat. The data indicate that operation of the HRT at the maximum design temperature (300°C) with the proposed solution composition will result in partial or complete precipitation of the uranium if the nickel concentration is allowed to rise to more than about 0.02 m. It is assumed that there will be 0.02 m excess acid (50% based on the uranium) plus enough acid to equal the nickel concentration. Conditions in the pressurizer appear to be in an even more doubtful state.

CHEMISTRY OF CORROSION

The program of fundamental studies dealing with the electrochemistry of corrosion comprises the following topics: passivity and the action of corrosion inhibitors of the type XO_4^{n-}; the action of foreign ions upon the electrode potential of iron and stainless steel; the polarization and corrosion properties of stainless steel; and the effect of radiation upon the electrochemistry of different systems.

PASSIVATION AND INHIBITION

G. H. Cartledge

In a previous report,[1] the passivating action of aqueous solutions of osmium(VIII) oxide (OsO_4) upon iron and carbon steel was described. This study was extended to determine quantitatively the electrode potential of electrolytic iron in 0.039 *f* osmic acid and the effect of foreign electrolytes upon the potential. These measurements were designed to supplement similar study[2] of the inhibiting ions TcO_4^-, MoO_4^{--}, and WO_4^{--}, all of which, in aerated solutions of sufficient concentration, produced noble electrode potentials, which, however, were sensitive to debasing by low concentrations of foreign ions. The results with these inhibitors were interpreted in terms of a labile, competitive adsorption of the inhibitor ions. The nobility was shown to be dependent also upon an oxidation process, however, since the weakly oxidizing molybdate and tungstate ions produced noble potentials only in the presence of oxygen.

In the osmium experiments, it was found that when electrolytic iron was immersed in 0.039 *f* osmic acid at 24°C the electrode potential came to a stable value within an hour or two, as a rule. This potential was measured in the manner described in previous reports, making use of a saturated calomel half cell as the reference electrode. No visible film formed during the few hours involved in making the potential measurements.

Since the literature contains no experimental value of the potential of the OsO_2-OsO_4 couple, this system was examined for comparative purposes. Platinum electrodes were coated electrolytically with a film of hydrated osmium(IV) oxide and measured in a supporting electrolyte consisting of sodium sulfate or sodium phosphate at various pH values. It was found possible to obtain reversible potentials in the pH range of 3.5 to 6.5. The measurements led to an E^0 value of −0.964 ± 0.002 v for the half-cell reaction

$$Os(OH)_4(ppt) \rightleftharpoons OsO_4(aq) + 4H^+ + 4e^-$$

The details of these measurements are to be published.[3]

Figure 29 shows measurements obtained when an electrolytic iron electrode and a coated platinum electrode were immersed in the same solution of 0.039 *f* osmic acid at different pH values. It will be seen that, within a few mv, the iron and platinum electrodes indicated the same potential. To demonstrate the independence of the platinum and iron electrodes in the system, another experiment is shown in which the iron electrode and two coated platinum electrodes were simultaneously measured. After the potentials had stabilized at the same value, the platinum electrodes were polarized by passage of a current of about 1 ma for 5 sec. As may be seen from Fig. 30, the three electrodes returned to essentially the same potential after the polarizing current was stopped.

In other measurements at 24°C it was shown that the noble potential in the osmium solution is also sensitive to the presence of added sulfate

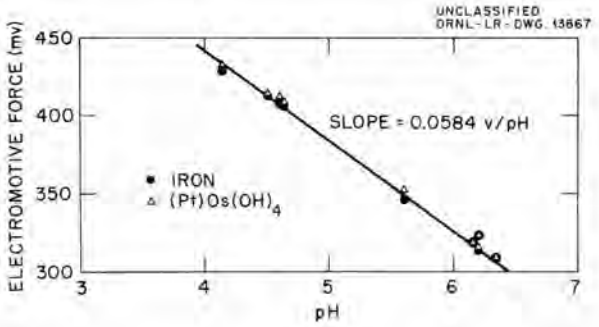

Fig. 29. Electrolytic Iron Passivated in Osmium(VIII) Oxide, 24°C.

[1] G. H. Cartledge, *Chem. Semiann. Prog. Rep. June 20, 1954*, ORNL-1755, p 13.

[2] G. H. Cartledge and R. F. Sympson, *Chem. Semiann. Prog. Rep. Dec. 20, 1955*, ORNL-2046, p 10; *J. Phys. Chem.* (in press).

[3] G. H. Cartledge, *J. Phys. Chem.* (in press).

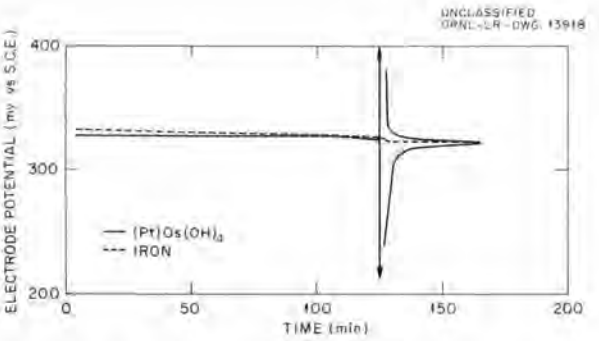

Fig. 30. Passivation of Iron by OsO_4.

and chloride ions, thus indicating that competitive adsorption plays a role in the action of osmic acid, as it does in the case of the inhibitors previously studied.

The fact that the iron electrode takes up the thermodynamic potential of the oxidation-reduction system in the osmium solution is of particular significance in connection with passivity and the nature of the passivating (Flade) potential. This observation means that the blocking off of metallic iron is so complete in this case that iron is not to be considered as an active reactant in the determination of the noble potential. The interpretation of the potential is therefore limited to processes involving either the oxidation-reduction system in solution or, in the absence of such, a process involving higher and lower oxidation states of iron in the thin film in contact with the solution. To account for the magnitude of the Flade potential and its experimentally known pH dependence it may be postulated that the higher oxidation state is Fe_2O_3, whereas the lower valence state is an abnormal oxide at the metallic interface, the "abnormality" consisting in a firmer binding of the first layer of oxygen than that which exists in the normal iron(II) oxide. On such a hypothesis the potential-determining process could be represented by the half-reaction

$$2e^- + Fe_2O_3 + 2H^+ \rightleftharpoons 2\text{''}FeO_i\text{''} + H_2O$$

From the magnitude of the Flade potential and the free energies of formation of Fe_2O_3 and H_2O, it may be calculated that the free energy of formation of the inner oxide, (FeO_i), would have to be -73.6 kcal·mole^{-1}, in comparison with

$$\Delta F^0 = -58.4 \text{ kcal·mole}^{-1}$$

for crystalline FeO.

The experiments with osmic acid and the pertechnetate ion are the only cases known in which iron is so completely blocked off as to serve as an indicator electrode for an oxidation-reduction process in neutral or weakly acidic solutions. Fuller discussion of these experiments and their bearing on passive potentials will soon be published.

In the study of the effect of foreign ions upon the electrode potential of inhibited electrolytic iron it was shown that addition of chloride and thiocyanate ions made the potential more noble until concentrations were reached at which debasing began. This effect has been studied further and it was found that similar ennobling by these ions occurs with stainless steel in an aerated solution of sodium sulfate without having an inhibitor present. It was found also that, in the instances so far investigated, the ennobling is related to the activity of the added electrolyte in accordance with an adsorption equation of the Freundlich type, namely $\Sigma(\Delta E) = K\alpha_i^{\rho}$, in which $\Sigma(\Delta E)$ represents the total ennobling when the chloride or thiocyanate ion is present at the activity α_i. These results are in harmony with the view that, in irreversible electrode systems, the electron must be assigned a chemical activity which is subject to alteration by factors that do not appear in the equation for the electrode process. Figure 31 shows a few of the preliminary results of this study. The metal was electrolytic iron in the solutions containing either the pertechnetate or tungstate ions as an inhibitor.

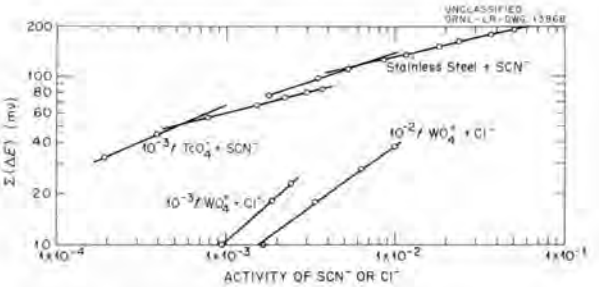

Fig. 31. Ennobling by Addition of KCl or KSCN, 57.5°C, Aerated.

POTENTIOSTATIC STUDIES ON STAINLESS STEEL ELECTRODES IN SULFURIC ACID SOLUTION

F. A. Posey G. H. Cartledge

Previous reports[4-6] have presented results of investigations on the spontaneous potential-time behavior of stainless steel electrodes in aerated, dilute sulfuric acid solutions at 40 to 90°C, under conditions where no current from an external source was passed through the metal-solution interphase. The present work represents a more searching examination of the relations existing between the potential and the rate of corrosion of stainless steel at potentials favoring a hydrogen-evolution type of attack. For this purpose, electrodes were maintained in selected environments at constant potential by means of a potentiostat or constant cathode potential device developed at the Laboratory.[7,8] The method of preparation of electrodes, the experimental conditions, and procedures for potential measurements have been described previously.[4] Rates of corrosion were estimated by using a sensitive spectrophotometric method based on complex ion formation between iron and thioglycolate ions.[9] The environment (aerated, 0.1 N H_2SO_4, stirred at approximately 600 rpm) and temperature (85 ± 1°C) were selected to correspond with the conditions used in previous work.

The electrical quantities measured in the potentiostatic experiments have simple significance only under steady-state conditions. Steady states of attackable electrodes are characterized by constancy with time of electrode potential, corrosion rate, and applied current and have the significance that the observed quantities, for example, current density, for a macroscopic electrode reflect conditions at each small element of area on the electrode. Steady states are attained with considerable difficulty even when using well-annealed electrodes. At constant potential, under the conditions of these experiments, several hours were necessary before the establishment of constant corrosion rate and applied current, and the time required was a function of electrode surface pretreatment. That electrodes made of the same batch of steel but having quite different surface pretreatments attain the same state was partially answered by experiments in which both initially emeried and initially electropolished specimens of type 347 stainless steel were used in 0.1 N H_2SO_4 at 85°C under a nitrogen atmosphere. They were observed to attain precisely the same potential after a period of time and to exhibit this potential unchanged for many hours. At this constant potential, however, the corrosion rate measured per square centimeter of apparent surface area of the initially emeried electrodes was greater by a factor of about 2 than that of the initially electropolished specimens of the same geometrical area.

In order to exhibit the same steady-state potential, the current densities of the partial processes which determine the electrode potential must be equal for both types of electrodes; therefore the variation in total rate of corrosion must be due to the difference in actual surface area. Hence, a knowledge of the actual area of the electrode interphase is necessary in order to convert electrical quantities based on measurements of geometrical surface areas to absolute values. In the potentiostatic experiments, corrosion rates were referred to unit apparent surface area of the initially emeried electrodes, and may be regarded as differing from true corrosion rates only by a small factor. This procedure is satisfactory for studying the variation of corrosion rate with electrode potential, and other experiments have demonstrated that electrodes subjected to emery-polishing exhibit a marked degree of reproducibility in their properties in the environment used in this work.

The experimental results on the variation of the steady-state rate of corrosion of initially emeried type 347 stainless steel electrodes with the electrode potential are portrayed in Fig. 32. Edeleanu,[10] also using a potentiostatic technique, has examined the potential-corrosion rate relation of a type 347 stainless steel in aerated, 20%

[4] G. H. Cartledge, *Chem. Semiann. Prog. Rep. June 20, 1954*, ORNL-1755, p 14.

[5] G. H. Cartledge, *Chem. Semiann. Prog. Rep. Dec. 20, 1954*, ORNL-1832, p 15.

[6] G. H. Cartledge and F. A. Posey, *Chem. Semiann. Prog. Rep. June 20, 1955*, ORNL-1940, p 10.

[7] R. W. Lamphere and L. B. Rogers, *Anal. Chem.* 22, 463 (1950).

[8] The author is indebted to M. H. Lietzke of the Chemistry Division for the loan of this instrument.

[9] H. W. Swank and M. G. Mellon, *Ind. Eng. Chem., Anal. Ed.* 10, 7 (1938).

[10] C. Edeleanu, *Nature* 173, 739 (1954).

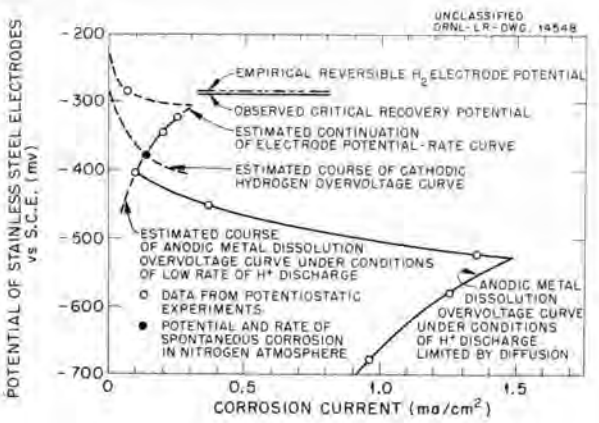

Fig. 32. Relationships Between Electrode Potential and Rate of Corrosion of Type 347 Stainless Steel in Aerated, 0.1 *N* H_2SO_4 at 85°C.

H_2SO_4 at 25°C. His results indicated a sharp maximum rate of corrosion in the vicinity of −250 mv vs the saturated calomel electrode. Work in this laboratory[11] has shown this to be very close to the reversible hydrogen electrode potential in that environment. The results of Fig. 32 are of practical as well as theoretical interest. The maximum rate of corrosion was observed at a potential of −530 mv vs S.C.E. This point is a characteristic of a particular steel and of the chosen environment and is useful for comparing the corrodibility of various steels in a common environment, since it represents the very highest rate of corrosion attainable, in the steady state, by a steel in hydrogen-evolution-type corrosion. At potentials far above that of the S.C.E., the formation of hexavalent chromium species becomes possible and leads to an enhanced rate of corrosion, which may even exceed the maximum attainable in hydrogen-evolution-type corrosion.

Under the conditions of the present experiments, the rates of the processes occurring at the metal-solution interphase, that is, cathodic reduction of H^+ and O_2 and anodic oxidative dissolution of metallic constituents (Fe as Fe^{++}, Cr as Cr^{+++}, Ni as Ni^{++}, etc.), are, in general, activation controlled, and the rates of these partial processes are describable in terms of anodic and cathodic overvoltage curves. Diffusion control, however, does become important for H^+ discharge on stainless steel at potentials sufficiently basic to the reversible hydrogen electrode potential. This is indicated by a departure from linearity of a plot of electrode potential vs the logarithm of the cathodic current density which occurs in the vicinity of −500 mv vs S.C.E.

Interpretation of the results of Fig. 32 is somewhat complicated by the presence of molecular oxygen in the system. The reversible oxygen potential in this environment lies approximately 1 v above S.C.E., so that the cathodic overvoltage curve for the reduction of oxygen has a large numerical value in the potential range of interest here; that is, the affinity of oxygen for electrons at the interphase is very large. However, hydrogen electrode overvoltage studies[12] have demonstrated that the rate of the reduction of oxygen becomes negligible compared with the rate of discharge of hydrogen ions at potentials lower by about 100 mv than the reversible hydrogen electrode potential. That this is also true for this system is indicated by evidence to be discussed presently.

The potential and rate of spontaneous corrosion of type 347 stainless steel in the steady state were determined in a nitrogen atmosphere, rigorously freed of oxygen, and are shown in Fig. 32 for comparison with the potentiostatic results obtained in the presence of air. This potential and rate, in the steady state, are uniquely determined by the intersection of the anodic and cathodic overvoltage curves for the partial processes occurring at the metal-solution interphase. Estimated overvoltage curves are sketched in Fig. 32 corresponding to the cathodic reduction of hydrogen ions and the anodic oxidative dissolution of metal ions. One important consequence of steady-state potential measurements for spontaneous corrosion in an aqueous environment where only these two partial processes are rate-determining is that, if the hydrogen-ion discharge overvoltage curve is nearly the same for all stainless steels, there will be a linear relationship between the steady-state potential for spontaneous corrosion of stainless steel and the logarithm of the corrosion rate. Several measurements of this type on various steels in the environment used in this work have been made, and the results obtained to date lend support to this conclusion. In the presence of oxygen or any other reducible

[11] G. H. Cartledge, *Nature* 177, 181 (1956).

[12] A. Hickling and F. W. Salt, *Trans. Faraday Soc.* 37, 319 (1941).

substance, such a correlation may still be possible, providing the effect of the substance is slight in the potential range of interest, or the total cathodic overvoltage curve is still similar for various steels undergoing spontaneous corrosion. Further work will be necessary before the feasibility of using steady-state spontaneous corrosion potential measurements as an index of the corrosion rate of different steels is established.

The steady-state rate measurements at the potentials −324, −344, and −401 mv vs S.C.E. lie on what may reasonably be presumed to be the anodic oxidative dissolution overvoltage curve for this stainless steel. A plot of electrode potential vs the logarithm of the corrosion rate for these points and the point corresponding to spontaneous corrosion in a nitrogen atmosphere at −378 mv is linear. The point at −285 mv vs S.C.E. is very near the empirical reversible hydrogen electrode potential in this environment and seems to be on the borderline between hydrogen-evolution-type corrosion and corrosion limited by diffusion through an oxide film. Corrosion rates in the noble region have been found generally to be an order of magnitude smaller than this value.

The important observation that, below potentials of approximately −400 mv vs S.C.E., the rate of corrosion no longer decreases as the antilogarithm of the electrode potential, but instead increases to a new maximum before again falling, requires interpretation. This behavior was apparently not noted in Edeleanu's experiments, as he did not carry his measurements to such low potentials and also worked under considerably different conditions. At potentials in the region of −300 to −400 mv, removal of hydrogen from the surface by admitting oxygen or by connecting the metal to a platinum electrode was shown to increase the corrosion rate.[5] The reduction of oxygen at these potentials does not produce an insoluble film, however, as it does at higher potentials. At potentials below about −400 mv the reduction of hydrogen ions is the strongly preferred cathodic process,[12] but there are at least three processes by which the hydrogen liberated may be consumed. These are: (1) recombination of atoms and escape as molecules; (2) surface combination with oxygen; and (3) penetration of the metal lattice. Furthermore, at sufficiently low potentials two additional factors become important, namely, limitation of the discharge of hydrogen ions by diffusion, and cathodic reduction of metal ions as the equilibrium potential of the metal is approached. The situation is obviously complicated and will not be discussed in detail at this point, but it will be apparent from the consideration of Fig. 33 that the hydrogen which diffuses into the metal plays an important role in the processes.

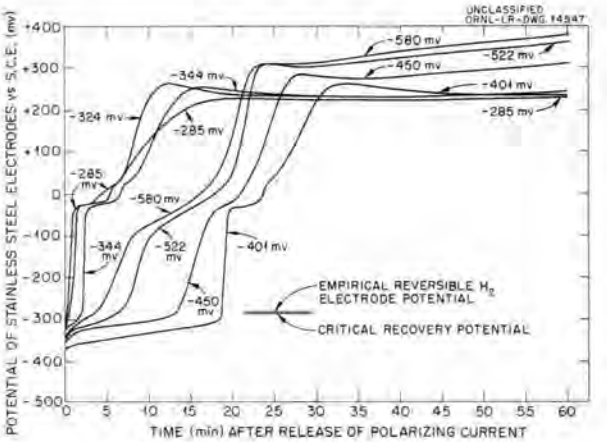

Fig. 33. Potential-Time Behavior of Type 347 Stainless Steel Electrodes on Recovery of Nobility Following Release of Potentiostatic Polarization at Various Potentials in Aerated, 0.1 *N* H_2SO_4 at 85°C.

Figure 33 shows the electrode potential-time behavior of the steel electrodes, held at the potentials indicated in Fig. 32, on spontaneous ennoblement after current from the potentiostat was shut off. Two fairly well-defined classes of recovery curves are apparent, one including those electrodes held at −285, −324, and −344 mv, and the other comprising those held at lower potentials. Features common to these curves are (1) an inflection at −25 mv vs S.C.E., (2) another less noticeable at +25 mv, and (3) a more or less prominent broad peak occurring above +200 mv.

Evidence to be discussed in a subsequent publication strongly suggests that the first inflection (at −25 mv) is a record of the net reaction of hydrogen from the metal with oxygen in solution at the interphase. This reaction becomes so important for electrodes held at the lower potentials (−522 and −580 mv) that the second inflection (at +25 mv) is completely obscured. The processes peculiar to the second inflection

and the broad peak lack precise identification. However, available evidence indicates that the reaction of Fe^{+++} in solution with hydrogen from the metal or with the metal itself causes the second inflection and that the broad peak is due to additional cathodic processes involving further reducible species generated during the first inflection, probably O_2^- or O_2^{--}, or their acid forms. Variations in the duration of the first inflection, the heights of the peaks, and the time required for ennoblement from the basic region are consistent with the interpretation advanced for the results of Fig. 32.

All stainless steel electrodes maintained at potentials below the reversible hydrogen electrode potential, either by an externally applied current or by spontaneous corrosion, assume a black color in a sufficient period of time. This happens both in the presence and in the absence of oxygen. This black color always disappears, or is at least greatly reduced, on spontaneous or forced ennoblement, at identically the position of the first inflection in the recovery curves at −25 mv vs S.C.E. Perhaps the color is due to a change in the reflectivity of the metal surface occasioned by the accommodation of hydrogen in the steel lattice. Further evidence is needed for the clarification of this interesting effect.

The previous types of observations are to be extended to a potentiostatic and galvanostatic study of hydrogen-evolution-type corrosion in an inert atmosphere, where the complication of the participation of partial processes due to oxygen reduction is eliminated. It is planned to cover a much wider range of potentials and to extend the work to an investigation of the very slow rates of corrosion which occur in the passive region.

ELECTRODE POTENTIALS UNDER RADIATION

W. E. Clark G. H. Cartledge

A program of investigation of the electrochemistry of corrosion in a radiation field was initiated, and a number of experiments were carried out in the high-intensity (8.5×10^{17} ev/g-min) gamma source. The approach employed was that previously described by Cartledge,[4,11] whose work on stainless steel supplied the background for comparison of potential-time behavior in radiation.

The principal difficulties encountered in this study are associated with the development of equipment which allows conditions to be controlled and measurements to be made with the same degree of accuracy and precision in the radiation field as outside. Thus far, attempts in this direction have not been entirely successful, but have been sufficiently so to indicate rather definitely that the differences are due to changes in the solution caused by radiolysis of the water.

The cell used in the majority of the experiments run thus far is shown in Fig. 34. The cell was made entirely of glass, the top and body being constructed from the two sections of a ground-glass joint. A silver–silver sulfate electrode using 0.1 *N* sulfuric acid as electrolyte was used as reference electrode. This electrode was

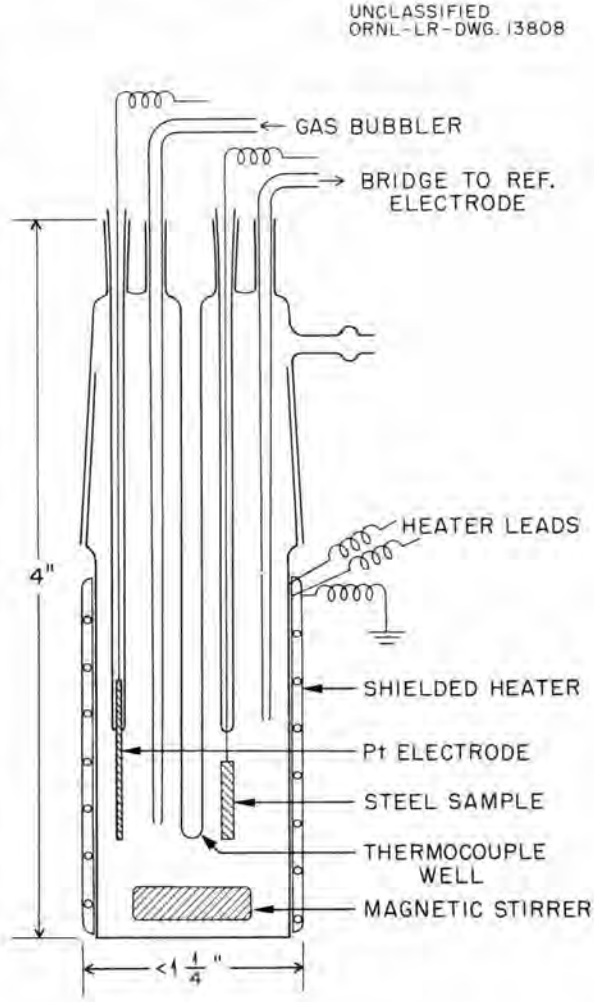

Fig. 34. Pyrex Cell For Measurement of Electrode Potentials in Gamma Radiation.

located entirely outside the source and was bridged into the cell as shown, using 0.1 *N* sulfuric acid as the bridge solution in a glass and Tygon bridge. The cell was stirred at 300 rpm, using a synchronous motor to activate the magnetic stirrer. This stirring rate produced a slight vortex in the solution. At normal filling the cell contained about 19 ml.

All experiments reported herein were carried out in 0.1 *N* sulfuric acid solution at 85°C. The temperature was controlled by means of a Honeywell Pyrovane controller actuated by an iron-constantan thermocouple located in the thermocouple well. When tested out of the source and checked by a thermometer, the temperature of the solution was controlled to within ±0.8°C. In the source, the control appeared to be more nearly ±1.5°C, probably because of the more rapid heat loss from the cell as a result of a tight fit inside the brass source holder. Potentials were measured by a modified Leeds and Northrup vacuum tube pH meter and a Brown recorder.

The stainless steel electrodes consisted of cylinders 1 cm in length and 0.16 cm in diameter, having a nominal area of 0.54 cm^2. The neck was approximately 2 cm long and 0.05 cm in diameter and was sealed into pyrex tubing. Since an absolutely tight glass-to-metal seal was difficult to obtain, it was usually necessary to complete the sealing operation by blowing a drop of sodium silicate into the bottom of the tube and then heating to 200°C for 2 or 3 hr. The electrode was then abraded with 2/0 emery paper, rinsed, and stored in an oven at 110°C until use. A few samples were heated in air at 200°C before use, in order to build up an oxide film. In most of these experiments, however, it was felt desirable to use metal with a minimum amount of oxide film to avoid the added complication of appreciable concentrations of iron in the solution during the early stages of the experiment.

In order to employ the platinum electrode as a monitor of the redox potential of the solution, it was necessary to investigate the effect of radiation on the potential of platinum. The only known study of this system was made by Veselovsky,[13] and few details are given.

[13] V. I. Veselovsky, *Peaceful Uses of Atomic Energy, Proceedings of the International Conference in Geneva, August 1955*, vol 7, p 599.

Figures 35 and 36 show the effect of gamma irradiation on smooth and platinized platinum electrodes, respectively. In both experiments the cell was open to air and no gas was bubbled through the cell. Figures 37 and 38 show the results obtained with platinized platinum electrodes when oxygen-free nitrogen and hydrogen, respectively, were bubbled through the solution before and during irradiation.

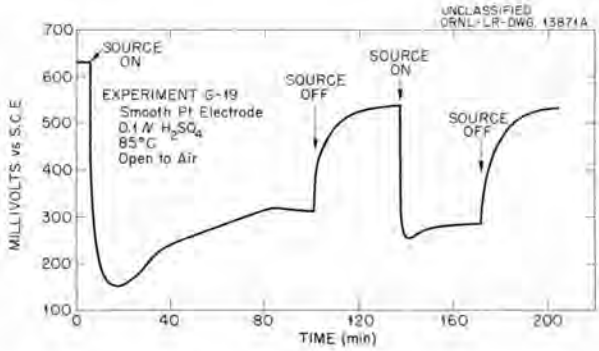

Fig. 35. Effect of Gamma Irradiations on a Smooth Platinum Electrode.

The potentials plotted are those vs the S.C.E., which is 470 mv negative to the silver–silver sulfate reference electrode actually employed.

As can be seen, the imposition of the gamma source had no appreciable effect on the potential of the platinum in the solution swept by hydrogen. In a solution swept by nitrogen, the debasement in the source stopped some 30 mv short of the reversible hydrogen potential.

During the debasement and ennoblement of the platinum electrodes before and after irradiation, several rather definite halts were observed in the potential vs time plots. It is planned to investigate this phenomenon more closely with the purpose of determining the reactions responsible for these halts.

Figure 39 shows the usual behavior of a sample of type 347 stainless steel in the gamma field, the cell being open to air. After the initial debasement and recovery of the steel, the imposition of the source causes a debasement which, however, is not sufficiently drastic to result in the evolution of hydrogen (−290 to −300 vs the S.C.E.). The steel gradually recovers and then continues to ennoble at a rate generally comparable

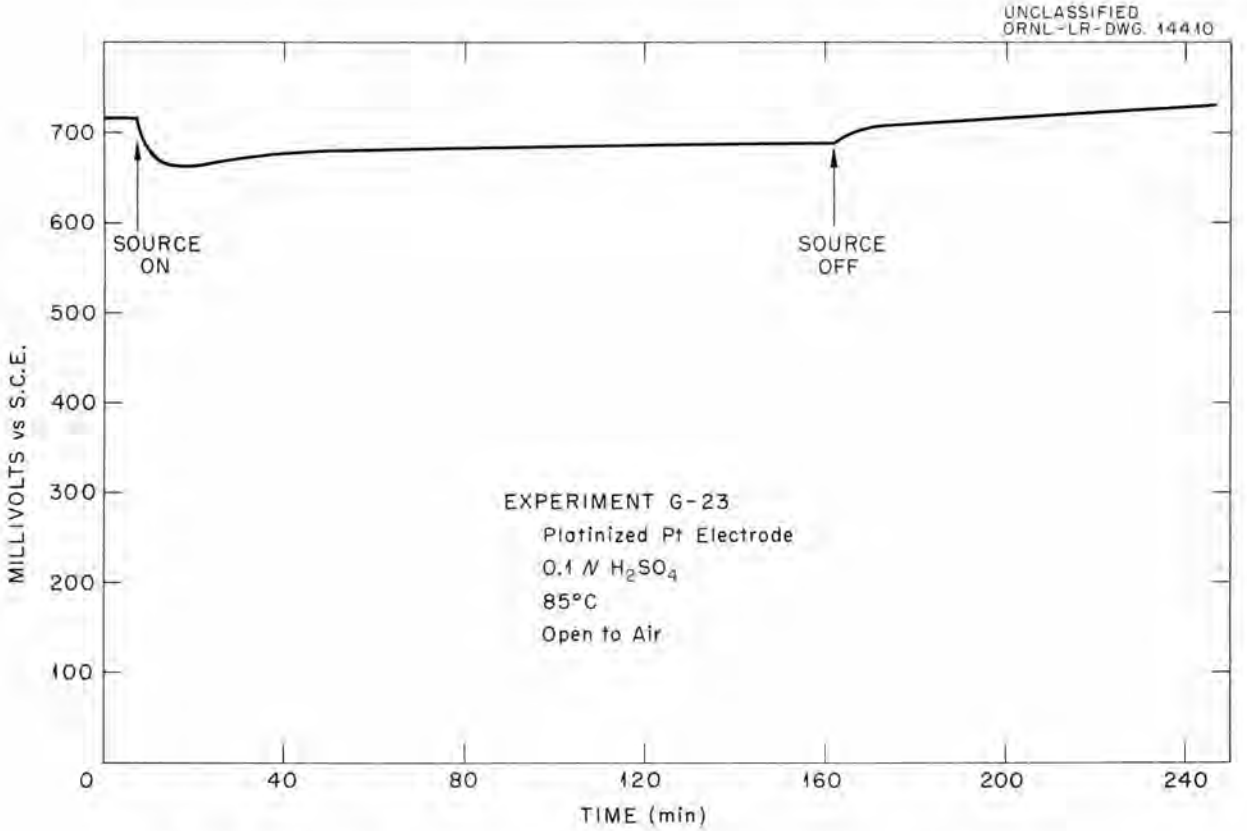

Fig. 36. Effect of Gamma Irradiation on a Platinized Platinum Electrode.

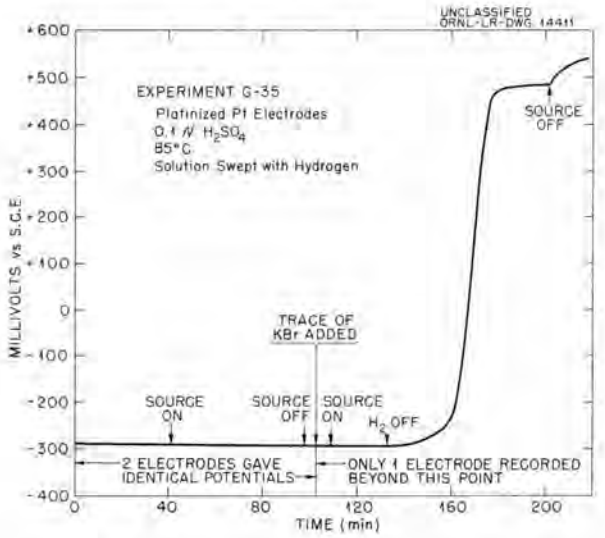

Fig. 37. Effect of Gamma Irradiation on a Platinized Platinum Electrode in a Hydrogen Atmosphere.

with that expected for a sample in the absence of irradiation and in a solution containing no appreciable amount of dissolved iron.

Occasionally the imposition of the source will cause debasement of the steel to potentials at which active corrosion can occur with the evolution of hydrogen. An example of this type of behavior is shown in Fig. 40. It will be noted that debasement of the steel is not so nearly instantaneous with the imposition of the source as is the case with the platinum; apparently a period of time is required for breakdown (or reduction) of the protective film. After about 1 hr of irradiation, this particular sample recovered.

Two further remarks appear to be of significance with respect to this experiment. The first is that the smooth platinum electrode remains at a relatively base potential so long as the steel corrodes, in spite of the fact that the radiation field favors the oxidation of Fe(II) to Fe(III). The second concerns a comparison of the time consumed at

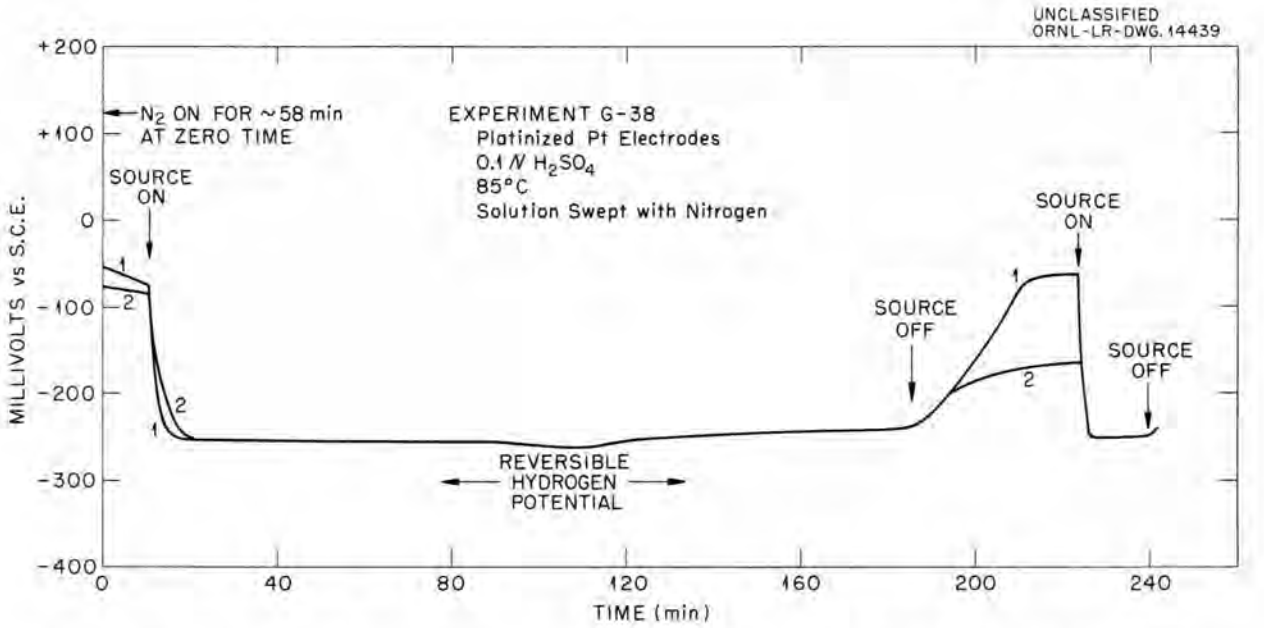

Fig. 38. Effect of Gamma Irradiation on a Platinized Platinum Electrode in a Nitrogen Atmosphere.

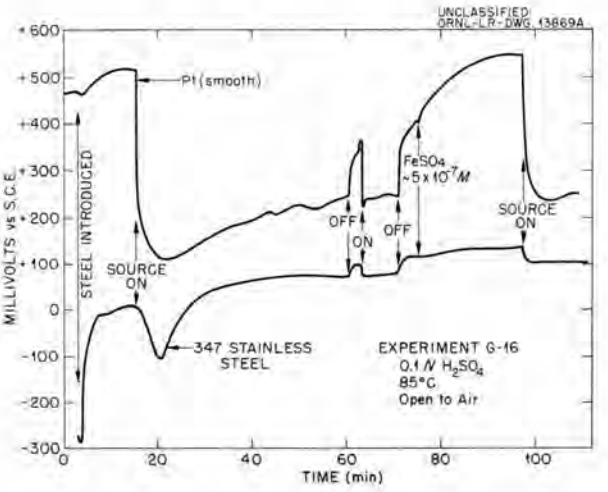

Fig. 39. Usual Potential Behavior of Type 347 Stainless Steel Under Gamma Irradiation.

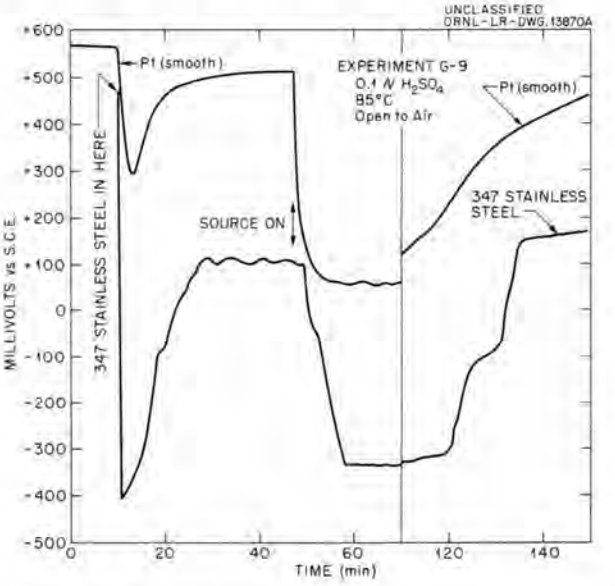

Fig. 40. Failure and Recovery of Type 347 Stainless Steel in Gamma Irradiation.

the halt in the recovery wave of the stainless steel in and out of irradiation (at approximately −100 mv vs the S.C.E.). The extra time required by the sample in radiation may possibly be due to the continuous formation of peroxide at the metal surface under irradiation.

A second type of exposure apparatus is the thermal loop shown in Fig. 41. This consists of the same cell shown in Fig. 34, attached to a larger cell or "cold leg" so that a slow circulation (1 to 2 ml/min) of the solution takes place. The intensity of irradiation in the cold leg is not accurately known but should be in the order of

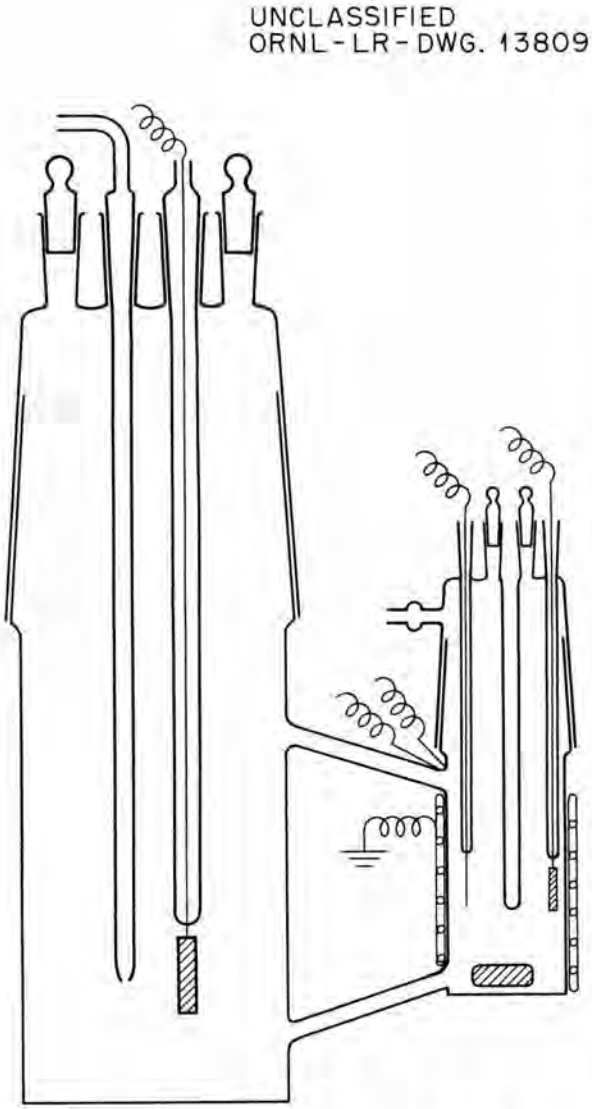

Fig. 41. Pyrex Thermal Loop for Gamma Radiation Studies.

10^{16} ev/g-min. The loop has distinct advantages over the small cell: it allows the use of larger volumes of solution, thus minimizing solution changes due to evaporation and buildup of corrosion products (the volume is about 170 ml for good circulation); it allows the direct comparison of as many as three steel samples at one time; and the manipulation and loading are much easier than that of the cell, since the bridge connection is made in the large cold leg. It does not, however, lend itself to control of the atmosphere as readily as does the cell.

Preliminary experiments in the loop involved comparison of type 347 stainless steel with samples of types 309 and 316, 309 and 321, and a comparison of types 304L, 302, and 310. The results indicated the probability that corrosion of these steels will show more differences out of radiation than in radiation, provided the solution is aerated. As expected, a platinum electrode in the hot leg of the loop open to air assumes a more noble potential than one located in the single cell under comparable conditions. Another manifestation of the more oxidizing potential of the solution is the fact that in the loop run in air all steels tested were ennobled instead of being debased on imposition of the source.

Hochanadel[14] lists the following reactions as being of importance in the radiolysis of water at 25°C:

(1) $H_2O \xrightarrow{\gamma} H_2O_2 + H_2 + H + OH$

(2) $H_2 + OH \longrightarrow H_2O + H$

(3) $O_2 + H \longrightarrow HO_2$

(4) $HO_2 + HO_2 \longrightarrow H_2O_2 + O_2$

As peroxide builds up in solution,

(5) $H_2O_2 + H \longrightarrow H_2O + OH$

(6) $H_2O_2 + OH \longrightarrow HO_2 + H_2O$

At elevated temperatures hydrogen peroxide decomposes thermally, but even at 150°C peroxide was present at the end of the irradiation.

The results reported herein are in complete agreement with the buildup of peroxide in the irradiated solution in air and oxygen. In hydrogen-swept solutions reaction 2 will be of greatest importance, since in the hydrogen stream the oxygen from thermal decomposition of peroxide will be swept from the solution and from the cell, thus maintaining the reversible hydrogen potentials on platinized platinum. In solutions swept by inert gases such as nitrogen, both oxygen and hydrogen from radiolysis will tend to be removed. The approach of the electrode potential to that of the hydrogen electrode is doubtless due to the great solubility of hydrogen in platinum and to the high

[14] C. J. Hochanadel, *Peaceful Uses of Atomic Energy, Proceedings of the International Conference in Geneva, August 1955*, vol 7, p 521.

degree of reversibility to hydrogen, as compared with oxygen.

A few exploratory potential-time measurements were made on Zircaloy-2 out of radiation to serve as a base line for future radiation corrosion experiments on this material. The solution used was aerated 0.1 *N* sulfuric acid, and the temperature was 85°C.

Abraded samples of Zircaloy-2 dropped rapidly to a very low potential, but recovered so quickly that the value of the minimum was difficult to determine with the present instrumentation. The minimum reading observed was −783 mv vs S.C.E. The recovery continued to about −80 mv vs the S.C.E., where it was observed to remain relatively constant for as long as experiments were run (several hours). Pretreatment of the sample caused very marked changes in the nature of the potential-time behavior. For example, a sample which had been heated to 450°C in air overnight debased only to −435 mv vs the S.C.E. and held this potential for two days, the temperature being held at 85°C during the day and allowed to cool to room temperature overnight.

NONAQUEOUS SYSTEMS AT HIGH TEMPERATURES

HIGH-TEMPERATURE CALORIMETRY

D. J. Sasmor R. Bevan
E. R. Van Artsdalen

Several extended series of measurements have been made with the high-temperature vacuum adiabatic calorimeter on (1) the empty sample container, (2) a sample of uranium trifluoride, UF_3, and (3) a standard sample of sapphire (aluminum oxide) from the National Bureau of Standards. The spread in the precision of these measurements varies from about ±3 to ±0.5%; the precision is a function of the equilibration time after the measured energy input. For short equilibration of the order of 15 min the precision is ±3% over the entire temperature range from 200 to 900°C. As the equilibration time is lengthened, the precision approaches ±0.5%. Unfortunately, long equilibration times introduce other uncertainties, and it is clear that the use of an extended equilibration period is not good calorimetric technique. Several changes have been made in the construction of the sample container in an attempt to shorten equilibration times. However, data obtained following these changes indicate that the slow attainment of temperature equilibrium is caused by thermal instability of the external shield system. Refinements are now in progress which it is hoped will improve the precision and accuracy of the results obtained.

FUSED SALTS

Electrical Conductance and Density of Fused Halides

I. S. Yaffe E. R. Van Artsdalen

The conductance of molten fluorides cannot be determined satisfactorily by using vitreous silica dip cells and a conventional Jones bridge because of rapid attack of silica by fluorides. Likewise, silica apparatus becomes progressively less satisfactory with most fused salts as the temperature is increased. Therefore, considerable effort has been spent to develop a satisfactory low-resistance transformer bridge which can be used in conjunction with a precious-metal electrode assembly to measure resistance of fused salts. The electric circuitry of the bridge was developed by Fairstein.[1] A simplified version of the circuit diagram is shown in Fig. 42, and the type of cell used is evident from the electrode assembly shown in Fig. 43. The principle of the method is to measure the potential drop across two probes located at fixed positions between two a-c current-carrying electrodes. Unfortunately, the electrode cell assembly must be calibrated in the appropriate temperature range against known fused-salt standards. This is necessary because the peculiar

[1] E. Fairstein, *Instrumentation and Controls Semiann. Prog. Rep. July 31, 1955*, ORNL-1997, p 9.

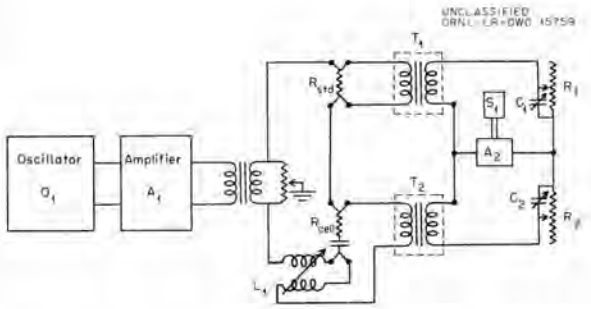

Fig. 42. Circuit Diagram of Low-Resistance Transformer Bridge.

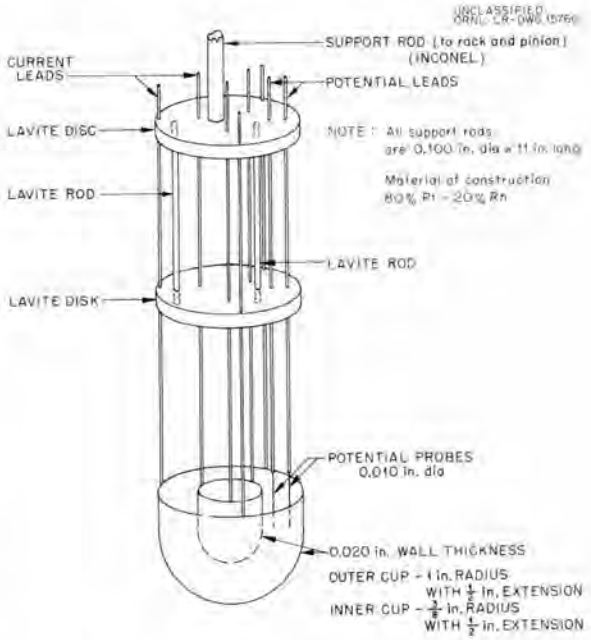

Fig. 43. Electrode Assembly.

geometry of the assembly precludes accurate predictions of expansion.

The cell was calibrated against molten potassium chloride;[2] the results are depicted in Fig. 44, where the circles show the initial calibration and the squares show the calibration following several runs. It is evident that the cell constant varies linearly with temperature and is stable over reasonable periods of time. A comparison of data obtained with this apparatus with that reported previously[2] for fused sodium chloride is illustrated in Fig. 45. Reproducibility of the measurements is excellent.

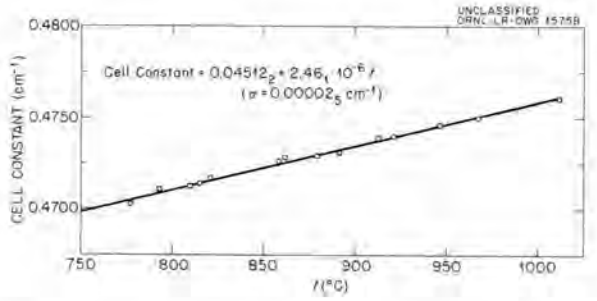

Fig. 44. Temperature Dependency of the Cell Constant.

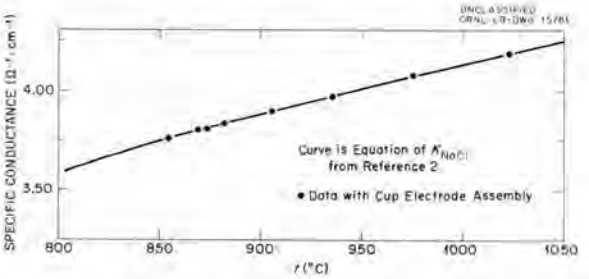

Fig. 45. Specific Conductance of Molten NaCl.

Data obtained for specific conductance and density of pure molten lithium, potassium, and cesium fluorides have been used to compute the equations given in Tables 24 and 25, respectively. It is significant that the equivalent conductance of cesium fluoride is higher than that of lithium fluoride. Cesium fluoride is the only salt studied in which the size of the cation is larger than that of the anion.

[2] E. R. Van Artsdalen and I. S. Yaffe, *J. Phys. Chem.* 59, 118 (1955).

When the equivalent conductances of the fluorides are compared with those of the other halides of the same cation, the order for potassium and cesium is $F^- > Cl^- > Br^- > I^-$, which might be considered regular. However, for the lithium halides, the order is $Br^- > Cl^- > I^- > F^-$. The relatively low position of LiF could be due to the high attraction between the two ions, which are the smallest and least polarizable of all simple ions. This same effect could also explain the smaller conductance[3] of LiCl as compared with that of LiBr.

The apparent heats of activation for equivalent conductance for these three alkali fluorides are plotted in Fig. 46. The variations with temperature are in line with previously reported data[2,3] and are interpretable by the hypotheses discussed in connection with those data.

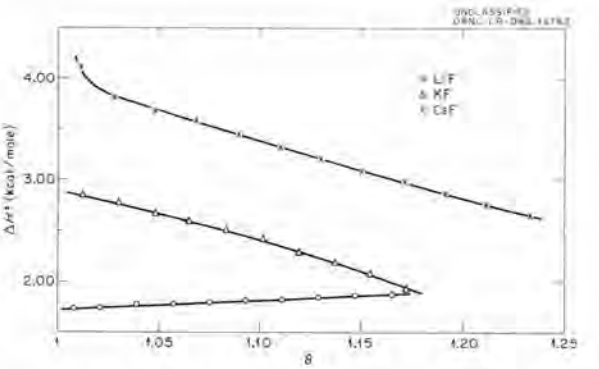

Fig. 46. Apparent Heats of Activation for Conduction for Alkali Fluorides.

The specific conductance and density of pure fused calcium, strontium, and barium chlorides, lanthanum chloride, and lanthanum and neodymium bromides were determined in the range of about 150 deg above their respective melting points. The equations representing specific conductance and density of these salts are listed in Tables 26 and 27, respectively. The conductance measurements were made with the usual vitreous silica dip cell and Jones bridge, and the density measurements by the submerged-bob method. Equivalent conductance, computed from these data, for the alkaline-earth chlorides was found to vary in the

[3] I. S. Yaffe and E. R. Van Artsdalen, *J. Phys. Chem.* (in press); *Chem. Semiann. Prog. Rep. Dec. 20, 1955*, ORNL-2046, p 21.

TABLE 24. CONSTANTS OF EQUATION FOR SPECIFIC CONDUCTANCE, κ, OF FUSED LITHIUM, POTASSIUM, AND CESIUM FLUORIDES

$\kappa = a + (b \times 10^{-2})t + (c \times 10^{-6})t^2$, $ohm^{-1} \cdot cm^{-1}$, where t is in °C

Salt	a	b	c	Standard Deviation ($ohm^{-1} \cdot cm^{-1}$)	Applicable Temperature Range (°C)
LiF	+3.805	+1.004	−3.516	0.008	847–1027
KF	−3.493	+1.480	−6.608	0.009	869–1040
CsF	−4.511	+1.642	−7.632	0.009	725–921

TABLE 25. CONSTANTS OF EQUATION FOR DENSITY, ρ, OF FUSED LITHIUM, POTASSIUM, AND CESIUM FLUORIDES

$\rho = a - (b \times 10^{-3})t$, g/cm^3, where t is in °C

Salt	a	b	Standard Deviation, σ (g/cm^3)	Experimental Temperature Range (°C)
LiF	2.2243	0.4902	0.0003	876–1047
KF	2.4685	0.6515	0.0003	881–1037
CsF	4.5489	1.2806	0.0004	712–912

TABLE 26. CONSTANTS OF EQUATION FOR SPECIFIC CONDUCTANCE, κ, FOR SOME FUSED POLYVALENT METAL HALIDES

$\kappa = a + (b \times 10^{-3})t + (c \times 10^{-6})t^2$, where t is in °C

Salt	a	b	c	Standard Deviation, σ ($ohm^{-1} \cdot cm^{-1}$)	Applicable Temperature Range (°C)
$CaCl_2$	-3.263_0	$+8.302_9$	-1.908_2	0.0012	784–958
$SrCl_2$	-1.744_0	$+4.087_9$	+0.2428	0.003_8	874–993
$BaCl_2$	-17.364_9	+34.647	−14.705	0.004_0	965–1100
$LaCl_3$	−8.004	+18.025	−8.167	0.009	874–987
$LaBr_3$	$+2.275_2$	-7.168_0	+6.700	0.003	777–912
$NdBr_3$	$+1.488_2$	-5.053_3	+4.800	0.003_6	690–873

TABLE 27. CONSTANTS OF EQUATION FOR DENSITY, ρ, FOR SOME FUSED POLYVALENT METAL HALIDES

$\rho = a - (b \times 10^{-3})t$, where t is in °C

Salt	a	b	Standard Deviation (g/cm^3)	Experimental Temperature Range (°C)
$CaCl_2$	2.4108	0.4225	0.0001	787–950
$SrCl_2$	3.2318	0.5781	0.0002	894–1037
$BaCl_2$	3.8292	0.6813	0.0001	966–1081
$LaCl_3$	3.8773	0.7774	0.0001	873–973
$LaBr_3$	5.0089	0.0960	0.0004	796–912
$NdBr_3$	4.7626	0.7779	0.0003	695–860

order $BaCl_2 > SrCl_2 > CaCl_2$. It is possible to attribute this order to higher complexing power of the smaller alkaline-earth ions. The equivalent conductance of the rare-earth halides computed from the data reported here shows that these are significantly poorer conductors than either alkali or alkaline-earth halides. Fused alkali halides have equivalent conductance about equal to their aqueous values at infinite dilution; fused alkaline-earth halides have values only slightly below the aqueous infinite dilution figures. However, the fused rare-earth halides show equivalent conductance about an order of magnitude smaller in the fused state than in the infinitely dilute aqueous solution. It is believed that these results can be attributed to the formation of complex ions within the rare-earth halide melts. The rapid rise of the equivalent conductance of the rare-earth halides with temperature and the concommittant decrease of apparent heat of activation (Fig. 47) are further arguments in favor of the concept of complex-ion formation, which decreases with rising temperature.

These results have been described in two papers which will be submitted for publication in the open literature.

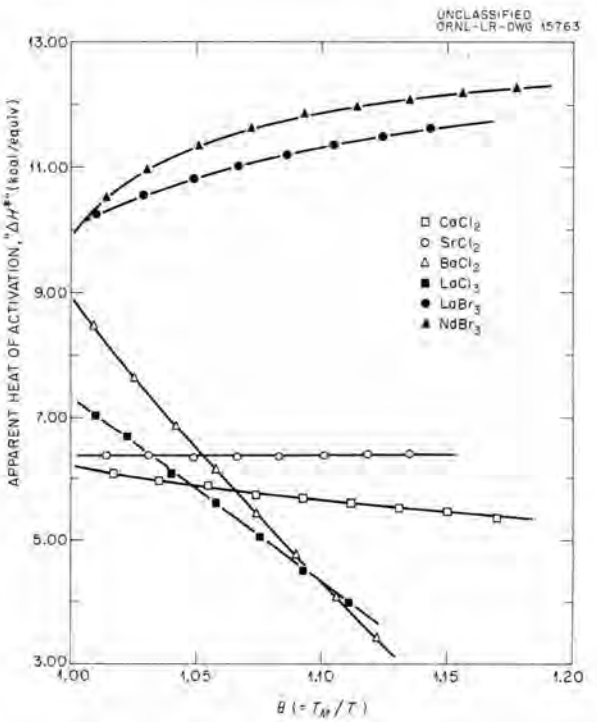

Fig. 47. "Heat of Activation" for Conduction.

Electrical Conductance and Density of Molten Nitrates

D. F. Smith[4] E. R. Van Artsdalen

Conductance and density of fused nitrates are of interest in connection with the investigation of self-diffusion. There are good data for several nitrates, but it was felt that new determinations were desirable for potassium and cesium nitrates because of inadequate data in the literature.

[4] Consultant and summer employee from the University of Alabama.

The Jones bridge and capillary dip cell method was used to measure the electrical resistance of fused potassium nitrate between 343 and 391°C. The melt was prepared from a cp sample of potassium nitrate dried under high vacuum at about 290°C for 18 hr. The specific conductance of potassium nitrate in this restricted range is given adequately by

$$\kappa = -0.4146_5 + 0.003074_5 t \text{ ohm}^{-1}\cdot\text{cm}^{-1} .$$

The density of this salt was determined on the same sample between 344 and 398°C by weighing a submerged bob in the customary manner, and the data may be expressed by the equation

$$\rho = 2.1360 - 7.758 \times 10^{-4} t \text{ g/cc} .$$

Data were obtained similarly for fused cesium nitrate. The cesium nitrate was prepared by adding a slight excess of silver nitrate to an aqueous solution of cp cesium chloride and filtering from the precipitated silver chloride. The excess silver nitrate was then removed with hydrogen sulfide and the cesium nitrate purified by recrystallization. After preliminary drying, it was dehydrated under high vacuum for 18 hr at 330°C. The specific conductance and density are given in the range 415 to 491°C by the equations

$$\kappa = -0.2452 + 1.8878_5 \times 10^{-3} t \text{ ohm}^{-1}\cdot\text{cm}^{-1}$$

and

$$\rho = 3.3023 - 1.1660_5 \times 10^{-3} t \text{ g/cc} .$$

Self-Diffusion in Molten Salts

A. S. Dworkin E. R. Van Artsdalen

The self-diffusion coefficients of the K^+ ion and the NO_3^- ion in molten KNO_3 have been measured. The method used was essentially the same as that used for the measurement of the self-diffusion coefficients in molten $NaNO_3$ and has been described in detail previously.[5] The tagged ions used to follow the diffusion were the stable isotopes K^{41} and O^{18}, the latter being incorporated in the NO_3^- ion.

[5] A. S. Dworkin and D. Brown, *Chem. Semiann. Prog. Rep. Dec. 20, 1955*, ORNL-2046, p 23; E. R. Van Artsdalen *et al.*, *J. Am. Chem. Soc.* 78, 1772 (1956).

The data may be expressed in the form of a rate equation:

$$(1) \qquad D = Ae^{-\Delta H^{\ddagger}/RT} ,$$

where D is the self-diffusion coefficient and $\Delta H^{\ddagger}$ is the heat of activation of self-diffusion. For K^+ and NO_3^-, Eqs. 2 and 3 are obtained by means of least-squares calculations:

$$(2) \qquad D_{K^+} = 1.95 \times 10^{-3} e^{-6005/RT} ,$$

$$(3) \qquad D_{NO_3^-} = 1.28 \times 10^{-3} e^{-5433/RT} .$$

The straight lines obtained by plotting log D vs $1/T$ are shown in Fig. 48. The probable error in D_{K^+} is ±0.05 (±2.4–3.4%), while that for $\Delta H^{\ddagger}_{K^+}$ is ±0.36 kcal (±6%). The probable error for $D_{NO_3^-}$ is ±0.036 (±1.7–2.4%) and that for $\Delta H^{\ddagger}_{NO_3^-}$ is 0.24 kcal (4.4%).

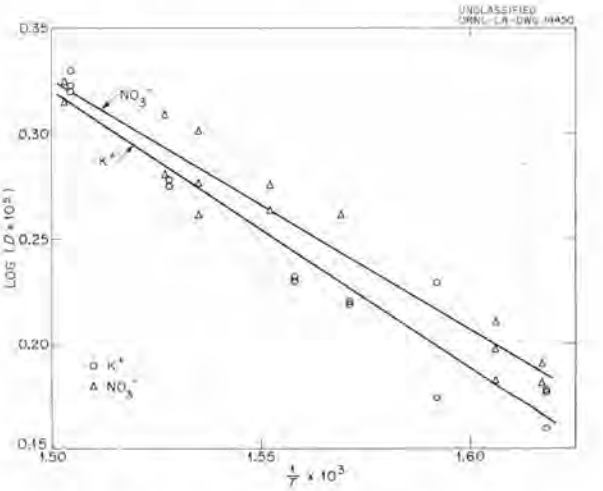

Fig. 48. Self-Diffusion Coefficients.

It was noted[5] in the study of $NaNO_3$ that the ratio of the self-diffusion coefficients of the ions is approximately equal to that of the inverse square root of their masses. This is not the case with KNO_3. If the same relationship held for KNO_3, the self-diffusion coefficient of the K^+ ion should be about 25% higher than that of the NO_3^- ion, whereas the data indicate that the NO_3^- coefficient is actually a few per cent higher

than that of the K^+. It should also be noted that the heats of activation of diffusion for the ions in the $NaNO_3$ melt agree to within about 0.1 kcal, whereas the heat of activation of diffusion of the K^+ ion is about 0.6 kcal greater than that of the NO_3^- ion in KNO_3. However, the limits of error are greater in the KNO_3 experiment, and the two figures $\Delta H_{K^+} = 6.00 \pm 0.36$ kcal and $\Delta H_{NO_3^-} = 5.43 \pm 0.24$ kcal fall just within these limits.

The measured equivalent conductance of potassium nitrate is about 63% less than that computed from the Nernst-Einstein equation and the self-diffusion data reported here. Similarly the measured conductance of sodium nitrate is about 30% below the computed value. Borucka, Bockris, and Kitchener[6] have reported self-diffusion data for fused sodium chloride, and they, too, find a similar effect for this salt. The self-diffusion of Tl^+ in fused TlCl has been determined by Berne and Klemm,[7] and although the diffusion coefficient for Cl^- is not known it seems likely that here, too, the Nernst-Einstein equation would indicate too high a conductance, because Tl^+ ion alone accounts for 95% of the measured value. Whether the Nernst-Einstein equation, which was derived as a limiting law for dilute aqueous solution, is applicable to fused salts is still uncertain. If it should be applicable, data of the type discussed here might indicate that some uncharged entities migrate in the diffusion experiments, and this view is expressed by Borucka, Bockris, and Kitchener. The problem is under active theoretical and experimental study, and it is hoped that further data will help to clarify the situation.

Measurements of the self-diffusion coefficients in molten $CsNO_3$ are under way. The stable isotope N^{15} has been obtained and will be incorporated in the salts $NaNO_3$ and KNO_3 so as to check the NO_3^- diffusion data previously obtained. The NO_3^- ion diffusion in $CsNO_3$ will also be measured in this manner. However, the mass spectrographic analysis of the N^{15} in the nitrates remains to be proved feasible.

Cryoscopy

J. E. Sutherland E. R. Van Artsdalen

Phase equilibrium studies show that calcium chloride forms addition compounds with potassium, rubidium, and cesium chlorides, of the type $CsCl{\cdot}CaCl_2$, which are stable. Corresponding compounds are not formed with lithium and sodium chlorides. The question whether these addition compounds are stable in the liquid state had not been answered. Freezing-point depression measurements of mixtures of calcium chloride and cesium chloride can be used to determine whether an addition compound is stable at high dilution in a particular fused-salt solvent. When molten sodium nitrate is used as the solvent, both cesium chloride and calcium chloride individually produce the ideal lowering of the freezing point up to at least 0.1 *m*. It was found that in the presence of 0.382 *m* CsCl calcium chloride gave ideal freezing-point lowering to concentrations in excess of 0.1 *m*. It is thereby demonstrated that the complex compound $CsCl{\cdot}CaCl_2$ is completely dissociated into its component ions at these concentrations in molten sodium nitrate at the freezing point.

Similar studies proved that magnesium chloride behaves ideally (is completely dissociated) in depressing the freezing point of sodium nitrate. The magnesium ion does not form anionic chloride complexes which are stable in sodium nitrate at the freezing point. The same relative lowering of the freezing point was produced by magnesium chloride alone and in the presence of 0.10 and 0.25 *m* sodium chloride.

On the other hand, magnesium bromide appears to be associated in sodium nitrate to form $MgBr^+$ and Br^-. Likewise, strontium bromide shows a small progressive deviation from ideality which increases with rising concentration and is suggestive of the formation of some sort of complex ion. These studies are incomplete. Barium fluoride has been shown to behave essentially ideally and it seems to be completely dissociated.

Fluorine Exchange Between Salts and Gases

T. A. Gens[8] R. Brosi
E. R. Van Artsdalen

Integrated apparatus for study of exchange of radioactive F^{18} has been built and tested. Techniques have been developed and improved for incorporating F^{18} into a number of inorganic fluorides.

[6] A. Z. Borucka, J. O'M. Bockris, and J. A. Kitchener, *J. Chem. Phys.* **24**, 1282 (1956).

[7] E. Berne and A. Klemm, *Z. Naturforsch.* **8a**, 400 (1953).

[8] ORINS Fellow 1955–56, University of Florida.

Exploratory measurements have been made with several fluorocarbon gases and a number of inorganic fluorides to determine whether fluorine exchange occurs. Thus far, the rather inconclusive evidence indicates the following:

1. Perfluoropropene, C_3F_6, begins to decompose in a flowing system at temperatures above 500°C, giving an increased pressure. This decomposition appears to be catalyzed by sodium fluoride but probably not by cesium fluoride.

2. Appreciable radioactive fluorine from tagged sodium fluoride appears in the vapor phase during the catalyzed decomposition. The chemical form of the fluorine is uncertain, although apparently it is not in elemental form.

3. Cesium fluoride appears to exchange fluorine without decomposition of C_3F_6.

4. Fluorine exchange could not be established between C_3F_6 and CrF_2.

5. Decomposition, as evidenced by a pressure rise, and fluorine exchange occurred with $CF_3N{=}CF_2$ and NaF.

LIQUID METAL–SALT SOLUTIONS

Phase Equilibria of the Potassium–Potassium Halide Systems[9]

J. W. Johnson M. A. Bredig

The investigation of the liquid-liquid and liquid-solid phase equilibria in the potassium metal–potassium halide systems was essentially completed with the study of the bromide and iodide systems.

In the earlier work,[10,11] sampling techniques were employed to delineate the solubility limits of these systems. The maintenance of constant temperature during the equilibration period and complete phase separation prior to sampling were required for reproducible results. A thermal analysis method has been developed which eliminates these requirements and all elaborate sampling devices. To detect small thermal effects, such as the separation of two liquid phases, the ratio of container weight to sample weight was reduced by employing thin-walled tubes fitted with a bottom thermocouple well. Temperatures were measured with a platinum–platinum 10% rhodium thermocouple inserted in the bottom thermocouple well. The emf of the couple was fed to a precision potentiometer which had a recorder with a chart span of 1 mv attached to the binding posts of the galvanometer. This arrangement permitted time-temperature curves to be recorded during the cooling and heating cycles. The temperatures at which the thermal effects occurred in the various systems could be read to the nearest 0.5°C and estimated to the nearest 0.1°C.

The validity of the data obtained by thermal analysis was checked in the potassium–potassium chloride system by comparison with results obtained by sampling techniques. The solubility of solid KCl in potassium metal was determined from 500 to 750°C by equilibration and decantation of the metal phase, and the curve through these data was found to meet the points obtained by thermal analysis very well.

Solubility in these systems was determined by thermal analysis over the whole concentration range, that is, from the pure salt to the pure metal (Fig. 49). The phase equilibria are of the same general type as those in the potassium–potassium fluoride system reported earlier.[11] They show a relatively large solubility of the solid salt in the liquid metal, with a positive temperature coefficient of that solubility, a relatively small, closed two-liquid phase region, and an appreciable solubility of the metal in the liquid salt near the monotectic temperature.

It was possible in these systems, because of the higher equilibrium metal concentrations at the monotectic reaction temperatures, to determine the freezing-point depression of the salt as a function of composition with greater accuracy than in the earlier studies. The upward curvature of the liquidus line corresponds to increasing positive deviation from Raoult's law as the metal concentration increases. At the monotectic temperature the solution contains almost twice as much metal as would be predicted theoretically, using the heat of fusion of the pure salt.[12] Moreover, an

[9] In cooperation with Wm. T. Smith, Jr., consultant, University of Tennessee.

[10] M. A. Bredig, J. W. Johnson, and Wm. T. Smith, Jr., *J. Am. Chem. Soc.* 77, 307 (1955).

[11] M. A. Bredig, H. R. Bronstein, and Wm. T. Smith, Jr., *J. Am. Chem. Soc.* 77, 1454 (1955).

[12] In the sodium systems, NaBr-Na and NaI-Na showed the same behavior; only in NaCl-Na did the melting-point depression seem to be nearly ideal. A careful reinvestigation with the new technique showed this to be in error due to an unsuspected small contamination of the sodium chloride with SiO_2. A strong positive deviation from Raoult's law, as expected, corresponding to a factor of approximately 2 at the monotectic, is now definitely established for the melting-point depression in this system as well.

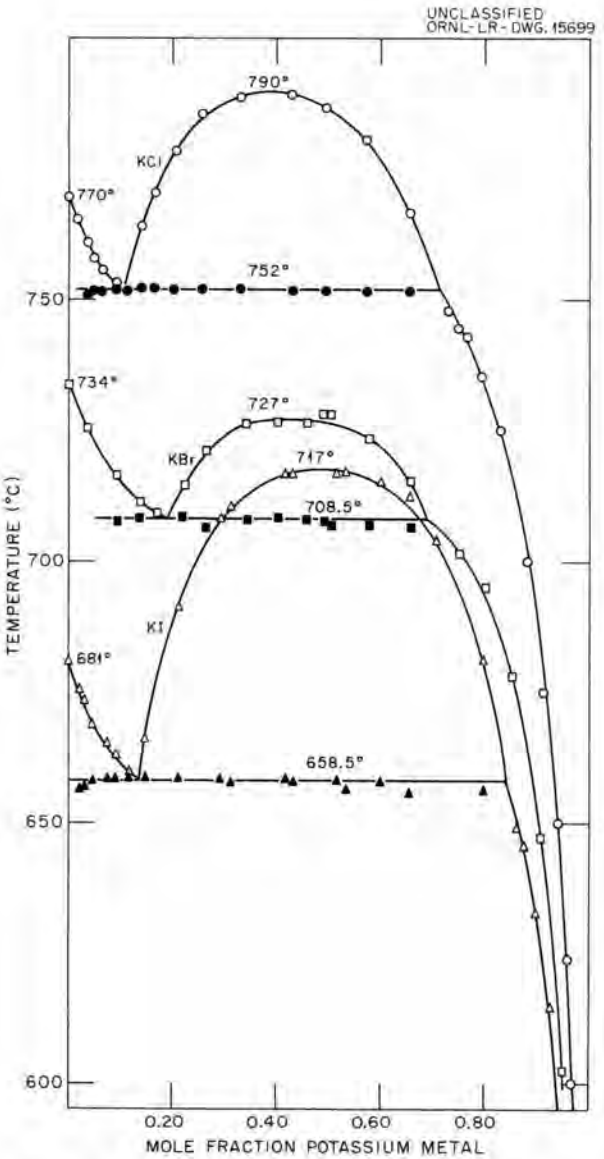

Fig. 49. The Potassium–Potassium Halide Systems.

extrapolation of the freezing-point depression curve to a region of very low metal concentration, where Raoult's law might be expected to hold, does not exactly yield the ideal limiting slope. Aside from insufficient accuracy of observed depressions, this may be due to a variety of factors such as solution of metal in the solid salt, lack of reliable values for the heats of fusion of the pure salts except in the case of potassium chloride, and lowering of the melting point of the pure salt in relation to the other temperatures because of the corrosion of the container in the absence of excess alkali metal. In the latter case a depression of 0.5 to 1°C in the melting point of the pure salt by corrosion products is sufficient to account for the observed discrepancy. The increasing positive deviation from ideality indicates an association of the dissolved potassium, probably an equilibrium between atoms and diatomic molecules, similar to that known in the metal vapor, with the concentration of the molecular species increasing as the metal concentration increases.

The span between the monotectic and the consolute temperatures decreases in going from the fluoride (60 deg) through the chloride (38 deg) to the bromide (19 deg) and then increases again for the iodide (60 deg). The critical temperature for the two-liquid phase region in the bromide system lies 7 deg below the melting point of the pure salt and probably represents a trend to the absence of a two-liquid phase region and complete miscibility at the melting point of the pure salt that occurs in the cesium–cesium halide systems.[11] Why this trend should be more pronounced in potassium bromide than in the other potassium halides is not quite clear. A factor which may be important is the similarity in molar volumes of the salt and metal, potassium metal having a molar volume 15 and 3.5% greater than its chloride and its bromide, respectively, and 17% less than its iodide. Of all the sodium and potassium metal-salt systems, the greatest similarity in molar volume of the molten salt and liquid metal occurs in the K-KBr system. No comparison can be made with the cesium systems, since the density of cesium metal has not been measured.

The solubility of the solid salt in the liquid metal below the monotectic temperature can be represented by the relation

$$N_2 = Ce^{AT/T_{mon}} ,$$

where N_2 is the mole fraction of the salt in solution, C is a constant for each salt, T is the temperature in degrees Kelvin, T_{mon} is the monotectic temperature for the system, and A is the same constant for chloride, bromide, and iodide. The validity of this equation would seem to indicate that the use of the reduced temperature, T/T_{mon}, furnishes equivalent temperatures in this region, since the temperature coefficient of solubility, A, is the same for all three salts.

Electrical Conductivity in Molten Salt-Metal Solutions[9]

H. R. Bronstein M. A. Bredig

Several modifications were made in the conductivity apparatus in order to overcome various experimental difficulties. The frequent cracking of the synthetic sapphire conductance cell on immersion into the molten salt was eliminated by preheating the cell in a small auxiliary electrical resistance furnace mounted inside the tank above the surface of the fused salt. While segregation of solid salt and liquid metal on freezing of the salt-metal mixture within the cell and the sampling crucible, when either was inserted cold into the melt, might have distorted the previous results, future data are believed to be free of this possible error.

The tank of the apparatus is now divided into an upper and a lower chamber separated by a horizontal partition. The cell assembly, the sampling device, a stirrer, and the liquid-metal loading tube are inserted into the melt, which is located in the lower chamber, through narrow tubes mounted in the partition. The tube openings can be closed and opened by shutters. It proved possible by these means to retain more than 90% of the volatile alkali metal in the molten salt during the time period required for the loading operation and the actual measurement, while previously, through vaporization of metal to the cold top of the tank, losses in excess of 50% were common.

Color of Liquid Alkali Metals Containing Salt

M. A. Bredig

It had been reported[13] that alkali halide dissolved in liquid alkali metal can produce intense colors at temperatures in excess of 500 to 600°C. It was stated further that the color of such solutions of salts in liquid metals was responsible for the coloration observed in molten alkali halides on electrolysis, since a colored metal phase was dispersed colloidally through the molten salt.

The result of the work on alkali metal–alkali halide phase equilibria performed during the last five years in this section of the Laboratory has been to provide final and quantitative evidence of the very large "true," rather than colloidal, solubility of the alkali metals in their molten halides. There can, therefore, be no question about any connection existing between the well-established coloration of solutions of alkali metals in the molten halides and any observations of a colored alkali metal phase.

A few experiments were undertaken with the objective of observing colors, if any, in liquid alkali metals under conditions in which the well-known deep coloration of the alkali metal vapors would not be a disturbing factor, as it appeared to have been in the tests cited above.

A 1-gal glass beaker covered with a watch glass contained a flat electric heating element on which was placed a shallow iron crucible cover which contained the liquid alkali metal. The temperature was read by a thermocouple welded to the crucible cover. When this assembly was heated with argon gas streaming rapidly through the beaker, thick clouds of intensely colored vapors, blue-green to purple, were seen above 500°C to issue from the surface of the liquid metal. Ever so often the whirling argon gas would displace enough of the vapors to permit a direct glance at the metal surface: It was the usual noncolored silvery-white liquid metal that became visible, irrespective of whether salt was added or not. On the basis of these observations it is suggested that the earlier finding[13] of a "colored liquid metal phase" was caused by the presence of clouds of sodium and potassium vapors containing appreciable fractions of diatomic, Na_2 and K_2, molecules well known to have absorption bands in the corresponding regions of the visible spectrum. In the deep, narrow crucible, and with the relatively still gas atmosphere in the large dry box that was used, with vertical observation,[13] these vapors may have escaped proper attention. The fact that liquid lithium metal was found to be not colored by the addition of salt at the temperatures employed, below 800°C, is readily explained by the much lower vapor pressure of this metal compared with that of sodium or potassium.

These remarks are not intended to exclude the possibility that, at higher temperatures and with much larger quantities of salt dissolved in the liquid metal, color may be produced. Certainly, above a minimum temperature, the consolute temperature, a continuous transition exists between the properties of the fused salt and the liquid metal, and somewhere in the whole concentration region the solutions of the salt in the liquid

[13] *Status and Prog. Rep. Feb. 1956*, ORNL-2062, p 23 (secret); B. H. Clampitt, *ANP Quar. Prog. Rep. March 10, 1956*, ORNL-2061, p 101 (secret).

metal must approach in appearance the solutions of the metal in the salt, many of which are deeply colored.

PARTIAL VAPOR PRESSURES OVER MIXTURES OF SALTS

S. Datz R. E. Minturn[14]

The vapor pressure of solid KCl has been measured from 10^{-5} to 10^{-1} mm Hg (730 to 1044°K), utilizing an effusion technique and a surface ionization detector.[15] The temperature coefficient as indicated in Fig. 50 appears in agreement with the reported value of Zimm and Mayer.[16] Measurements have also been made on solid NaCl in this range but are not yet complete. The data for liquid KCl and NaCl have been irreproducible, presumably because of the tendency of the liquids to creep up the walls of the platinum crucible and vaporize from areas of higher temperature, causing a nonequilibrium situation.

[14] On loan from U.S. Air Force.

[15] S. Datz and R. E. Minturn, *Chem. Semiann. Prog. Rep. Dec. 20, 1955*, ORNL-2046, p 52.

[16] B. H. Zimm and J. E. Mayer, *J. Chem. Phys.* **12**, 362 (1944).

DIFFRACTION STUDIES OF LIQUIDS

An X-Ray Study of Molten Cesium Iodide

P. A. Agron M. D. Danford
M. A. Bredig H. A. Levy

Introduction. – Cesium iodide was chosen for this study as one of the four extreme cases among the combinations of alkali metals with halogens, namely, the one in which both ions are so large that dispersion (Van der Waals) forces between them are more important than in the other salts. These additional forces lead, according to Mayer,[17]

[17] J. E. Mayer, *J. Chem. Phys.* **1**, 270 (1933); *J. Chem. Phys.* **1**, 327 (1933).

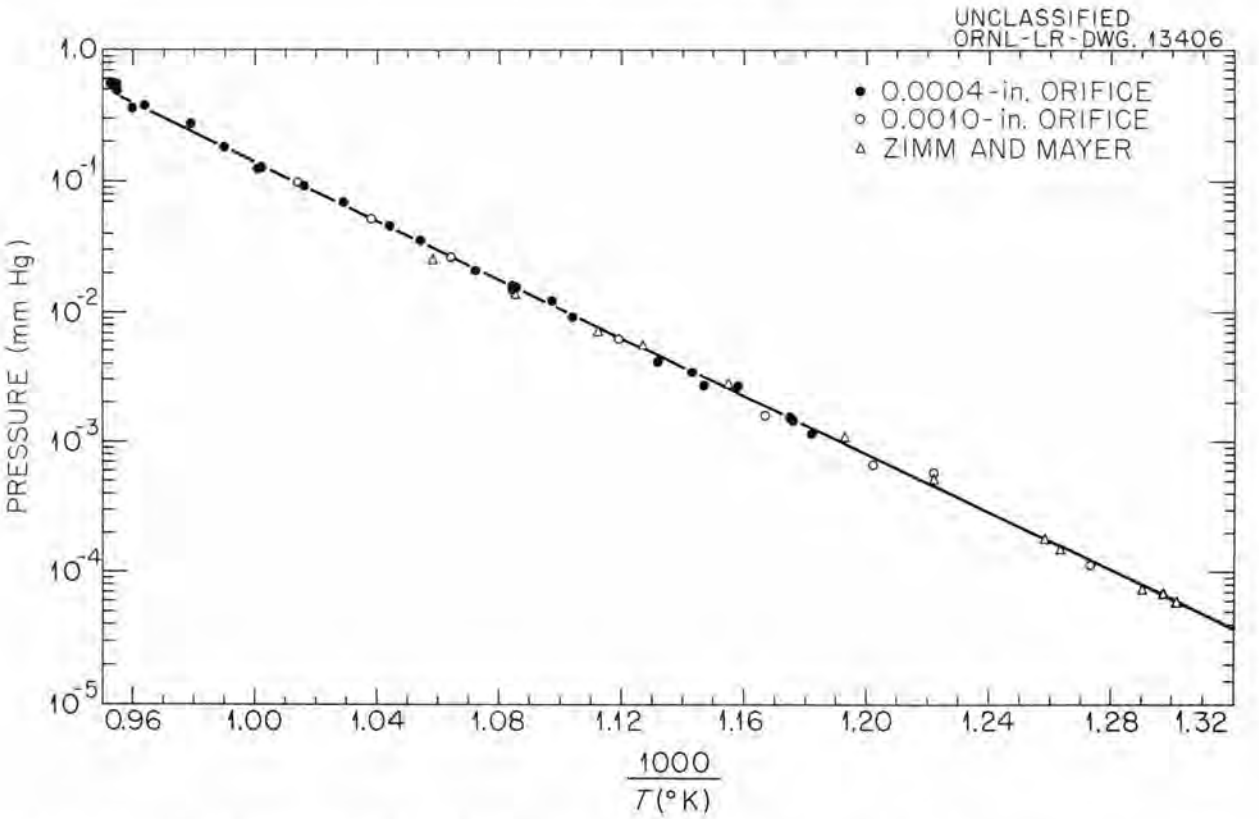

Fig. 50. Vapor Pressure of Solid Potassium Chloride as a Function of Reciprocal Temperature. The pressure correspondence is established by reference to the values of Zimm and Mayer, some of which are plotted above.

to the higher coordination number of 8 in cesium chloride at room temperature, and, as expected, this structure was found to be even more stable in cesium bromide and iodide.[18] The structure of the molten iodide is of particular interest in connection with the comparatively large volume change occurring on melting, which suggested a considerable decrease in the average coordination number.[18] The choice of this salt was also favored by the following factors: (1) its relatively low melting point (621°C), (2) the similarity of the form factors of Cs^+ and I^-, which simplifies interpretation of the x-ray scattering data, and (3) the low intensity of Compton-modified radiation when scattered from heavy atoms, which facilitates a satisfactory correction of the data for this effect.

Experimental. – The diffractometer used in obtaining the diffraction pattern of molten cesium iodide has been described previously.[19] The sample was obtained from a single crystal of cesium iodide and placed in a tray cut from a single crystal of magnesium oxide. Intensity patterns were recorded, with the sample of cesium iodide being held at 640°C. Both rate-meter traces and step scanning were employed to obtain the intensity pattern shown in Fig. 51, the region from $s = 4\pi(\sin \phi/2)/\lambda = 1.10$ to $s = 4.60$ being obtained from rate-meter traces, while the remaining portion of the pattern was obtained by step-scanning procedures. The times for a predetermined number of counts were recorded by a Clary printing timer, with the number of counts being chosen to keep the statistical error in the $si(s)$ curve shown at the top of Fig. 51 approximately constant. Points from $s = 4.75$ to $s = 8.73$, $s = 8.86$ to $s = 12.73$, and $s = 12.84$ to $s = 16.10$ represent 20,000, 30,000, and 40,000 counts,

[18] J. W. Johnson, P. A. Agron, and M. A. Bredig, *J. Am. Chem. Soc.* 77, 2734 (1955).

[19] P. C. Sharrah *et al.*, *Chem. Semiann. Prog. Rep. June 20, 1955*, ORNL-1940, p 39.

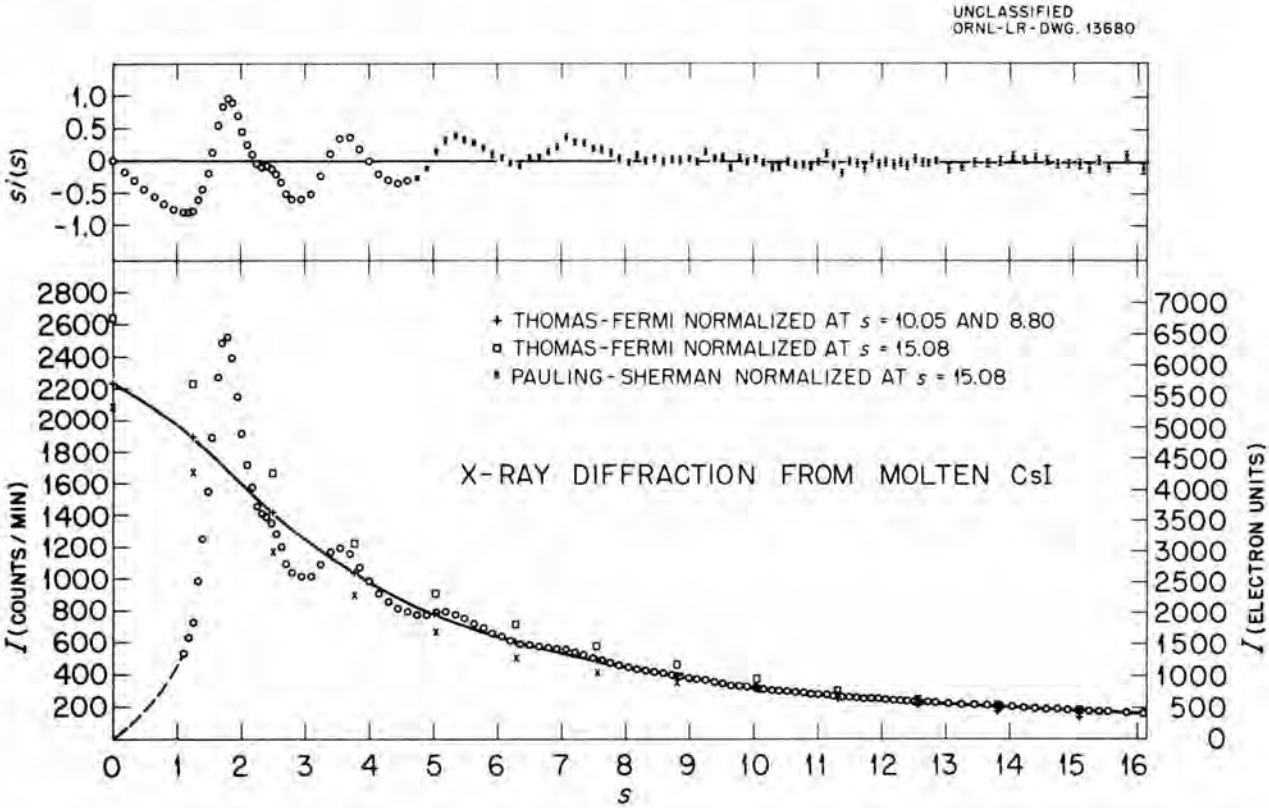

Fig. 51. Intensity Pattern for Molten CsI (Bottom); Reduced Intensity Function $s[(I/N/^2) - 1]$ for Molten CsI (Top).

respectively. The raw intensity curve was corrected for instrument background and converted to absolute intensity by normalizing at large diffraction angle to the theoretical (Fermi-Thomas corrected for dispersion) scattering from independent cesium and iodine atoms, with Compton modified scattering assumed to be negligible. The radial distribution function, shown at the center of Fig. 52, was obtained by the method of Zernicke and Prins[20] and Debye and Menke,[21] using Beevers-Lipsom strips.

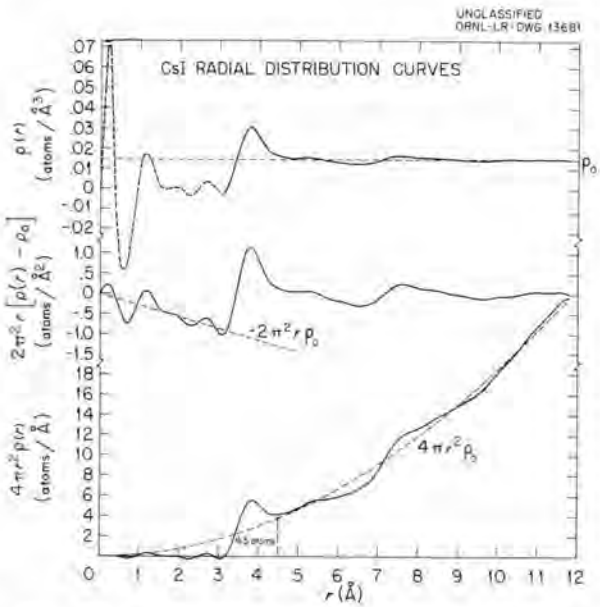

Fig. 52. Radial Distribution Function, $4\pi r^2\rho(r)$, for Molten CsI (Bottom); Distribution Function, $2\pi^2 r[\rho(r) - \rho_0]$, for CsI (This Function Is the Sine Fourier Transform of the Reduced Intensity Function Shown at Top of Fig. 51) (Center); Radial Density Function $\rho(r)$ for Molten CsI (Top).

Results. – The intensity pattern shown in Fig. 51 has been corrected for polarization and is seen to follow the shape of the sum of the squares of the atomic form factors for cesium and iodine, as calculated by the Thomas-Fermi method[22,23] and normalized at s = 10.05 and 8.80, quite satisfactorily to s = 11. Beyond s = 11, the observed intensity curve rises above the theoretical, independent atomic-scattering curve. The theoretical curve normalized at s = 15.08 and the corresponding independent scattering curve calculated by the Pauling-Sherman method[24] are entirely unsatisfactory. These deviations may arise from either instrumental causes or from deficiencies in the scattering theory, and which of these is the case remains to be determined. The reduced intensity function shown at the top of Fig. 51 shows no structure beyond s = 8. The Fourier inversion of the reduced intensity curve is shown at the center of Fig. 52 and is proportional to $r\rho(r)$, $\rho(r)$ being the radial atomic density function, while the straight line is the function $-2\pi^2 r\rho_0$, where ρ_0 is the average atomic density. The radial atomic density function $\rho(r)$, which represents the mean density of atoms at distance r from any one atom, and the radial distribution $4\pi r^2\rho(r)$ are shown at the top and bottom of Fig. 52, respectively. The area under the first peak of the radial distribution curve, when this is bounded in the manner shown by the dotted line, is approximately 4.5 atoms at a distance of 3.85 Å.

Discussion. – The value of 3.85 Å obtained for the Cs-I distance in this investigation, which corresponds approximately to the sum of the ionic crystal radii for coordination number 6 (refs 25, 26, and 27), is considerably smaller than 4.09 Å, the distance for coordination number 8 in the crystal measured just below the melting point.[18]

The average coordination number of 4.5 is considerably lower than the value of 5.8 reported[28] for KCl. It seems worthwhile to point out that the minimum beyond the first peak in the radial density curve at the top of Fig. 51 does not fall below the average atomic density and that the $\rho(r)$ function rapidly approaches the average atomic density and follows it quite closely. Thus it would appear that there is less structure in molten cesium iodide than had been previously supposed for fused salt systems, but further work will be necessary before general conclusions can be drawn.

[20] F. Zernicke and J. Prins, *Z. Physik* 41, 184 (1927).

[21] P. Debye and H. Menke, *Ergeb. d. Tech. Röntgenk.* II, Adademische Verlagsgesellschaft, Leipzig, 1931.

[22] L. H. Thomas, *Proc. Cambridge Phil. Soc.* 23, 542 (1927).

[23] E. Fermi, *Z. Physik* 48, 73 (1928).

[24] L. Pauling and J. Sherman, *Z. Krist.* 81, 1 (1932).

[25] V. M. Goldschmidt, *Ber.* 60, 1263 (1927).

[26] L. Pauling, *J. Am. Chem. Soc.* 49, 765 (1927).

[27] W. H. Zachariasen, *Z. Krist.* 80, 137 (1931).

[28] K. Lark-Horovitz and E. P. Miller, *Phys. Rev.* 49, 418 (1936).

CHEMICAL PHYSICS

RADIO-FREQUENCY SPECTROSCOPY

Gas Yields from Irradiated Acids

A. Weinberger R. Livingston

Atomic hydrogen has been found by means of its paramagnetic resonance in several substances irradiated with Co^{60} gamma rays at liquid-nitrogen temperature.[1] A study has been started on the yields of gas from these irradiated substances to see whether there is a correlation with the atomic-hydrogen yield. It is not necessary that there be a correlation, since molecular hydrogen might be formed from a species other than atomic hydrogen that appears stably trapped at 77°K, and also since the stably trapped atomic hydrogen observed at 77°K need not become molecular hydrogen when the sample is warmed.

Gas-yield measurements have been made on several concentrations of sulfuric acid. The degassed, frozen acid was irradiated at 77°K with Co^{60} gamma rays. Following the irradiation the samples were warmed and the amounts of hydrogen and oxygen assayed. For a range of concentrations, the acid can be frozen either to a glassy solid or to a crystalline solid. The yields, in units of molecules of gas formed per 100 ev of energy absorbed, varied from about 0.2 to 0.6 for hydrogen and from about 0.01 to 0.09 for oxygen over the concentration range of 2 to 33 mole % of H_2SO_4. The yield values scattered considerably, and there appeared to be a definite dependence on whether the frozen sample was glassy or crystalline. The yields were higher in the glassy material. In order to determine more carefully the effect of the state of the frozen acid, a sample was prepared with the concentration adjusted to the one-hydrate composition (50 mole %), and irradiations were carried out with portions quickly frozen to a glass and with other portions slowly crystallized. Duplicate samples agreed well, and the yields for hydrogen and oxygen, respectively, in the crystalline material were 0.005 and 0.0005, while in the glass material they were 0.166 and 0.023. Atomic-hydrogen yields have not yet been measured at this acid concentration. Yields of atomic hydrogen have, however, been measured more accurately than previously[1] on glassy 17 mole % acid, and the values were much higher, making them much more nearly comparable with the higher gas yields quoted above.

Pure Quadrupole Spectroscopy

H. Zeldes R. Livingston

The final results of a study of the Zeeman effect on the pure quadrupole spectrum of iodine in iodic acid have been submitted for publication.[2] Similarly, the results of a Zeeman study[3] on the chlorine resonances in potassium, sodium, and barium chlorates will be submitted for publication soon. These results will not be treated further here. The electric field gradient terms that arise from the ionic environment of a chlorine atom in the $NaClO_3$ and $KClO_3$ lattices are being computed on the Oracle. The objective is to find out whether the electric charges associated with the ionic environment can explain the difference in chlorine quadrupole coupling in the two salts and to see whether the small field gradient tensor asymmetry found[3] in $KClO_3$ can be explained. The calculations are not complete, but it appears possible that the field gradient asymmetry can be explained by the charges of ions in the environment. It is not possible yet to say whether the coupling difference can be explained on this basis, but it looks likely that it cannot.

Paramagnetic Resonance

R. Livingston H. Zeldes

The first results obtained with calcium hydroxide were described earlier.[4] The main paramagnetic effect after gamma irradiation of a single crystal at 77°K was the appearance of a strong absorption line. The g value clearly showed axial symmetry with $g_{\parallel} = 2.0018$ and $g_{\perp} = 2.0743$, where the parallel value is along the c axis of the hexagonal crystal. This absorption line showed a large width anistropy. It also showed small satellite lines arising from interactions of the unpaired electron with near-neighbor protons. A second pair of weak absorption lines was also found and these were due to a small yield of atomic hydrogen. The width

[1] R. Livingston, H. Zeldes, and E. H. Taylor, *Discussions Faraday Soc.* 19, 166 (1955).

[2] R. Livingston and H. Zeldes, *J. Chem. Phys.* (in press).

[3] H. Zeldes and R. Livingston, paper to be submitted to *J. Chem. Phys.*

[4] H. Zeldes and R. Livingston, *Chem. Semiann. Prog. Rep. Dec. 20, 1955*, ORNL-2046, p 49.

anisotropy found for the hydrogen absorption lines showed sixfold symmetry about the c axis, indicating that the atomic hydrogen is on one of the threefold axes of the lattice.

A number of new observations have been made. The main, strong absorption line is formed with a yield of about 2.6 unpaired electrons for every 100 ev of gamma energy absorbed. The effect saturates only after extremely heavy irradiation. After 8.7×10^{19} ev of energy was absorbed in a 9.8-mg crystal it was estimated that the number of unpaired electrons was roughly 0.7% of the total number of $Ca(OH)_2$ molecules present. This irradiation essentially produced saturation. The species giving rise to the absorption line disappeared at a moderate rate at 0°C, and in the one quantitative rate experiment which was made it appeared to follow second-order kinetics. In any case, from several observations, the rate definitely follows higher than first-order kinetics.

The main absorption had been attributed to the OH radical formed by the simple reaction $OH^- \rightarrow OH + e$. In order to further test this idea the optical absorption of single crystals of calcium hydroxide irradiated at 77°K was examined. A well-known transition appears in gaseous OH radical at about 3065 Å corresponding to the $\Pi \longleftrightarrow \Sigma$ transition. A very strong absorption was found in the solid at about 3075 Å which is in excellent agreement with the known transition in gaseous OH. The absorption is somewhat masked at 77°K by a general increase in the absorption throughout much of the ultraviolet region, but quickly warming the sample to, say, 200°K and then cooling to 77°K reduces much of the background. The 3075-Å optical absorption disappears at a moderate rate at 0°C at higher than first-order kinetics, and is thus similar to the paramagnetic absorption line.

Although the above evidence indicates that the paramagnetic resonance may be the OH radical, this interpretation causes some concern. In particular, a difficulty is the smallness of the hyperfine interaction that would have to be ascribed to the OH radical. Since the optical observations give strong evidence for the formation of OH by the reaction $OH^- \rightarrow OH + e$, the paramagnetic species observed may be the electron formed in the reaction, or a new product resulting from this electron. The OH and the new product would then be created in one-to-one correspondence, and back reaction would cause them to disappear together, thus explaining why the paramagnetic line (not OH) disappeared concurrently with the optical line (OH).

Only two reactions for this electron were considered reasonable. The first was $Ca^{++} + e \rightarrow Ca^+$, and the second was simply the electron going to a negative ion vacancy to form an F center. In order to determine whether the first reaction was the correct one, a single crystal of $Ca(OH)_2$ was made, using Ca^{43}. Since Ca^+ has an S ground state, a large hyperfine interaction would have to be present. No hyperfine effects appeared, and the absorption line was only slightly broadened, clearly showing that the electron was not on the calcium. Judging from the small increase in line width, the electron might be quite far from the calcium. If an electron is placed at an OH^- vacancy and *highly localized* (F center with a deep potential well), the line width change in the Ca^{43} crystal is reasonable. Moreover, if the electron is considered localized in an OH^- vacancy, an approximate calculation, using the intensity of the satellites of the line, gives a distance to the near-neighbor protons quite close to that deduced from the known crystal structure. Finally, a start has been made in applying the Van Vleck theory of line widths,[5] assuming a localized electron. The results so far have been encouraging. The Van Vleck theory gives the second moment of the line. As an approximation the line shape can be assumed to be gaussian and the second moments translated to full widths at half height.

The calculations thus far have given a width of 2.9 gauss for the $g_{\parallel}$ orientation and 2.2 gauss for $g_{\perp}$, with the field along the a crystallographic axis. For an intermediate orientation the computed width is very much greater. Since the paramagnetic line sharpens as the sample is cooled, the width measurements must be made at a very low temperature, where only the spin-spin interactions remain. Most width measurements made thus far[4] have been at 77°K, which is known to be too high a temperature. One approximate measurement at 20°K for the $g_{\parallel}$ orientation has been made, giving a value of 2.7 gauss. The $g_{\perp}$ width is larger and the intermediate width very much larger. Although the above observations are in good agreement with the electron being in a negative ion vacancy, other models might fit equally well at this stage of interpretation.

Additional lines, not previously reported, have also been observed in irradiated $Ca(OH)_2$. At 0°C

[5] J. H. Van Vleck, *Phys. Rev.* 74, 1168 (1948).

the main line slowly disappears and in its place three very weak lines appear. Quantitative measurements have not been made, but the number of unpaired electrons involved is roughly in the order of 1% of those causing the main line. The three lines show anistropy and are *not* axially symmetric. The most reasonable explanation appears to be that the unpaired electron species are interstitials located off the symmetry axes. This would account for three crystallographically related lines, since for any one interstitial location there would have to be two others related by crystal symmetry. Another possible explanation might be that the species lie in a normal lattice site, but that a lattice site in the immediate neighborhood is not occupied in a normal manner. Studies have been started that will give some information on the location of the unpaired electron. The Auger effect has been proposed as a mechanism for forming interstitials with gamma irradiation, and it appears that the observed yield attributed to interstitials may be reasonable for such a process. The nature of the species is subject to speculation at this time, but O^- is being considered. The atomic H might reasonably be formed concurrently with the formation of an interstitial species.

NEUTRON DIFFRACTION STUDIES

A Single-Crystal Neutron Diffraction Study of AlO(OH)

W. R. Busing H. A. Levy

Diaspore, AlO(OH), crystallizes in space group D_{2h}^{16}-*Pbnm*. There are four molecules per unit cell and crystallographically two kinds of oxygen atoms. All atoms are situated in mirror planes and have the coordinates $\pm(u,v,-\frac{1}{4})$; $\pm(\frac{1}{2}-u,\frac{1}{2}+v,-\frac{1}{4})$. The x-ray structure was discussed in detail by Ewing,[6] and Hoppe[7] determined the position parameters of the Al and O atoms. Ewing assumed that the short O_I–O_{II} bond distance of 2.65 Å indicated the presence of a hydrogen bond.

[6]F. J. Ewing, *J. Chem. Phys.* 3, 203 (1935).

[7]W. Hoppe, *Z. Krist.* 104A, 11 (1942).

A single-crystal neutron diffraction study of diaspore has been made, and the intensities of 70 reflections of the *hk*0 zone have been measured. Signs of the structure factors were assigned on the basis of the hydrogen-bonded model, and a Fourier projection indicated that this model was essentially correct. A least-squares refinement including two position parameters and three temperature-factor coefficients for each atom, together with an over-all scale factor, reduced the conventional discrepancy factor

$$R = \frac{\Sigma||F_o| - |F_c||}{\Sigma|F_o|}$$

to 2.8%.

The position parameters, u and v, are given in Table 28, together with Hoppe's values for comparison. These results indicate that the H atom is at a distance of 0.990 Å from O_{II} and 1.691 Å from O_I. It does not lie on the line of centers between the O atoms, but instead the O_{II}–H bond makes an angle of 11.9 deg with this line. If the hydrogen atom were on the O–O line, the Al–O_{II}–H bond angle would be 140.9 deg, but the displacement of the H atom reduces this angle to 129.0 deg.

Data from the 0*kl* zone are now being processed, and these will provide a complete description of the thermal motions of the various atoms.

TABLE 28. POSITION PARAMETERS OF THE ATOMS IN DIASPORE FROM X-RAY WORK OF HOPPE AND FROM CURRENT NEUTRON DIFFRACTION STUDIES

	Hoppe*	Present Work
u (Al)	−0.048	−0.0452
v (Al)	+0.146	+0.1442
u (O_I)	+0.287	+0.2880
v (O_I)	−0.199	−0.1990
u (O_{II})	−0.198	−0.1971
v (O_{II})	−0.056	−0.0533
u (H)		−0.4096
v (H)		−0.0879

*W. Hoppe, *Z. Krist.* 104 A, 11 (1942).

VIBRATIONAL SPECTRA OF DEUTERATED ETHANOLS

J. G. Burr, Jr.

The infrared spectra of CD_3CH_2OH, CH_3CD_2OH, CH_3CH_2OD, and C_2D_6O have been obtained on a Perkin-Elmer model 21 spectrometer with rock-salt optics. Since this series of spectra presents a unique opportunity for analysis of the vibrations in ethanol, they are being examined in collaboration with H. W. Morgan of the Molecular Spectroscopy Group.

EXPERIMENTS WITH MOLECULAR BEAMS

S. Datz

R. E. Minturn E. H. Taylor

Work in this field was concerned with the application of techniques developed previously to the measurement of vapor pressures of fused salts. It is reported in the section of this report entitled "Partial Vapor Pressures Over Mixtures of Salts."